

Ulm University, Institute of Biochemistry and Molecular Biology

Prof. Dr. Michael Kühl

**Investigation of the extent of cardiomyocyte
regeneration in the injured zebrafish heart and
the role of Wnt signaling during cardiac repair**

Dissertation

submitted in partial fulfillment of the requirements for the degree of
“Doctor of Philosophy” (PhD) of the International Graduate School in Molecular
Medicine Ulm of the Medical Faculty of Ulm University

Alberto Bertozzi

Place of birth: Castel San Pietro Terme, Italy

2018

Current Dean of the Faculty of Medicine:

Prof. Dr. Thomas Wirth

Chairman of the International Graduate School:

Prof. Dr. Michael Kühl

Thesis Advisory Committee:

First supervisor: Prof. Dr. Gilbert Weidinger, Ulm, Germany

Second supervisor: Prof. Dr. Steffen Just, Ulm, Germany

Third supervisor: Prof. Dr. Didier Stainier, Bad Nauheim, Germany

External reviewer:

Prof. Dr. Jörg Heineke, Mannheim, Germany

Day doctorate awarded:

06.05.2019

Table of Contents

List of abbreviations	6
Introduction	10
Heart regeneration in zebrafish.....	10
Cryoinjury model in the zebrafish heart	11
Cellular responses to cardiac injury in zebrafish	13
The Wnt/ β -catenin signaling pathway	15
Wnt signaling in repair and cardiac development.....	16
Motivation and aim of the study	18
Materials and methods	20
Results	29
Quantitative time-course of cardiomyocyte regeneration in injured zebrafish hearts	29
Establishment of a semi-automatic method for cardiomyocyte number quantification on cryosections.....	29
Cardiomyocyte numbers are fully restored during heart regeneration within 30 days.....	32
The extent of cardiomyocyte regeneration and wound size do not fully correlate	36
Myocardial morphology regenerates, but cardiomyocytes remain smaller in areas enclosing residual scars.....	39
Wnt/ β -catenin signaling in zebrafish heart regeneration	42
Wnt/ β -catenin signaling is upregulated upon cryoinjury	42
Manipulation of Wnt/ β -catenin signaling in the adult heart using inducible transgenes	48

Global prolonged inhibition of Wnt/ β -catenin signaling reduces cardiomyocyte proliferation.....	51
Global Wnt/ β -catenin inhibition impairs fetal cardiac myosin re-expression in dedifferentiating cardiomyocytes	54
Cell-autonomous Wnt/ β -catenin inhibition impairs cardiomyocyte cell cycle re-entry	56
Global Wnt/ β -catenin loss of function does not impact on morphological regeneration	61
A small qPCR screen of selected Wnt ligands identifies <i>wnt9a</i> upregulation upon injury	63
Discussion	68
A model for zebrafish heart regeneration by complete cardiomyocyte regeneration	68
Wnt/ β -catenin signaling in zebrafish heart regeneration	72
Activation of Wnt/ β -catenin in the regenerating adult zebrafish hearts	72
The role of Wnt/ β -catenin in zebrafish cardiac repair	73
Expression of Wnt ligands in the zebrafish heart in response to injury	76
Conclusion	79
Summary	80
List of references.....	82
Statutory declaration.....	95

List of abbreviations

+	Positive
-	Negative
AFOG	Acid fuchsin-orange G
Aldh1a2	Aldehyde dehydrogenase 1 family, member A2
ANOVA	Analysis of variance
Apc	Adenomatous polyposis coli
BMP	Bone morphogenetic protein
BrdU	5-bromo-2'-deoxyuridine
C.I.	Confidence interval
Ck	Casein kinase
Coro1a	Coronin, actin binding protein, 1A
CM	Cardiomyocyte
Ctnnb	Catenin (cadherin-associated protein), beta
DAPI	6-diamidino-2-phenylindole
DEAB	N,N-diethylaminobenzaldehyde
DEX	Dexamethasone
Dkk	Dickkopf
DMSO	Dimethylsulfoxide
DOX	Doxycycline
dpa	days post amputation
dpi	days post cryoinjury
dps	days post sham-injury

Dvl	Dishevelled
ECM	Extracellular matrix
EdU	5-ethynyl-2'-deoxyuridine
e.g.	exempli gratia (for example)
EGFP	Enhanced green fluorescent protein
EMT	Epithelial-mesenchymal transition
EndMT	Endothelial-mesenchymal transition
ESC	Embryonic stem cell
EtOH	Ethanol
Fgf	Fibroblast growth factor
Fli1a	Fli-1 proto-oncogene, ETS transcription factor a
Fzd	Frizzled
Gata4	GATA binding protein 4
GFP	Green fluorescent protein
Gsk3	Glycogen synthase kinase 3
hs	heat shock
hpa	hours post amputation
hpi	hours post injury
hsp70l	heat shock cognate 70-kd protein, like
Igf	Insulin-like growth factor
IP	Intraperitoneal
IWR-1	Inhibitor of Wnt response 1
Kdr1	Kinase insert domain receptor like

Lef	Lymphoid enhancer factor
Lrp5/6	Low-density lipoprotein receptor-related protein 5/6
Luc	Luciferase
Mef2	Myocyte enhancer factor-2
MHC	Myosin heavy chain
MI	Myocardial infarction
Myh7	Myosin, Heavy Chain 7
Myl7	Myosin, Light Chain 7
NCS	Newborn calf serum
NF- κ B	Nuclear factor of kappa light polypeptide gene enhancer in B-cells 2
NLS	Nuclear localization sequence
Nrg1	Neuregulin 1
n.s.	not significant
nT	Nuclear Tomato
o/n	over night
OTM	Optimal Tcf motif
PBS	Phosphate-buffered saline
PCNA	Proliferative cell nuclear antigen
PCP	Planar cell polarity
PEM	PIPES-EGTA-MgCl ₂
PH3	Phospho-histone 3
PFA	Paraformaldehyde
RA	Retinoic acid

Rho-GTPase	Ras homologue Guanosine triphosphate hydrolase
RT	Room temperature
sFrp	Secreted frizzled-related protein
Shh	Sonic hedgehog
Tcf	T cell factor
TetA	TetActivator
TetRE	TetResponder
Tgf β	Transforming growth factor β
Tx	Triton X-100
Vegf	Vascular endothelial growth factor
w/v	Weight per volume
Wnt	Wingless-type MMTV integration site family
wt	Wild-type
YFP	Yellow fluorescent protein

Introduction

Acute myocardial infarction is a leading cause of worldwide morbidity and mortality. Typically myocardial infarction occurs due to obstruction of a coronary artery resulting in necrosis of a portion of the myocardium. The human heart has an extremely low turnover rate of cardiomyocytes in physiological conditions, and injury to the myocardium does not result in elevated proliferation and replacement of the lost cardiomyocytes (Kikuchi and Poss 2012). If the injury is compatible with survival, healing is further impeded by permanent scarring. Because the scar is not contractile, the ventricular wall undergoes remodeling associated with cardiomyocyte hypertrophy in order to maintain pumping functions of the heart. Over a period of time heart function deteriorates resulting in heart failure (reviewed in Laflamme and Murry 2011). This non-regenerative response to heart injury is conserved also in the typical mammalian model organisms like mice, rats and pigs. It is now clear that the neonatal mouse responds to cardiac injury by cardiomyocyte proliferation, a feature which is somehow lost after the first week post birth, suggesting that an intrinsic ability to regenerate is still preserved in murine cardiomyocytes (Porrello et al. 2011). In nature, there are several vertebrate species, such as teleost fish and urodele amphibians, that hold remarkable ability to regenerate lost body parts throughout the entire lifespan. Zebrafish is one of these species that can regenerate multiple tissue types even in adulthood (Gemberling et al. 2013; Sehring et al. 2016). Strikingly, zebrafish initiate a response to cardiac injury which includes cardiomyocyte proliferation and leads to almost scar-free repair (Chablais and Jazwinska 2012; González-Rosa et al. 2011; Poss et al. 2002; Schnabel et al. 2011). Due to its robust regenerative capability, zebrafish has developed rapidly over the past years as an important heart regeneration model. Understanding the molecular mechanisms behind zebrafish heart regeneration could therefore offer crucial insights into cardiomyocyte biology that has potential translational value, which could unlock the secret to human cardiomyocyte proliferation.

Heart regeneration in zebrafish

In adult mammals, heart injuries result in permanent scarring and lost cardiomyocytes cannot be regenerated. Thus, the discovery that zebrafish hearts can recover from substantial loss of myocardium (Poss et al. 2002) has raised great interest in the underlying cellular and molecular mechanisms. Several types of injuries, such as milder stabs and

scratch injuries, resection or cryoinjury which results in death of at least 20% of the myocardium, and genetic ablation of up to 65% of ventricular cardiomyocytes are all compatible with survival and trigger a pro-regenerative response, albeit at different intensities (Chablais et al. 2011; González-Rosa et al. 2011; Itou et al. 2014; Parente et al. 2013; Poss et al. 2002; Schnabel et al. 2011; Wang et al. 2011).

Cryoinjury model in the zebrafish heart

The ability of zebrafish to regenerate the adult heart was first reported by resection of the ventricle (Poss et al. 2002). After surgical removal of around 20% of the apex of the ventricle, a fibrin-rich clot seals the injury within days. In contrast to mammalian hearts after myocardial infarction (MI), little or no collagen deposition is left one or two months after injury, indicating that scarring is not permanent. Rather, the damaged area shows signs of muscle restoration and sustained cardiomyocyte proliferation. Apical resection has since been the most frequently used injury model but recent studies have suggested new ways to damage the heart, which better resemble cardiac ischemia.

In contrast to most mammalian heart injuries, apical resection does not cause widespread tissue death and thus has less value as a clinically relevant model. Hence, cryoinjury has been employed in zebrafish to better mimic aspects of MI (Chablais et al. 2011; González-Rosa et al. 2011; Schnabel et al. 2011). A small piece of dry ice or a thin metal filament cooled by liquid nitrogen is applied to the surface of the ventricle to cause a sudden freezing which results in massive tissue necrosis. Zebrafish can tolerate cryoinjury-induced death of around 30% of the ventricle. As first response to damage, cellular debris and dead cells must be cleared from the affected area by immune cells infiltrating into the wound (Schnabel et al. 2011). Later on, the injured area shows collagen deposition and thus scarring starting as early as 3 dpi, a response considered to be essential to maintain tissue integrity (Richardson et al. 2015). However, the deposited ECM is progressively resolved during the course of regeneration, resulting in resorption of most of the scar between 60 and 130 days post injury (dpi) (Figure 1) (Chablais and Jazwinska, 2012; González-Rosa et al. 2011; Poss et al. 2002; Schnabel et al. 2011). The necessary clearing of necrotic and scar tissue, concomitant to the restoration of myocardium, might explain at least partially the longer time required for cryoinjured hearts to repair compared to resected hearts, which need only about 30 days. Nevertheless, other cellular responses are substantially identical between the two models, including cardiomyocyte cell cycle re-entry and reactivation of developmental gene programs (Kikuchi et al. 2011; Lepilina et al. 2006).

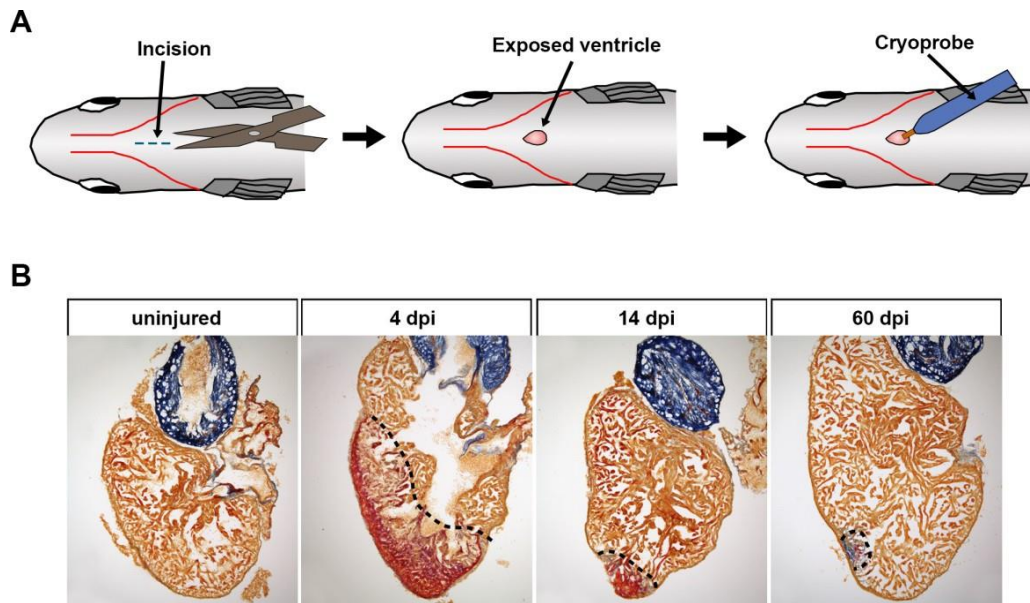


Figure 1. Cryoinjury model in the zebrafish heart

(A) Schematic representation of cryoinjury of the zebrafish heart. After the fish is anesthetized, an incision is made through the body wall and pericardial sac (blue dashed line). The ventricle is then exposed by gently pressing on the sides of the fish. Next, the ventricle is touched by a liquid nitrogen-cooled cryoprobe until it thaws completely to avoid tearing of the ventricle. Finally, the fish is transferred back to fish water for recovery. (B) Acid fuchsin orange G (AFOG) staining on longitudinal sections of cryoinjured hearts at different time points after injury. At 4 days post injury (dpi), the injured area is characterized by fibrin deposition (red). The wound tissue progressively reduces in size from 4 to 60 dpi where little or no collagen deposition is observed. Dashed lines, wound boundary. Figure 1B is obtained from Schnabel K, Wu C-C, Kurth T, Weidinger G (2011) Regeneration of Cryoinjury Induced Necrotic Heart Lesions in Zebrafish Is Associated with Epicardial Activation and Cardiomyocyte Proliferation. PLoS ONE 6(4): e18503. doi:10.1371/journal.pone.0018503. (© 2011 Schnabel et al. This is an open-access article distributed under the terms of the Creative Commons Attribution License CC BY 4.0, <https://creativecommons.org/licenses/by/4.0/>, which permits unrestricted use, distribution, and reproduction in any medium, provided the original author and source are credited.)

Cellular responses to cardiac injury in zebrafish

Earlier studies focused on the source of restored myocardium and found by genetic lineage-tracing approaches that spared pre-existing differentiated cardiomyocytes are the major contributors to the regenerated tissue, based on the location of labeled cells relative to the resection plane (Jopling et al. 2010; Kikuchi et al. 2010). However, only by means of genetic lineage-tracing, these studies could not clearly quantify the amount of newly produced cardiomyocytes in the regenerate, or clarify whether those pre-existing cardiomyocytes undergo hypertrophy in response to injury. Cardiomyocytes close to the wound area acquire certain characteristics associated with a less mature state, such as rounded mitochondria and disassembled sarcomeres (Jopling et al. 2010), as well as reactivation of the cardiac developmental gene *gata4* (Kikuchi et al. 2010). It was found that cardiomyocytes re-expressing the *gata4* reporter are the primary contributors to the proliferating cardiomyocyte pool. Other studies have shown that border zone cardiomyocytes also downregulate mature cardiomyocyte genes like *myl7* (myosin light chain 7) and upregulate certain embryonic forms of myosin heavy chain (MHC) like *myh7* (myosin heavy chain 7) (Sallin et al. 2015; Wu et al. 2016). Altogether such changes, which include downregulation of mature markers while certain embryonic features are upregulated, are collectively termed dedifferentiation (Jopling et al. 2010; Kikuchi et al. 2010). Since direct inhibition of cardiomyocyte dedifferentiation upon over-expression of a dominant negative form of *gata4* results in impaired proliferation (Gupta et al. 2013), it is generally assumed that dedifferentiation might be a necessary step that allows cardiomyocytes to re-enter the cell cycle and replicate.

Regenerative cardiomyocyte proliferation in the zebrafish heart requires activation of several signaling pathways, directly or indirectly. The main cellular sources of mitogens and ligands that activate cardiomyocyte proliferation appear to be the endocardium and epicardium. Immediately after injury, as early as 1 hour post amputation (hpa), the endocardium upregulates expression of aldehyde dehydrogenase 1 family, member a2 (*aldh1a2*), which is the rate-limiting factor in production of the signaling molecule retinoic acid, in an organ-wide fashion (Kikuchi et al. 2011). Already at 1 day post amputation (dpa), *aldh1a2* expression is limited to regions close to the wound area (Kikuchi et al. 2011). The production of retinoic acid is essential for cardiomyocyte proliferation since overexpression of *cyp26a*, a retinoic acid degrading enzyme, blocks cardiomyocyte proliferation. Retinoic acid is also produced by the epicardium in a similar organ-wide

manner by 3 dpa (Kikuchi et al. 2011; Lepilina et al. 2006). The epicardium and epicardial-derived cells are major sources of growth factors and extracellular matrix proteins (Masters and Riley 2014). By 3 dpa, epicardial cells undergo EMT which results in perivascular supportive cells and fibroblasts that invade into the wound tissue (Lepilina et al. 2006). These perivascular cells produce Neuregulin 1 (Nrg1), which is a potent activator of cardiomyocyte proliferation (Gemberling et al. 2015). Epicardial cells are also sources of the Sonic hedgehog ligand (Shha) which plays a pro-proliferative role in cardiomyocytes (Choi et al. 2013; Sugimoto et al. 2017). Furthermore, spatially resolved transcriptomics revealed activation of Bone Morphogenetic Protein (BMP) signaling in border zone cardiomyocytes which is essential for cardiomyocyte proliferation (Wu et al. 2016). In addition, myocardial activation of NF- κ B signaling was found as early as 1 dpa but peaked by 2 weeks after amputation and is also required for cardiomyocyte cell cycle re-entry (Karra et al. 2015). Many additional pathways, such as Transforming Growth Factor β (TGF β), Notch and Igf signaling, were also shown to promote cardiomyocyte proliferation and scar removal (Chablais and Jazwinska 2012, Zhao et al. 2014, Huang et al. 2013).

Several other signaling pathways affect the process of revascularization, which supports cardiomyocyte proliferation. Re-vascularization is rapid and begins as early as 6 hours post cryoinjury (hpi) (Marín-Juez et al. 2016). This is dependent on the vascular endothelial growth factor aa (Vegfaa). Overexpression of a dominant negative version of Vegfaa in the heart blocks endothelial proliferation, in addition to suppressing cardiomyocyte proliferation. Similarly, upon macrophage depletion, there is a reduction in cardiomyocyte proliferation presumably due to revascularization defects and failure to remove necrotic tissue from the injured area (Lai et al. 2017).

The Wnt/ β -catenin signaling pathway

The Wnt/ β -catenin signaling pathway plays multiple functions during embryonic development, adult homeostasis, and tissue regeneration (MacDonald et al. 2009, Logan and Nusse 2004). Its name comes from a family of proteins, the Wnt proteins, which act as secreted ligands, and from the downstream effector molecule, β -catenin (Willert and Nusse 2012, Clevers and Nusse 2012). In the absence of an active Wnt ligand, β -catenin is phosphorylated by a cytoplasmic complex (the “destruction complex”) composed of two serine/threonine kinases, namely Glycogen synthase kinase 3 β (Gsk3 β) and Casein kinase 1 (Ck1), the scaffolding protein Axin and the tumor suppressor Adenomatous polyposis coli (Apc) (Figure 2) (Angers and Moon 2009, Stamos and Weis 2013). Phosphorylated β -catenin is ubiquitinated and targeted for degradation via the proteasome (MacDonald et al. 2009, Clevers and Nusse 2012, Behrens et al. 1996, Kimelman and Xu 2006). If active Wnt ligands are secreted, they interact with Frizzled (Fzd) receptors and the coreceptor Low-density lipoprotein receptor-related proteins 5/6 (Lrp5/6) (Angers and Moon 2009, MacDonald and He 2012). Lrp5/6 is then phosphorylated by Gsk3 β and Ck1, and this event recruits the cytoplasmic scaffolding proteins Dishevelled (Dvl) and Axin to the receptor, leading to deactivation of the destruction complex and thus inhibition of β -catenin phosphorylation (Figure 2) (Angers and Moon 2009). This results in β -catenin stabilization and its translocation into the nucleus. Nuclear β -catenin regulates target gene expression by forming a complex with transcription factors of the T cell factor (Tcf)/Lymphoid enhancer factor (Lef) family (MacDonald et al. 2009, Angers and Moon 2009, Cadigan and Waterman 2012). Wnt/ β -catenin signaling is under negative regulation by many extracellular inhibitors of the pathway, which act by binding either to Wnt ligands, such as secreted Frizzled-related proteins (sFrps), or to the Lrp5/6 coreceptor, such as Dickkopf (Dkk) (Moon et al. 2004).

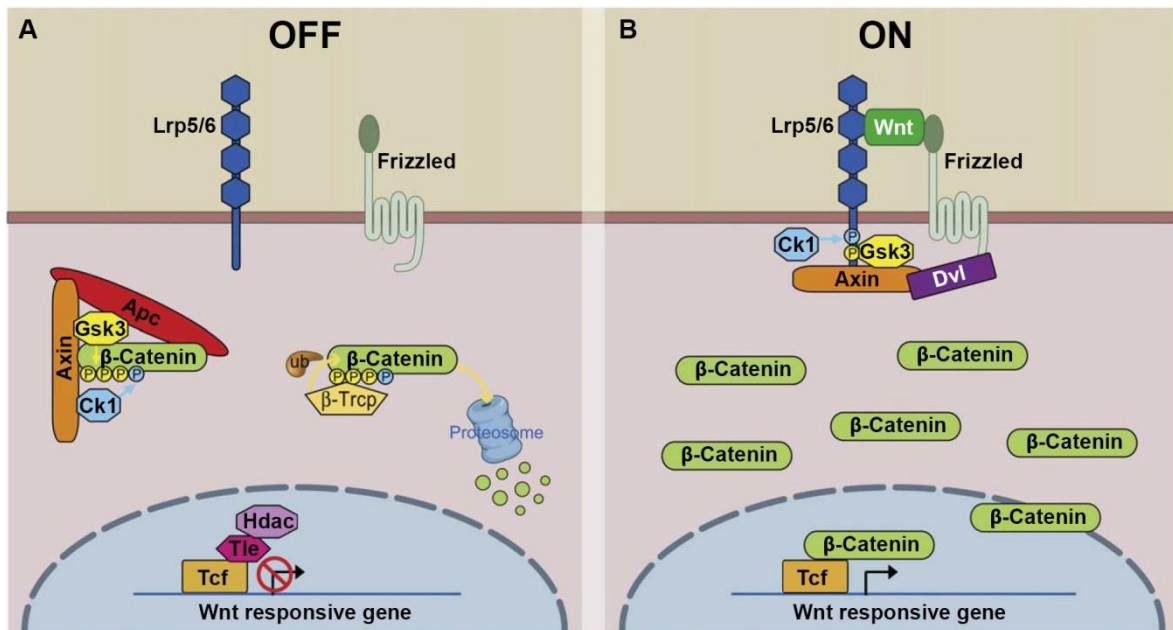


Figure 2. The Wnt/β-catenin signaling pathway

Shown is a simplified overview of signaling events and protein interactions in the absence (A) or in the presence (B) of Wnt ligands. In the inactive state (A), β-catenin is phosphorylated by the destruction complex (formed from the two kinases Gsk3 and Ck1, the scaffolding protein Axin, and the tumor suppressor Apc) and degraded by ubiquitin-mediated proteolysis. In the active state (B), secreted Wnt ligands bind to Frizzled receptors and the Lrp5/6 coreceptor. Phosphorylation of Lrp5/6 by Gsk3 and Ck1 recruits Dvl and Axin to the ligand-bound receptors, inhibiting the destruction complex. This, in turn, prevents β-catenin phosphorylation and results in β-catenin stabilization in the cytoplasm. Stabilized β-catenin is translocated into the nucleus, where it regulates target gene expression together with the Tcf/Lef transcription factors. (Reprinted from *Developmental Cell*, Vol. 17, MacDonald B.T., Tamai K., He X., Wnt/β-Catenin Signaling: Components, Mechanisms, and Diseases, Pages 9-26, © (2009), with permission from Elsevier).

Wnt signaling in repair and cardiac development

Wnt signaling is induced in different organs by disparate types of injury, such as planarian transection (Petersen and Reddien 2009), exposure to ionizing radiation (Gurung et al. 2009) and inhalation of hazardous chemicals into the airway (Villar et al. 2011, Beers and Morrisey 2011). In organs with high regenerative capacities, inhibition of Wnt signaling blocks the repair response. For instance, Wnt signaling has been implicated in hydra head regeneration (Galliot and Chera 2010), newt lens (Hayashi et al. 2008) and amniote retina regeneration (Kubo and Nakagawa 2008), mammalian pancreas regeneration (Figeac et al. 2010) and lung repair (Zhang et al. 2008). The Wnt pathway is active also during blastema formation in both zebrafish fin regeneration and urodele limb regrowth after amputation,

where it regulates tissue organization and is required for differentiation or proliferation of blastema cells (Yokoyama et al. 2007, Poss et al. 2000, Wehner et al. 2014, Stoick-Cooper et al. 2007). Taken together, these studies demonstrate that endogenous Wnt signaling is generally required for tissue repair. Even in organs with limited regenerative capacity, Wnt signaling is still usually necessary for the healing process, e.g. after skeletal fracture (Chen et al. 2007, Kim et al. 2007, Leucht et al. 2008) and skin wounding (Ito et al. 2007). In the infarcted rodent heart, several studies have shown induced expression of Wnt ligands and of the feedback regulators Dkk1 and Dkk2 (Aisagbonhi et al. 2011, Duan et al. 2012). Wnt signaling has been reported to induce a pro-fibrotic response to cardiac ischemia, via inducing epithelial- and endothelial-mesenchymal transition and production of myofibroblasts, even though scar deposition was important to prevent myocardial ruptures due to the sudden loss of cardiac muscle (Aisagbonhi et al. 2011, Chen et al. 2004, Zelarayán et al. 2008, Duan et al. 2012). In addition, Wnt/ β -catenin was also found to increase infarct size and worsen cardiac performance, since it prevents progenitor cells from differentiating into new mature cardiomyocytes (Zelarayán et al. 2008, also reviewed in Bastakoty and Young 2016). Another study reported that injection of Wnt3a into infarcted mouse hearts results in lower proliferation of the cardiac side population (Oikonomopoulos et al. 2011). Taken together, these data point to a detrimental role of Wnt/ β -catenin to heart repair after MI (also reviewed in Ozhan and Weidinger 2015).

In addition to functions in tissue repair, Wnt signaling is implicated also in whole-body patterning and organ specification during embryogenesis (Huelsken and Birchmeier 2001). Beside many other organs, Wnt/ β -catenin is essential also for vertebrate heart development (Lickert et al. 2002). Several studies in zebrafish and mouse embryos, as well as in mouse and human embryonic stem cells (hESCs), have identified temporally distinct roles for Wnt/ β -catenin signaling during vertebrate heart development. The pathway induces cardiac specification during early developmental stages, whereas it inhibits cardiomyocyte differentiation at later stages (Gessert and Kühl 2010, Ueno et al. 2007, Klaus et al. 2007, Naito et al. 2006, Paige et al. 2010). Wnt/ β -catenin signaling might also positively regulate proliferation during heart development, since it induces cell cycle re-entry of neonatal or adult rat cardiomyocytes *in vitro* (Tseng et al. 2006) and promotes cardiac precursor cell proliferation *in vivo* (Heallen et al. 2011).

Motivation and aim of the study

Does cardiomyocyte proliferation fully restore the pre-injury cardiomyocyte number in the zebrafish heart?

While scar-free healing is an important aspect of regeneration, full restoration of pre-injury cell numbers is certainly equally important. Zebrafish heart regeneration has been stipulated to be “complete” in many publications, but it has actually not been shown whether the full number of pre-injury cardiomyocytes is restored. One reason for this is that it is not trivial to assess the extent of regeneration in the heart since, unlike for example in an amputated limb or fin, the original injury plane is not visible anymore in the regenerated organ and cannot be standardized to occur at a defined location (Figure 3). Thus, it is not possible to quantify the amount of regenerated myocardium directly in the same heart, and all studies on zebrafish heart regeneration have so far relied on indirect evidence for myocardial regeneration, e.g. restoration of the area covered by muscle tissue to pre-injury levels (Poss et al. 2002), disappearance of wound tissue (Poss et al. 2002, Chablais et al. 2011, Gonzalez-Rosa et al. 2011, Schnabel et al. 2011), cell cycle activity of cardiomyocytes (Poss et al. 2002, Chablais et al. 2011, Gonzalez-Rosa et al. 2011, Schnabel et al. 2011, Wang et al. 2011, Sallin et al. 2015, Wu et al. 2016) and expansion of genetically labelled clones of cardiomyocytes (Kikuchi et al. 2010). However, it is unknown whether and to which extent cardiomyocyte hypertrophy, which is a major response to heart injury in mammals (Zebrowski et al. 2013), could also contribute to these processes in the injured zebrafish heart.

Another puzzling issue in zebrafish heart regeneration is that cardiomyocyte cell cycle re-entry and wound size do not fully correlate. While the rate of cycling cardiomyocytes peaks around 7 dpi and then declines gradually, reaching baseline by 30 dpi, wound healing usually requires a longer time, between 60 and 130 days depending on the study (Chablais et al. 2011, Gonzalez-Rosa et al. 2011). This apparent discrepancy between the dynamics of cardiomyocyte cell cycle re-entry and wound resorption could either indicate that wound size is not a good proxy for the extent of cardiomyocyte regeneration or that cardiomyocytes do not fully regenerate to pre-injury numbers.

In this work, we set out to clarify this open question, employing cardiomyocyte counting to quantify the true extent of zebrafish cardiomyocyte restoration and myocardial regeneration.

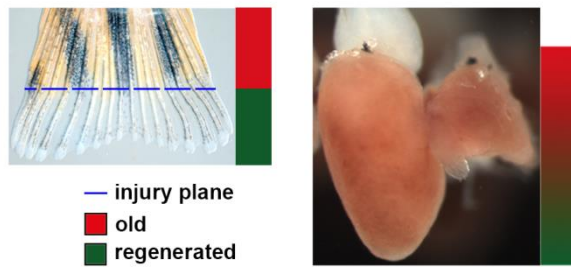


Figure 3. Old and new tissue in the regenerating zebrafish fin and heart

In the zebrafish fin, old (red) and regenerating (green) tissue can be easily distinguished based on pigmentation of the tissue and position of the amputation plane along the long axis of the fin. In the heart, position of the initial wound border is unknown, thus old and regenerated myocardium cannot be unambiguously distinguished.

Is Wnt signaling involved in zebrafish heart regeneration?

Heart regeneration is a complex mechanism that requires several processes such as dedifferentiation, proliferation and patterning to take place in concert in a highly regulated manner. Wnt/ β -catenin signaling is crucial for orchestration of the regeneration process in other organs, such as in the zebrafish fin and in planarian (Wehner et al. 2014, Reuter et al. 2015). Although a large amount of data shows that Wnt/ β -catenin has an important role in mammalian cardiac remodeling in response to injury, its potential role in organisms truly capable of heart regeneration remains to be investigated. In particular, the aim of this work was to study whether its role is similar or different to the functions that Wnt signaling plays after MI in mice, i.e. a factor promoting scar deposition while inhibiting restoration of new cardiomyocytes. Naturally regenerating species such as zebrafish provide an excellent experimental model to address these questions, combined with the available tools to achieve genetic manipulation at ease.

Materials and methods

Reagents and Buffers

Phosphate Buffered Saline: 1.7 mM KH_2PO_4 , 5.2 mM Na_2HPO_4 , 150 mM NaCl , pH 7.4

Phosphate buffer: 0.1 M $\text{Na}_2\text{HPO}_4 \cdot 2\text{H}_2\text{O}$, 18.8 μM $\text{NaH}_2\text{PO}_4 \cdot \text{H}_2\text{O}$ in H_2O , pH 7.4

PEM: 80 mM Na-Pipes, 5 mM EGTA, 1 mM $\text{MgCl}_2 \cdot 6\text{H}_2\text{O}$, pH 7.4

PEMTx: 0.2 % Triton X-100 in PEM

PEMTx/NCS: 89 % PEMTx, 1% DMSO, 10% Newborn Calf Serum

Sodium citrate buffer: 10 mM sodium citrate (tri-sodium citrate dihydrate), pH 6.0

E3 embryo medium: 5 mM NaCl , 0.17 mM KCl , 0.33 mM $\text{CaCl}_2 \cdot 2\text{H}_2\text{O}$,
0.33 mM $\text{MgSO}_4 \cdot 7\text{H}_2\text{O}$, 0.2% (w/v) methylene blue, pH 6.5

Paraformaldehyde fixative: 4% paraformaldehyde in 0.1 M phosphate buffer, pH 7.4

4% Sucrose solution: 4% (w/v) sucrose in 0.1 M Phosphate buffer

30% Sucrose solution: 30% (w/v) sucrose in 0.1 M Phosphate buffer

DAPI: 10 mg/ml stock solution (Sigma) diluted 1:10,000 in PEM

Tricaine solution (24x): 0.4% (v/w) Tricaine in 15 mM Tris, pH 7

Bouin's solution: Sigma #HT10132

Phosphomolybdic acid: Sigma #HT153

Mounting medium for fluorescence: Vectashield (Hard Set) H-1400, Vector

Tricaine methanesulfonate (MS-222): Sigma #E10521

Tissue freezing medium (TFM): NEG-50 colorless, Thermo Scientific

Drugs

Nocodazole: Sigma #M1404

IWR-1: Sigma #I0161

Retinoic acid: Sigma #R2625

DEAB: Sigma #D86256

Citral: Sigma #C83007

Dexamethasone: Sigma #D1756

Doxycycline: Sigma #D9891

Fish lines and husbandry

All experiments using adult zebrafish have been approved by the state of Baden-Württemberg (Tierversuch Nr. 1193 and 1352) and the animal protection representative of Ulm University. Zebrafish of ~ 6 to 12 months of age were used. The following previously published transgenic fish lines were used: *fli1a:eGFP^{y1Tg}* (Lawson and Weinstein 2002), - *14.8gata4:GFP^{ae1}* (Heicklen-Klein and Evans 2004), *coro1a:eGFP^{hkz04tTg}* (Li et al. 2012), *myl7:GFP^{twu34Tg}* (Huang et al. 2003), *hsp70l:Axin1^{w35Tg}* (Kagermeier-Schenk et al. 2011), *hsp70l:dkk1b-GFP^{w32Tg}* (Ueno et al. 2007), *hsp70l:wnt8a-GFP^{w34Tg}* (Weidinger et al. 2005), *HSE:Xla.Cttnb-MYC,EGFP^{w75Tg}* (Veldman et al. 2013), *fli1a:nEGFP^{y7Tg}* (Roman et al. 2002), *kdrl:EGFP^{s843Tg}* (Jin et al. 2005), *myl7:H2B-GFP^{zf521Tg}* (Mickoleit et al. 2014), *myl7:TETA-GBD-2A-mCherry^{tud3Tg}* (Knopf et al. 2010), *myl7:TETAM2-2A-mCherry^{ulm8Tg}* (Wehner et al. 2015), *TETRE:Mmu.Axin1-YFP^{tud1}* (Knopf et al. 2010), *OTM:d2EGFP^{kyu2Tg}* (Shimizu et al. 2012), *top:GFP^{w25Tg}* (Dorsky et al. 2002), and - *5.1myl7:DsRed2-NLS^{f2Tg}* (Mably et al. 2003).

Zebrafish embryos were collected shortly after fertilization and housed in an incubator at 28.5 °C in embryo E3 medium until 6 days post fertilization (dpf), then they were transferred in our housing facility. Zebrafish housing conditions in the facility for all fish irrespective of age were as follows: 27 °C water temperature, pH 7.4, 14/10 h light/dark cycle, ~6-10 fish per liter.

Cryoinjury, heat-shocks and drug treatment

Cryoinjury was performed as reported before (Wu et al. 2016). Fish were anesthetized with 0.02% Tricaine (MS-222) and transferred to a moist sponge for surgery. An incision through the body wall and the pericardial sac was made anteriorly to the posterior medial margin of the heart with a pair of straight iridectomy scissors, reaching about 2/3 of the length of the heart. The incision was spread open with a pair of fine forceps. The ventricle was exposed by gently pressing against the sides of the fish. A liquid nitrogen-cooled copper filament of 0.5 mm diameter was applied to the apex of the ventricle for around 15 seconds to cause the cryoinjury. After surgery, the fish were returned to fish system water. To revitalize the fish a pipette was used to vigorously squirt water over the gills until the fish started to breathe regularly. Fish were then returned to circulating water in the housing facility after recovery. For sham operations, fish were treated the same way in which the pericardial sac was opened but the heart left untouched.

For experiments involving heat-shock inducible gene expression, fish were incubated at 37°C for 1 hour in a heat shock tank, after which the water temperature was reduced back to 27°C within 15 minutes. For short-term heat shock regimes, fish were heat shocked once at 7 dpi; for long-term heat shock regimes, fish were heat-shocked once daily.

Nocodazole (Sigma M1404) and IWR-1 (Sigma I0161) were reconstituted in DMSO at 33 mM and 10 mM, respectively. Stock solutions of 100 mM retinoic acid (Sigma R2625), 250 mM DEAB (Sigma D86256), 250 mM Citral (Sigma C83007) and 25 mM dexamethasone (Sigma D1756) were prepared in 100% ethanol, while doxycycline (Sigma D9891) was dissolved in 50% ethanol at the final concentration of 50 mg/ml. All stock solutions were stored at -20 °C in the dark. For treatment by soaking, fish were kept in an incubator at 25 °C in the dark at ~ 1 fish / 100 ml density in fish system water, and drugs were exchanged daily. Drugs were used at the following final concentration: nocodazole, 5 µM; retinoic acid, 5 µM; DEAB, 10 µM; Citral, 50 µM; dexamethasone, 100 µM; doxycycline, 25 µg/mL. For retinoic acid, DEAB and Citral treatment, fish in the control group were incubated in the same conditions with the respective equivalent concentration of ethanol. EdU (10 mM in PBS) and IWR-1 (diluted 1:10 in PBS at the final concentration of 1 mM) were administered by intraperitoneal injection of 20 µl for each fish. For IWR-1 treatment, fish in the control group were injected with an equal volume of 10% DMSO/PBS.

Tissue fixation and sectioning

For immunofluorescence and histological staining, hearts were extracted, fixed in 4% paraformaldehyde (PFA) (in phosphate buffer) at room temperature for 1 h, washed three times for 10 min in 4% sucrose/phosphate buffer and equilibrated in 30% sucrose (in phosphate buffer) overnight at 4 °C. Hearts were then embedded into tissue freezing medium and cryosectioned into 10 µm sections.

For quantitative regeneration experiments, hearts were sectioned with a random orientation to ensure that no stereological bias was introduced in our analysis. Heart sections were equally distributed onto six or its multiples serial slides so each slide contained sections representing all areas of the ventricle.

Immunofluorescence and histological staining

DsRed in *-5.1myl7:DsRed2-nls* transgenic fish was detected by imaging of native DsRed fluorescence. All other markers were detected via immunofluorescence. Immunostainings were performed as previously described (Wu et al. 2016). The sections were washed three times in PEMTx for 10 min and blocked with PEMTx/NCS for 1 h at room temperature in a humidified chamber. For PCNA and Mef2c, antigen retrieval was performed by heating slides containing heart sections at 85 °C in 10 mM sodium citrate buffer (pH 6.0) for 10 min before the blocking step. After blocking the primary antibodies were applied at 4 °C in a humidified chamber overnight. The slides were washed again in PEMTx three times for 15 min. Secondary antibodies were applied and the slides were incubated for 1 h at room temperature in a humidified chamber, followed by three steps of washing 10 min each in PEMTx. Nuclei were counterstained by incubation with DAPI solution for 10 min. Finally the slides were mounted with Vectashield anti-fade mounting medium and cover glasses.

Primary antibodies used were anti-aldh1a2 (Abmart #P30011), anti-PH3 (Cell-Signaling #9706), anti-dsRed (Clontech #632496), anti-PCNA (Dako #M0879), anti-GFP (Abcam #ab13970), , anti-laminin (Sigma-Aldrich, #L9393), anti-MF20 (Developmental Studies Hybridoma Bank), anti-Myh7 (Developmental Studies Hybridoma Bank #AB_531790), anti-Myl7 (Genetex#GTX128346) and anti-Mef2c (Santa Cruz #SC313). Secondary antibodies conjugated to Alexa 488, 555 or 633 (Invitrogen) were used at a dilution of 1:1000. Nuclei were shown by DAPI (4',6-diamidino-2-phenylindole) staining.

EdU staining was performed using the Edu-Click 647 kit according to the manufacturer's instructions (Baseclick).

Acid fuchsin orange G (AFOG) staining was performed on cryosections as previously described (Poss et al. 2002). In brief, after drying slides at RT for 1 h, they were incubated in pre- heated (60 °C) Bouin's solution (Sigma) for 2 h, followed by incubation at RT for an additional hour. Slides were then rinsed in slowly running water for 30 min and rinsed in 1% Phosphomolybdic acid (Sigma) for 5 min. Slides were then rinsed in H₂O for 5 min and stained with AFOG solution (1 g aniline blue, 2 g orange G and 3 g acid fuchsin in 200 ml H₂O, pH 1.09) for 5 min. Afterwards, slides were rinsed in H₂O for two min and dehydrated by incubating two times in 95% EtOH and then two times in 100% EtOH (5 min each). Slides were then washed two times in Xylen (2 min each) and mounted in pertex (Medite).

***In situ* hybridization**

RNAscope *in situ* hybridization (ACDBio) was performed on cryosectioned hearts according to the manufacturer's protocol for fixed frozen sections (RNAscope Multiplex Fluorescent Assay v2, Cat. No. 323100), except without target retrieval pretreatment.

Probes used were *axin2* (Cat. No 465351), *dkk1b* (Cat. No. 523391), *aldh1a2* (Cat. No. 455681), *egfp* (Cat. No. 400281), *sp5a* (Cat. No. 487271), *sp5l* (Cat. No 487281) and *wnt9a* (Cat. No 525351).

Quantitative PCR

Hearts were extracted and homogenized with Minilys tissue homogenizer (Bertin). RNA was then extracted using the RNeasy fibrous tissue mini kit (Qiagen) as per the manufacturer's instructions. cDNA was synthesized using iScript Advanced cDNA Synthesis Kit for RT-qPCR (Bio-Rad) as per the manufacturer's instructions. qPCR was performed in duplicate for each sample using SsoAdvanced Universal SYBR Green Supermix (Bio-Rad). C(t) values were normalized to 18S rRNA expression levels and fold change was calculated using the $2^{-\Delta\Delta C_t}$ method (Livak and Schmittgen 2001).

The following primers were used for qPCR:

18S rRNA (fw): CGCTATTGGAGCTGGAATTACC

18S rRNA (rv): GAAACGGCTACCACATCCAA

lef1 (fw): TAAGTATTACGAATTAGCCCGCAAG
lef1 (rv): CTAGCAGGCTTCCATCTCTAAAAG
axin2 (fw): CCAATGACAGTGAAGTTTCTAGTGA
axin2 (rv): CTCCAGTCTGGCTATCAACTGTG
wnt2ba (fw): TCGAGATTACAAGAGAACGACCAAA
wnt2ba (rv): ATTTGGTCATGCGGTTTACACG
wnt3 (fw): AGGACAGTCTAGCAATATTTGGACC
wnt3 (rv): CTTTATGATGGGAGTCACAGCCACA
wnt3a (fw): GTCATGGCAAGCTACCCGATATG
wnt3a (rv): GCCAGGAATTGAGCTACACATTATG
wnt4a (fw): ATTCCACTAAAGATGTCATCGGAGT
wnt4a (rv): ACCTCCACATTACGTTTACAGATCT
wnt5a (fw): TAGGAGAGTCTTGTTATGATGCTGC
wnt5a (rv): CGATCACATACTTCAGGAATCAG
wnt5b (fw): CAGAACAATGAAGCCGGAAGAAT
wnt5b (rv): AGCTCTAGTTTTCCACGTCGG
wnt7ba (fw): ACGTCAAATATGGAGTGGAGTTCTC
wnt7ba (rv): ACCATGACATTTACATTCCAGCTTC
wnt8a (fw): AAAATGGATCATCTGTGCAGCAAG
wnt8a (rv): CATATAGACATAACCAACGACGCAA
wnt9a (fw): CCATTATAGTGCATCTGATCAGCCT
wnt9a (rv): TGCTTCTTTTCCAGTTTGAGTCGAT
wnt9b (fw): CGCCCAGATTGACGCACATAACATA

wnt9b (rv): GCTGTGTCATAGCGGTA CTTCAACA

wnt10a (fw): CGAGACGTACAGAGACATTCACT

wnt10a (rv): CATTTCGATTTCCCTCCTCATGTGG

wnt11 (fw): CGGTTGGAGAGAATGAACTAGTC

wnt11 (rv): ACCTCTGTGTAGGCATTATAACCC

wnt16 (fw): CCAAACCTCAGTTCAGACACGAAC

wnt16 (rv): ATGGATGAACGCTGTCTCTTTAGTC

Imaging

All images of immunofluorescence stainings are single optical planes acquired at 20X magnification with Leica Sp5 or Sp8 confocal microscopes. For wound size quantification and for quantitative regeneration experiments, widefield fluorescent images were acquired at 10X magnification with a Keyence microscope, and z-stack images were acquired at 63X magnification with a Leica SP5 confocal microscope.

Cardiomyocyte number quantifications

For quantitative regeneration experiments, all sections on 1/6th of the slides, over which the sections of each heart were distributed, were analyzed. If heart sections were distributed on 12 or 18 slides, 2 or 3 non-consecutive slides were selected, respectively. Image analysis was performed with ImageJ. Ventricle and wound area, as well as base and apex regions, were defined manually based on overlay of DsRed2 and DAPI fluorescence or on AFOG staining. Automatic quantification of cardiomyocyte number was performed using the Find Maxima function. Noise tolerance was set to a value which creates a single point selection for each cardiomyocyte nucleus based on native DsRed2 fluorescence, while giving no false positive selections in the background. Imaging conditions and noise tolerance parameters were kept constant within the same experimental pool, as well as among the three main experiments with different final time-points. Estimation of the total number of cardiomyocytes in the whole ventricle was performed by multiplying the measured number of cardiomyocytes by 6 (since we analyzed 1/6th of sections) and by multiplying with 0.715, a factor designed to correct for the fact that a certain number of cardiomyocyte nuclei are shared between adjacent sections, since they were cut through. To determine this correction factor, 50 μ m thick cryosections were imaged to produce confocal stacks of the

entire section, and the number of nuclei within a virtual 10 μm -thick sub-stack was manually counted. Cardiomyocyte nuclei present in the first and last optical plane of the sub-stack were considered severed if they were detected also in the adjacent optical planes of the original 50 μm stack. This analysis showed that 57% of the cardiomyocyte nuclei are cut through and thus shared between sections, while 43% are not shared between sections. All shared cardiomyocytes in the bottom optical plane (half of the cut cardiomyocytes, i.e. 28.5%) were assigned to the same analyzed sub-stack, while all shared cardiomyocytes in the top optical plane (the other 28.5%) were assigned to the optical planes above the sub-stack. Thus only 43% plus 28.5% (71.5%) of all counted cardiomyocytes were considered unique to a 10 μm -thick sub-stack, and therefore the same ratio was applied to correct the number of cardiomyocytes in each physical 10 μm section. Total ventricle volume was estimated by multiplying the measured ventricular area by $6 \times 10 \mu\text{m}$. For comparison of manual and automatic counting and for analysis of superimposed cardiomyocyte nuclei, a $150 \times 150 \mu\text{m}$ region was randomly selected in 1-2 sections from 3-4 hearts. Manual and automatic counting of confocal images was performed on maximum projections of z-stacks. Superimposed cardiomyocytes were quantified by analyzing overlapping nuclei in two focal planes 5 μm apart of z-stack confocal images.

Quantification of cardiomyocyte density and compact layer width

Cardiomyocyte density was calculated by dividing the number of cardiomyocyte nuclei by the volume containing the selected cardiomyocytes. The apex volume was defined as the entire region containing the myocardial layer that forms the external wall surrounding the remaining wound, while the base volume was defined as a $\sim 250 \mu\text{m} \times 250 \mu\text{m}$ region most distal from the apex, in close proximity to the bulbus arteriosus. Width of the myocardial compact layer was calculated by manually outlining the region of the myocardium labeled with laminin with an inner and outer line, and averaging the minimum distance between all coordinate points of the two lines. Width was measured for the compact layer surrounding the apex of the ventricle or only for the portion encompassing the wound edge, defined as the region of the regenerated myocardium which encloses any internalized wound of hearts with a remaining scar.

Modeling of cardiomyocyte regeneration time-course

Theoretical numbers of regenerated cardiomyocytes were calculated based on a timecourse for PCNA+ cardiomyocytes, according to the following equation:

$$\% CM(n) = \% CM(0) * \left[\prod_{t=0}^n (1 + F_t)^t \right]^{(1/i)}$$

where n is the time point (days post injury), t is the time interval (days) between two consecutive time points, F_t is the cardiomyocyte proliferation rate during t (calculated as the average of the PCNA+ cardiomyocyte rates at two consecutive time points flanking t), and i the cell-cycle length in days. Values were calculated assuming that all PCNA+ cardiomyocytes divide and assuming a constant cell-cycle length of 24 hours ($i=1$). Curve fitting was performed using the built-in exponential recovery function of ImageJ.

Quantification and statistical analyses

For all other quantifications, 2 to 3 sections displaying the biggest wounds were analyzed per heart. Quantifications of PCNA, EdU and PH3 expression were performed in cardiomyocytes situated within 150 μm from the wound border. For dedifferentiation assays, ImageJ was used to select and quantify the region of interest by using threshold function. Quantification of RNAscope in situ hybridization was performed automatically using the Find Maxima function in ImageJ, and number of dots (representing mRNA transcripts) was normalized to the area in μm^2 .

Measurements of the size of the wound area and of the ventricle area on sections of myosin heavy chain-immunostained sections on wild-type or transgenics hearts were performed manually with ImageJ software on all sections of one serial slide, representing approximately one-sixth of the total ventricle.

All quantifications were plotted using Prism 6 software. Error bars represent confidence intervals 95% (C.I. 95%). For testing significance between two groups, two-tailed unpaired student's t-test was used, except where otherwise indicated. For testing significance in case of multiple groups, one way ANOVA was performed which was then followed by a Tukey post hoc multiple comparison test. In figures, n.s. indicates $p > 0.05$, * indicates $p < 0.05$, ** indicates $p < 0.01$, *** indicates $p < 0.001$ and **** indicates $p < 0.0001$.

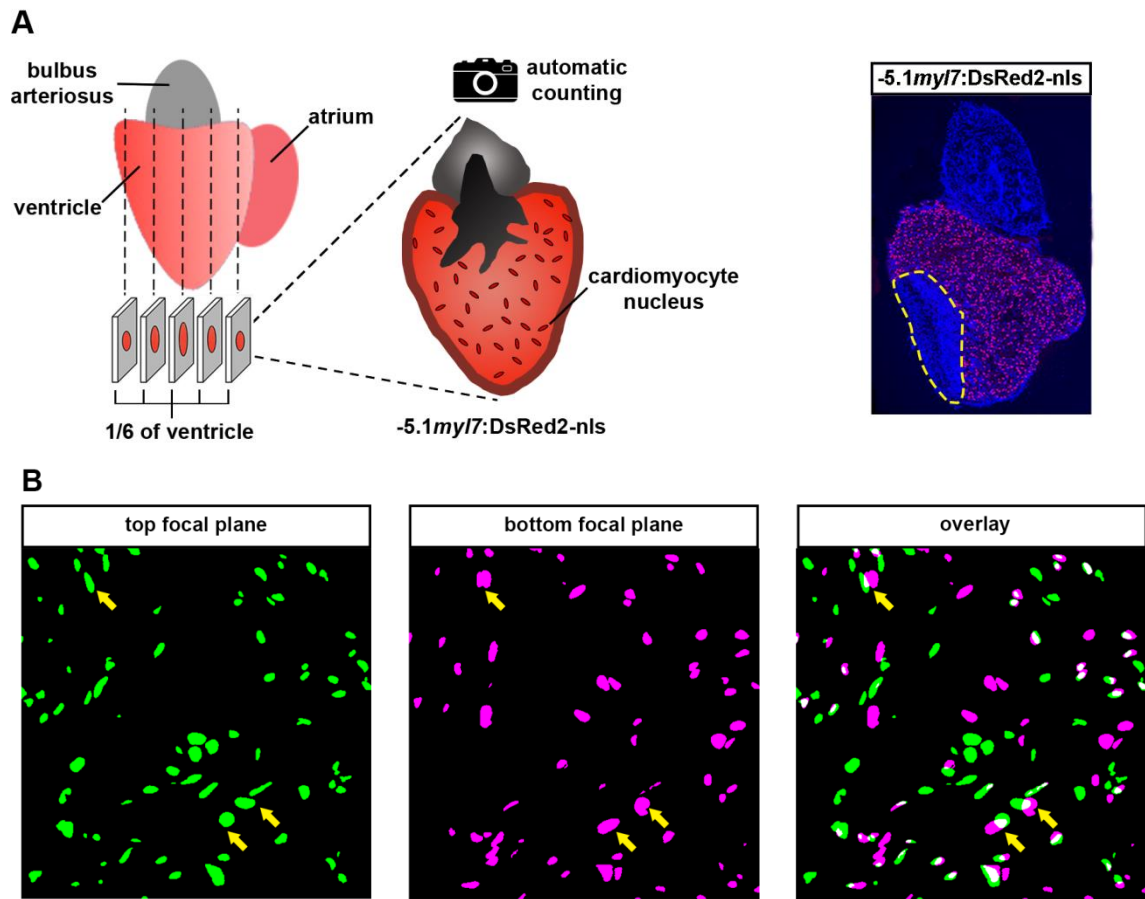
Results

Quantitative time-course of cardiomyocyte regeneration in injured zebrafish hearts

Establishment of a semi-automatic method for cardiomyocyte number quantification on cryosections

To quantify the extent of cardiomyocyte regeneration, we set out to count the absolute number of cardiomyocytes in sham injured and cryoinjured hearts after wound healing was complete. Since ~95% of adult zebrafish cardiomyocytes are mononucleated (Wills et al. 2008), we decided to determine cardiomyocyte numbers by counting cardiomyocyte nuclei labeled by DsRed expression in *-5.1myl7:DsRed2-nls^{f2Tg}* transgenic fish. We avoided counting dissociated cells since in our hands dissociation from fixed samples produced clumps and cellular debris in addition to single cells, and thus this procedure would have introduced biases in estimation of cardiomyocyte numbers. We rather counted cardiomyocytes on cryosections, using stereological methods to derive absolute cardiomyocyte numbers in the entire ventricle from the quantification performed on sections (Figure 4A). To develop a reliable method for reconstructing the total number of ventricular cardiomyocytes from heart sections, I first determined how many cardiomyocyte nuclei appear superimposed on each other in 10 μm thick sections. To do so, I acquired z-stacks of 10 μm thick sections, compared the top and the bottom optical plane of the z-stack and determined that the ratio of superimposed cardiomyocyte nuclei within the stack is low (~ 4%) and thus only few overlapping nuclei in the section would erroneously be counted as one in maximum projections of stacks or wide-field images (Figure 4B). We then concluded that 10 μm is a thickness low enough that it does not introduce a significant bias in the quantification. We then proceeded to compare manual counting and automatic counting (as described in the Materials and Methods) on images acquired with confocal or widefield microscopy. By analyzing same regions of interest in the same sections, we determined that automatic counting on images from a widefield microscope detects comparable cardiomyocyte numbers as automatic or manual counting on maximum projections of confocal z-stacks (Figure 4C). To quantify the percentage of cardiomyocyte nuclei which are severed by cryosectioning and would thus be present in 2 adjacent sections, we selected a 10 μm thick confocal substack centered in the middle of a 50 μm thick cryosection. This substack would thus represent a virtual 10 μm thick

cryosection. We then determined the total number of cardiomyocyte nuclei within the stack, plus the number of cut nuclei, according to the procedure described in the Materials and Methods. We found that on average, 57% of cardiomyocyte nuclei are severed in 10 μm -thick cryosections, and conversely 43% are not cut through (Figure 4D). This percentage was then converted into a correction factor to correctly estimate the total number of cardiomyocytes in the whole heart (described in detail in the Materials and Methods). Finally, since sectioning of adult zebrafish hearts at 10 μm thickness produces several slides from the same samples, we compared the absolute cardiomyocyte numbers derived from the analysis of all sections of individual hearts obtained from cryosectioning, with the estimate from analyzing only different subsets of slides (each representing 1/6th of all sections). We observed no significant difference in absolute numbers between the two approaches (Figure 4E), indicating that quantification performed on just a fraction of sections provides the correct estimation for the whole ventricle. Taken all these results together, we concluded that a semi-automated analysis of images of a subset of 10 μm thick cryosections acquired by widefield fluorescent microscopy represented a reliable method to determine absolute cardiomyocyte numbers.



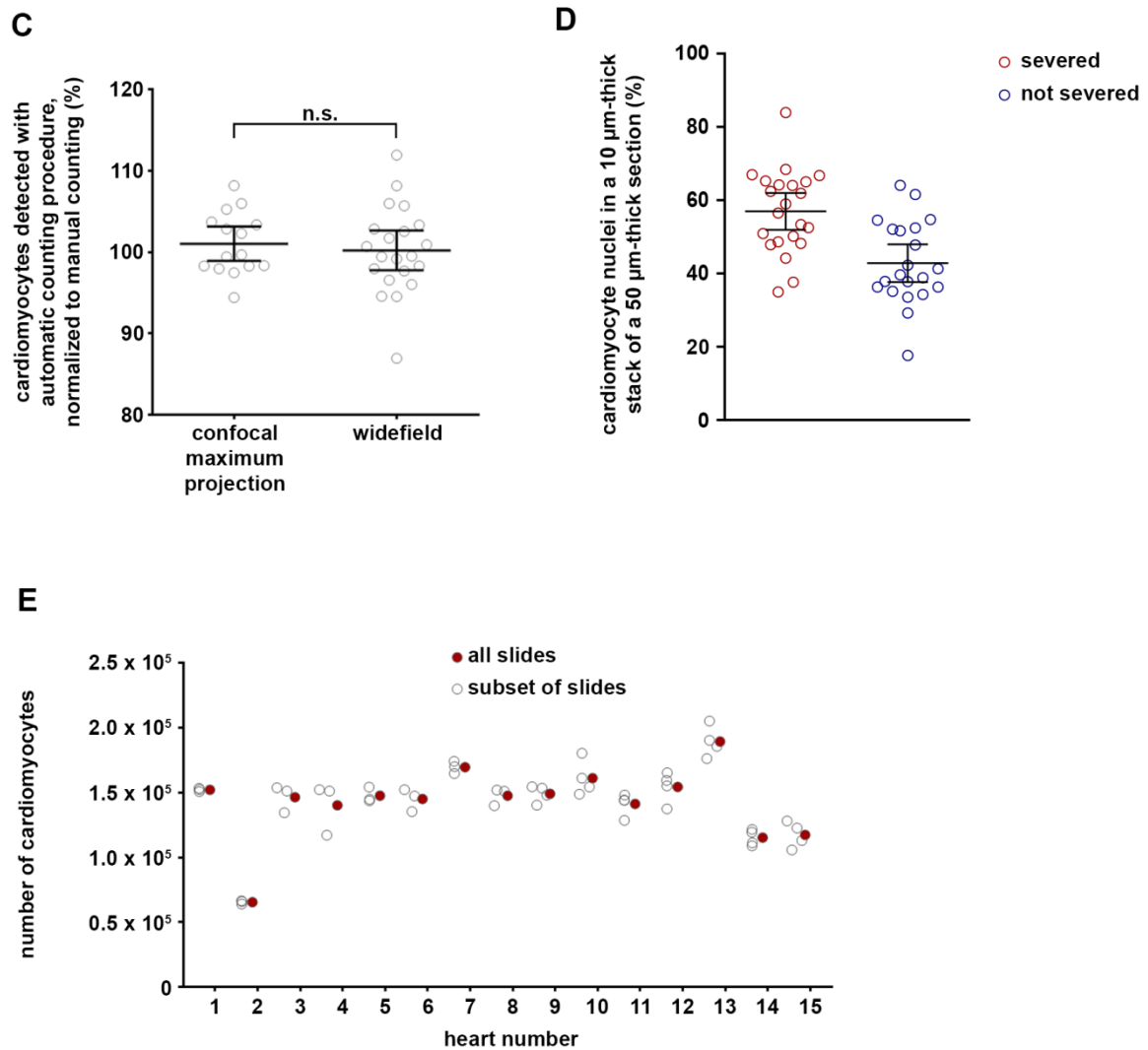


Figure 4. Establishment of a semi-automatic method for cardiomyocyte number quantification on cryosections

(A) Experimental design for quantification of cardiomyocytes. Serial sections were collected through the entire ventricle, 1/6th of the sections was imaged and the number of cardiomyocytes was determined by automatic counting of DsRed+ nuclei. Picture on the right panel shows an example of a heart of - *5.1myl7:DsRed2-nls* transgenic fish at 3 dpi (wound area is outlined with dashed yellow line).

(B) The number of cardiomyocyte nuclei that are superimposed on maximum projection confocal stacks of 10 μm heart sections is low. Nuclei were outlined in the top (green) and bottom (magenta) optical plane of a confocal z-stack of 10 μm cryosections, 6-7 μm apart from each other, and overlap regions (white) were analyzed. Distinct overlapping cardiomyocyte nuclei are marked with yellow arrows. n=3.

(C) Automatic counting using widefield microscopy images detects comparable numbers of cardiomyocytes as automatic or manual counting using confocal z-stack images (the latter normalized to 100%). Error bars, mean \pm CI 95%. n=9; unpaired two-tail t-test; n.s.: $p > 0.05$.

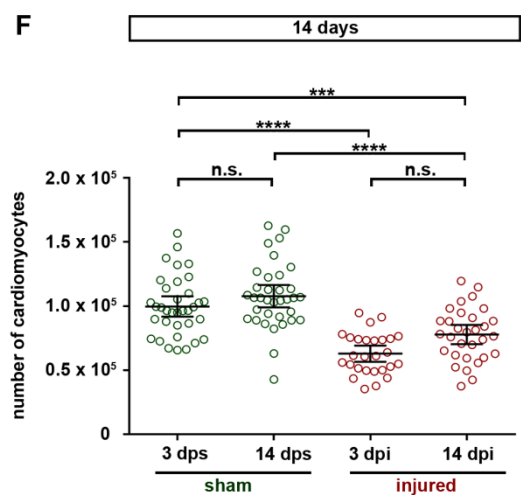
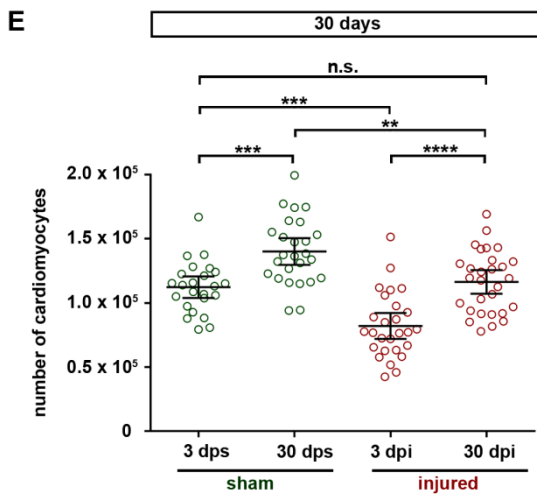
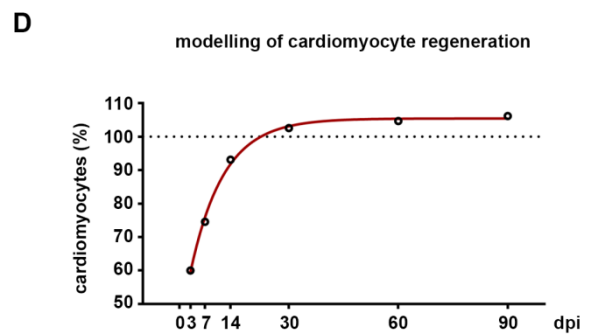
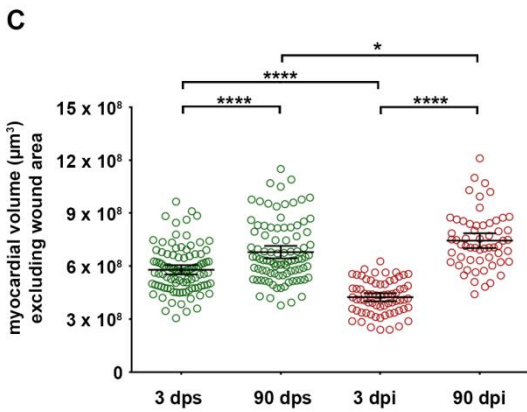
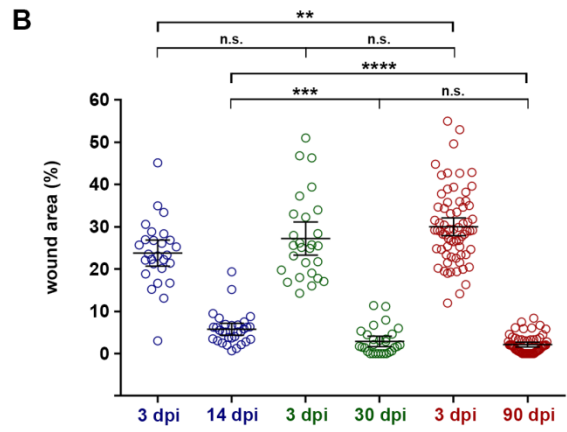
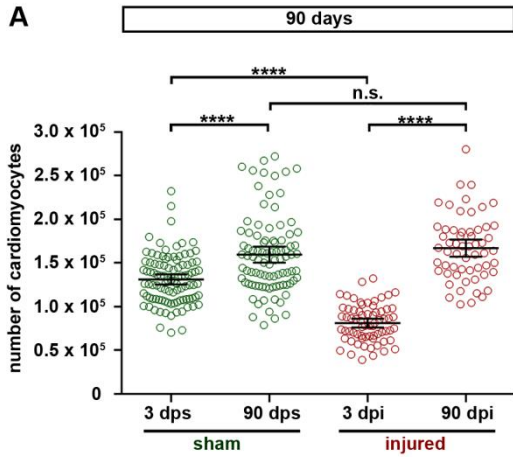
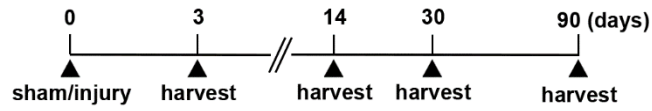
(D) The number of cardiomyocyte nuclei was determined within a 10 μm thick confocal sub-stack centered in the middle of a 50 μm thick cryosection. Nuclei that could be detected in the top or bottom z-plane of the sub-stack and at the same time in the adjacent z-plane outside the sub-stack were considered "severed", meaning that they were cut by cryosectioning. On average, 57% of cardiomyocyte nuclei are severed in 10 μm -thick cryosections, and conversely 43% are not cut through, that is they could only be detected within the substack. Error bars, mean \pm CI 95%. n=6.

(E) Subsampling does not significantly affect the estimation of total number of cardiomyocytes. Comparison of the total number of cardiomyocytes per heart estimated from different subsets of slides, each representing 1/6th of the sections of the whole ventricle, with the total number determined by counting all sections. n=15.

Cardiomyocyte numbers are fully restored during heart regeneration within 30 days

To determine cardiomyocyte numbers pre- and post-injury, we randomly assigned *-5.1myl7:DsRed2-nls^{f2Tg}* transgenic individuals from a large cohort of fish to either sham injury or ventricle cryoinjury. Within each group, fish were randomly assigned to heart extraction for analysis at 3 days post intervention, to quantify initial wound size and the number of killed cardiomyocytes in injured fish, or at 90 days post intervention, to quantify residual wound size and the number of regenerated cardiomyocytes in injured fish (Figure 5, upper panel). This end time point was chosen because wounds should have largely been resolved by then, as previously shown (Poss et al. 2002, Chablais et al. 2011, Gonzalez-Rosa et al. 2011, Schnabel et al. 2011). Control ventricles contained on average $131 \pm 5 \times 10^3$ cardiomyocytes at 3 days post sham injury (dps) (Figure 5A). In cryoinjured hearts, wound size (measured as the percentage of cardiomyocyte-negative area relative to the entire ventricle) represented $30 \pm 2\%$ of the ventricle area at 3 dpi, and the percentage of cardiomyocytes killed because of injury (represented by the relative difference in average cardiomyocyte numbers between 3 dps and 3 dpi) amounted to $38 \pm 5\%$ (Figure 5A,B). At 90 dps, cardiomyocyte numbers and the ventricular volume had increased significantly in sham injured hearts, indicating that our housing conditions stimulated cardiomyocyte hyperplasia in adult fish over this time period (Figure 5A,C). At 90 days post cryoinjury, regenerated hearts contained the same number of cardiomyocytes as sham injured hearts, and also volume of healthy myocardium was restored (Figure 5A,C). We concluded that zebrafish hearts can fully regenerate the pre-injury cardiomyocyte number. Intriguingly, at 90 dpi the average number of regenerated cardiomyocytes was $172 \pm 20\%$ of the number of cardiomyocytes lost to injury (the number of cells missing at 3 dpi, Figure 5G). Thus, 90 days post injury were sufficient not only to restore the lost

cardiomyocytes, but also to generate the same additional numbers of cardiomyocytes beyond those present at day 0 as sham injured hearts (Figure 5A). We next wondered what constitutes the minimum time frame to achieve complete cardiomyocyte regeneration. To address this, we modelled the time-course of cardiomyocyte number increase in regenerating hearts, using the assumptions that all PCNA+ cardiomyocytes actually divide, and that cardiomyocyte cell cycle length is 24 hours and constant during regeneration. We estimated that the pre-injury cardiomyocyte number should already be fully restored by 30 dpi (Figure 5D). To verify this, we repeated the same experimental procedure outlined above at 3, 14 and 30 days post sham or cryoinjury. We again observed a significant increase in cardiomyocyte numbers in sham injured hearts within 27 days (Figure 5E). Average wound area and percentage of lost cardiomyocytes at 3 dpi showed that the extent of cryoinjury was similar to the first experiment (Figure 5B,E). As predicted by our mathematical model, injured hearts at 30 dpi contained the same number of cardiomyocytes as sham injured hearts at 3 dpi (Figure 5E). $114 \pm 30\%$ of the killed cardiomyocytes at 3 dpi had been regenerated at 30 dpi (Figure 5G). Thus, complete cardiomyocyte regeneration was already achieved within four weeks, earlier than what is commonly considered the end point for zebrafish heart regeneration after cryoinjury based on morphological or functional markers (Chablais et al. 2011, Gonzalez-Rosa et al. 2011, Schnabel et al. 2011). Cardiomyocyte numbers at 30 dpi were lower than those seen in sham injured hearts at 30 dpi (Figure 5E), indicating that four weeks were just sufficient to complete cardiomyocyte regeneration, but not to induce additional hyperplasia of the myocardium. As expected from our mathematical model, at 14 dpi cardiomyocyte regeneration was only $40 \pm 20\%$ of the missing cardiomyocytes at 3 dpi (Figure 5F,G). Likewise, wounds were also still significantly bigger at 14 dpi than at 30 and 90 dpi (Figure 5B).



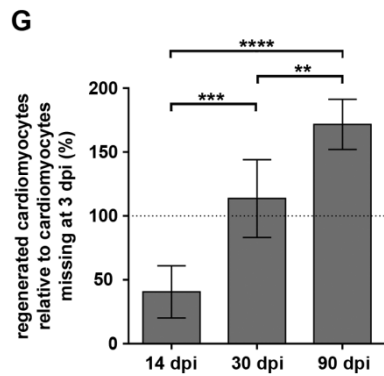


Figure 5. Cardiomyocyte numbers are fully restored during heart regeneration within 30 days

Upper panel: Experimental design for quantification of cardiomyocytes. -5.1myl7:DsRed2-nls transgenic fish were randomly assigned to two groups (sham or injury) and fish again randomly picked for heart extraction at 3, 14, 30 or 90 dpi or days post sham (dps).

(A) Cardiomyocytes regenerate to the same number as found in sham injured hearts within 90 days. The absolute total number of cardiomyocytes per heart is plotted in sham and injured fish (green and red, respectively), at 3 and 90 dps or dpi. Error bars, mean \pm CI 95%. n=99, 92, 68, 58; one-way ANOVA plus Tukey's multiple comparisons test; n.s.: $p>0.05$, ****: $p<0.0001$.

(B) Wound area at 3 dpi accounts for 25-30% of the ventricle area. The average wound area has dropped to 6%, 3% and 2% at 14, 30 and 90 dpi, respectively. Different colors indicate data from the three cohorts of fish that we injured, each with its own 3 dpi control. Error bars, mean \pm CI 95%. n=27, 31 (14 dpi group); n=27, 29 (30 dpi group); n=68, 58 (90 dpi group); one-way ANOVA plus Tukey's multiple comparisons test; n.s : $p>0.05$, **: $p<0.01$, ***: $p<0.001$, ****: $p<0.0001$.

(C) Volume of the healthy myocardium (ventricular volume minus the wound area) recovers in injured hearts to levels similar to those of sham injured hearts within 90 days. Error bars, mean \pm CI 95%. n=99, 92, 68, 58; one-way ANOVA plus Tukey's multiple comparisons test; n.s.: $p>0.05$, *: $p<0.05$, ****: $p<0.0001$.

(D) Modelling of the time-course of cardiomyocyte regeneration in response to injury that kills 38% of cardiomyocytes, based on the ratio of PCNA+ cardiomyocytes at different time points after injury and assuming a cell cycle length of 24 hours that remains constant during regeneration.

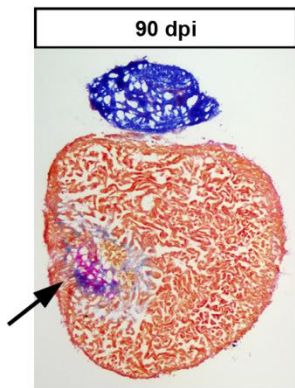
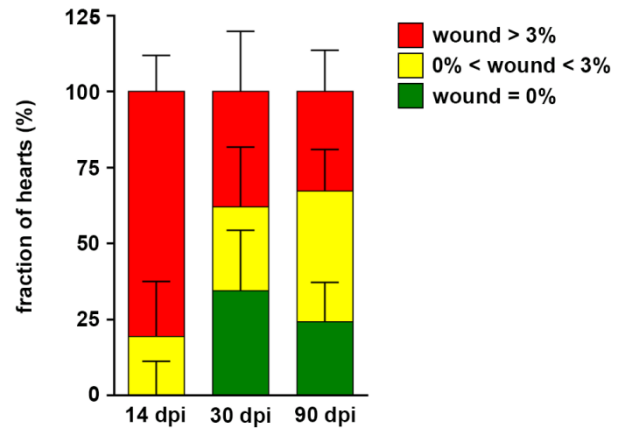
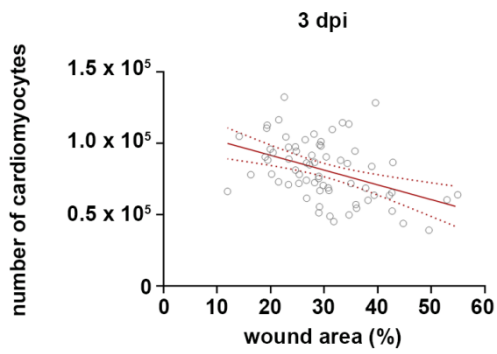
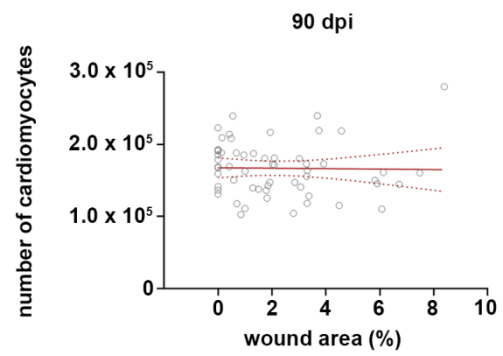
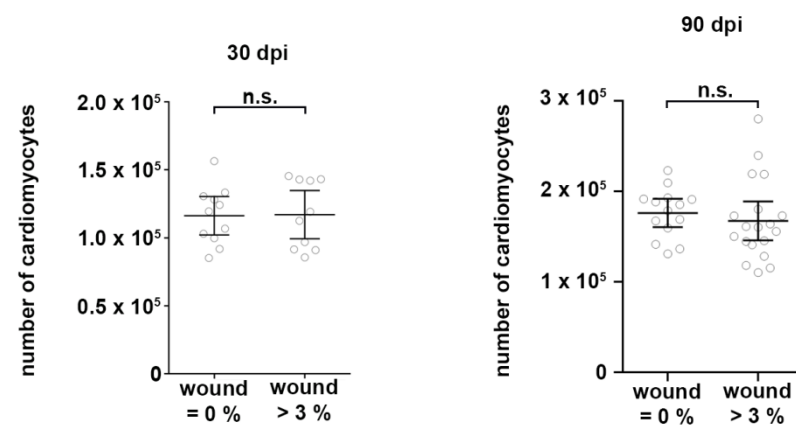
(E) Cardiomyocyte regeneration is complete already at 30 dpi. The absolute total number of cardiomyocytes per heart is plotted in sham and injured fish (green and red, respectively), at 3 and 30 dps or dpi. Error bars, mean \pm CI 95%. n=24, 26, 27, 29; one-way ANOVA plus Tukey's multiple comparisons test; n.s : $p>0.05$, **: $p<0.01$, ***: $p<0.001$, ****: $p<0.0001$.

(F) Cardiomyocyte regeneration is not complete at 14 dpi. The absolute total number of cardiomyocytes per heart is plotted in sham and injured fish (green and red, respectively), at 3 and 14 dps or dpi. Error bars, mean \pm CI 95%. n=35, 35, 27, 31; one-way ANOVA plus Tukey's multiple comparisons test; n.s : $p>0.05$, ***: $p<0.001$, ****: $p<0.0001$.

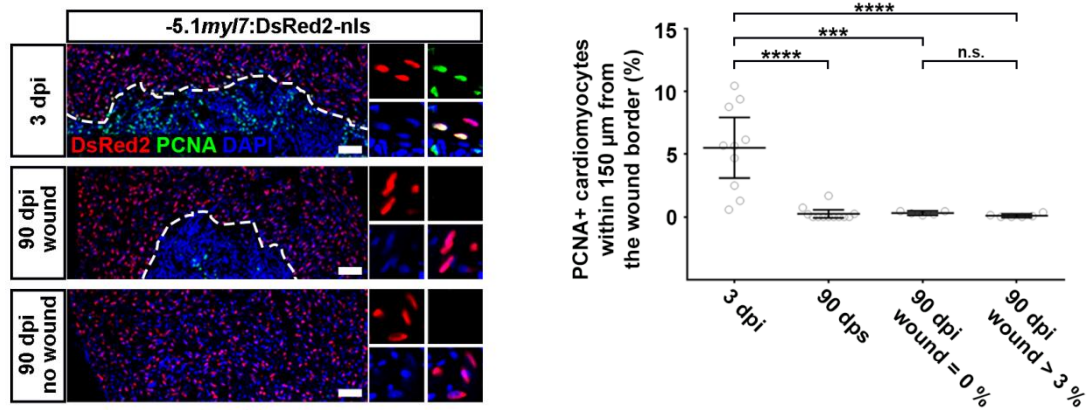
(G) Percentage of regenerated cardiomyocytes at 14, 30 and 90 dpi, normalized to their respective 3 dpi group (0% of regenerated cardiomyocytes at 3 dpi). Dotted line represents complete regeneration (100% of cardiomyocytes lost to injury were restored). Error bars, mean \pm CI 95%. One-way ANOVA plus Tukey's multiple comparisons test; **: $p < 0.01$, ***: $p < 0.001$, ****: $p < 0.0001$.

The extent of cardiomyocyte regeneration and wound size do not fully correlate

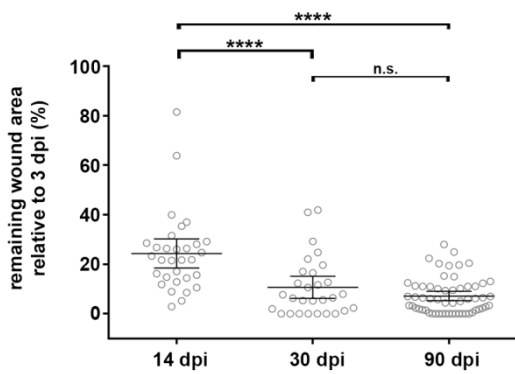
Even though cardiomyocytes had been fully restored by 90 dpi and average wound area had dropped to only 2%, the majority of regenerated hearts still contained some residual scarring (Figure 6A). 33% of the total number of analyzed hearts had a wound area higher than 3% of ventricle area (Figure 6B). Thus, we wondered whether hearts containing such scar tissue had failed to regenerate all cardiomyocytes. However, while wound size inversely correlated with cardiomyocyte number in 3 dpi hearts (Figure 6C), such correlation was not observed in 90 dpi hearts (Figure 6D). In addition, hearts that contained no wound at all and hearts that contained the biggest wounds, both at 30 and 90 dpi, had the same number of cardiomyocytes (Figure 6E). Also, cardiomyocyte proliferation was the same in 90 dpi hearts containing wounds and in those not containing wounds (Figure 6F). Thus, we concluded that complete cardiomyocyte regeneration can occur despite the presence of scar tissue. Interestingly, neither the average wound area nor the fraction of hearts retaining a significant wound (wound area $>$ 3% of ventricle area) changed significantly between 30 dpi and 90 dpi (Figure 6B,G). This suggests that those hearts with residual wounds at 30 dpi might never achieve scar-free regeneration. However, during early phases of regeneration, the average size of the wound was smaller than the fraction of cardiomyocytes lost to injury (Figure 6H). Taken together, these data indicate that wound size is not always a reliable proxy for the number of regenerated cardiomyocytes.

A**B****C****D****E**

F



G



H

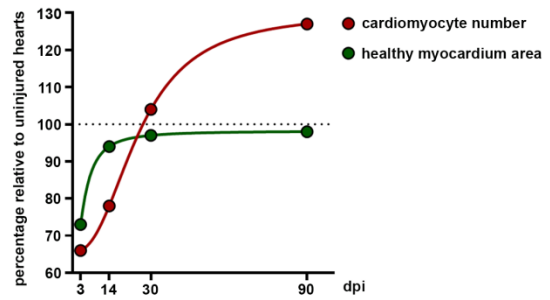


Figure 6. The extent of cardiomyocyte regeneration and wound size do not fully correlate

(A) Example of an acid fuchsin orange (AFOG) stained ventricle section at 90 dpi displaying incomplete wound healing, evident by presence of fibrin (purple) and collagen (blue, arrow).

(B) Percentage of hearts with no residual wounds (= 0% of ventricle area), small wounds (between 0% and 3%) or bigger wounds (> 3%) at 14, 30 and 90 dpi. Error bars, mean \pm CI 95%. n=31, 29, 58.

(C) Number of cardiomyocytes plotted against relative wound area at 3 dpi. Red and dotted lines indicate linear regression \pm CI 95%. Data are from the first experiment, where the other half of fish was analyzed at 90 dpi. n=68.

(D) Number of cardiomyocytes plotted against relative wound area at 90 dpi. Red and dotted lines indicate linear regression \pm CI 95%. n=58.

(E) At 30 and 90 dpi, the number of cardiomyocytes present in hearts displaying no wound (wound area = 0%) and in those hearts displaying the biggest wounds (wound area > 3%) does not differ. Error bars, mean \pm CI 95%. n=10, 11 (30 dpi); n=14, 19 (90 dpi); unpaired two-tail t-test; n.s.: $p > 0.05$.

(F) PCNA+ cardiomyocytes (identified by nuclear DsRed in *-5.1myl7:DsRed2-nls* transgenic fish) can be found at the wound border at 3 dpi, but not in 90 dpi hearts with or without residual wound. Scale bar, 100 μ m. In the right graph, quantification of data shown in the left figure. Error bars, mean \pm CI 95%. n=10, 12, 5, 6; one-way ANOVA plus Tukey's multiple comparisons test; n.s : $p>0.05$, ***: $p<0.001$, ****: $p<0.0001$.

(G) Percentage of remaining wound area at 14, 30 and 90 dpi, normalized to their respective 3 dpi group (100% of remaining wound area at 3 dpi). Error bars, mean \pm CI 95%. n=31, 29, 58; one-way ANOVA plus Tukey's multiple comparisons test; n.s : $p>0.05$, ****: $p<0.0001$.

(H) Percentage of cardiomyocyte numbers (red) and healthy myocardium area (green), relative to uninjured hearts, at 3, 14, 30 and 90 dpi. The 3 dpi data is the average from all three cohorts of fish we injured.

Myocardial morphology regenerates, but cardiomyocytes remain smaller in areas enclosing residual scars

Since the majority of cryoinjured hearts at 30 or 90 dpi retained some scar tissue in our experiments, we investigated whether morphology of the regenerated myocardium was altered. However, we observed no difference in myocardial volume at 30 dpi compared to sham-injured hearts (Figure 7A), as well as no difference in overall cardiomyocyte density at 90 days post intervention (Figure 7B), suggesting that cardiomyocytes do not become hypertrophic. It has recently been reported that regenerated muscle can be identified as localized thickening of the cortical layer of the myocardium (Gonzalez-Rosa et al. 2018). In contrast, at 30 dpi we did not observe any difference in thickness of the cortical layer, identified using laminin as a marker (Sanchez-Iranzo et al. 2018a) (Figure 7C). In addition, in the subset of hearts containing wounds at 30 dpi, we could not detect significant localized cortical thickening in the region of the myocardium enclosing residual wounds (Figure 7C). However, we found that at 30 and 90 dpi those hearts that contained scars had a higher cardiomyocyte density in the myocardial layer that surrounds the remaining wound at the heart apex (Figure 7D).

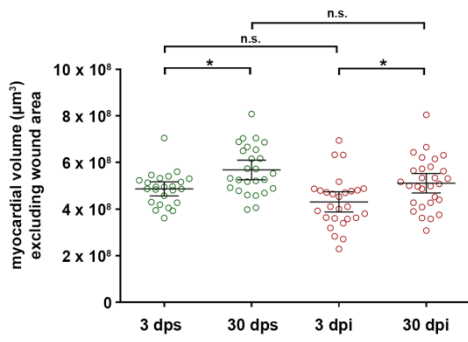
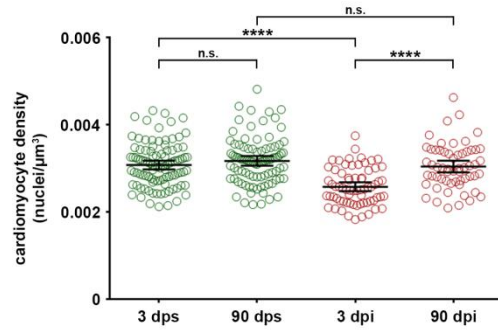
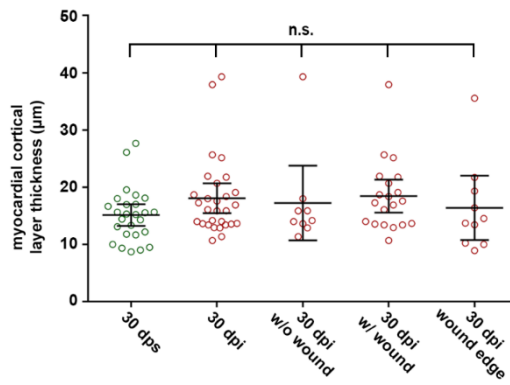
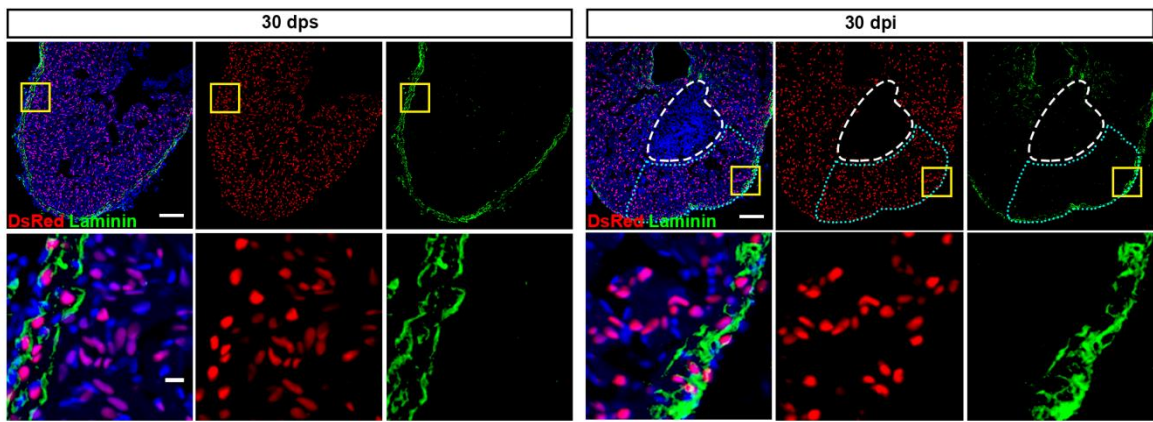
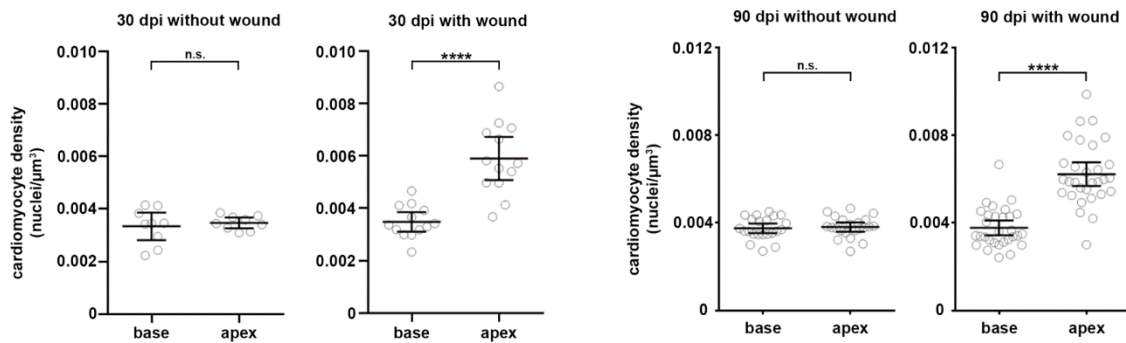
A**B****C****D**

Figure 7. Myocardial morphology regenerates, but cardiomyocytes remain smaller in areas enclosing residual scars

(A) Volume of the healthy myocardium (ventricular volume minus the wound area) recovers in injured hearts to levels similar to those of sham injured hearts within 30 days. Error bars, mean \pm CI 95%. n=24, 26, 27, 29; one-way ANOVA plus Tukey's multiple comparisons test; n.s.: $p>0.05$, *: $p<0.05$.

(B) Average cardiomyocyte density in the whole ventricle does not differ between injured fish at 90 dpi and sham-injured fish at 90 dps. Error bars, mean \pm CI 95%. n=99, 92, 68, 58; one-way ANOVA plus Tukey's multiple comparisons test; n.s.: $p>0.05$, ****: $p<0.0001$.

(C) Representative pictures of the outer cortical layer of cardiomyocytes, labeled by laminin immunostaining, at 30 days post sham-injury or injury. In the 30 dpi panel, dashed white lines indicate the remaining wound area and the dotted cyan outline marks the wound edge. Yellow rectangles mark the region in the top figures magnified in the bottom insets. Scale bar, 100 μ m. In the lower panel, quantification of data shown in the upper panel shows no difference in the average myocardial cortical layer thickness at 30 days post sham injury or cryoinjury, as well as in 30 dpi hearts with or without residual wound. Error bars, mean \pm CI 95%. n=26, 29, 9, 20, 10; one-way ANOVA plus Tukey's multiple comparisons test; n.s.: $p>0.05$.

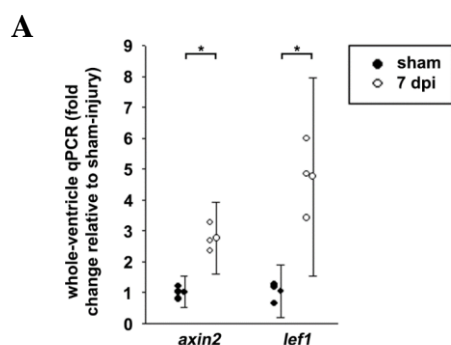
(D) Cardiomyocyte density is higher in the apex of 30 and 90 dpi hearts that contain a wound ($> 0\%$ of ventricle area) compared to the base region. No difference is observed between base and apex in 30 and 90 dpi hearts without wound. Error bars, mean \pm CI 95%. n=9, 13 (30 dpi); n=22, 30 (90 dpi); unpaired two-tail t-test; n.s.: $p>0.05$, ****: $p<0.0001$.

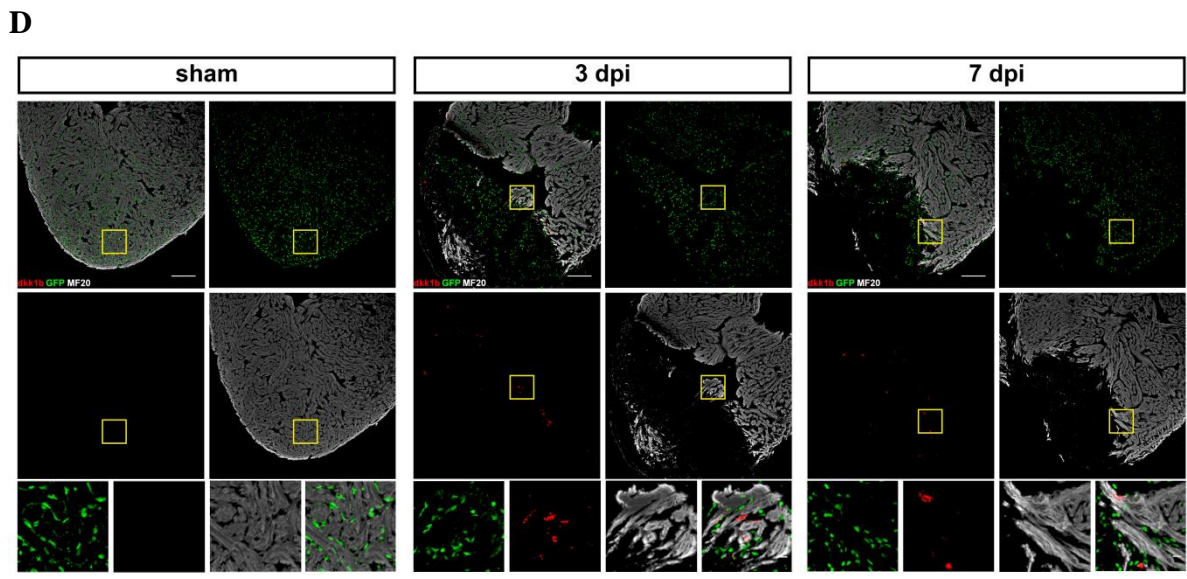
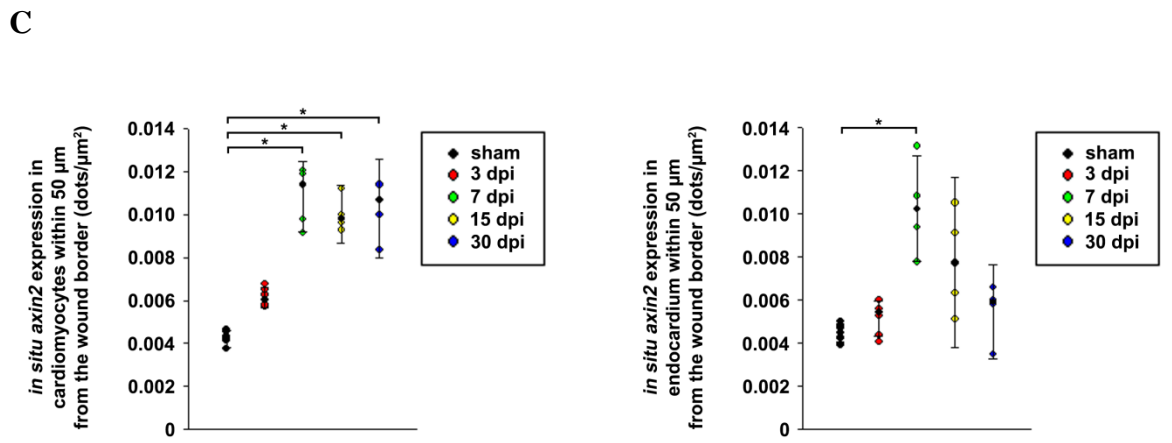
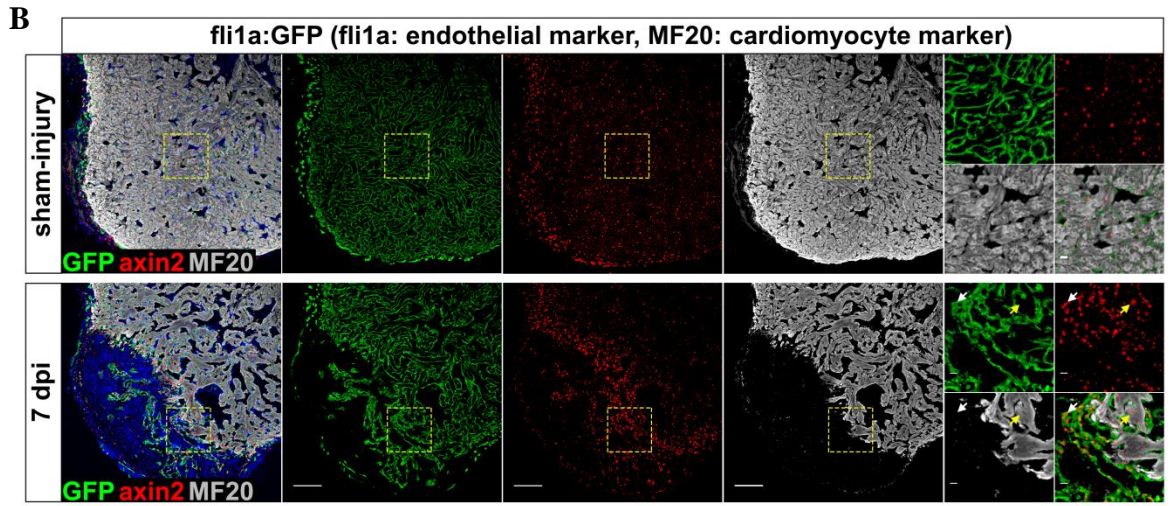
Wnt/ β -catenin signaling in zebrafish heart regeneration

Wnt/ β -catenin signaling is upregulated upon cryoinjury

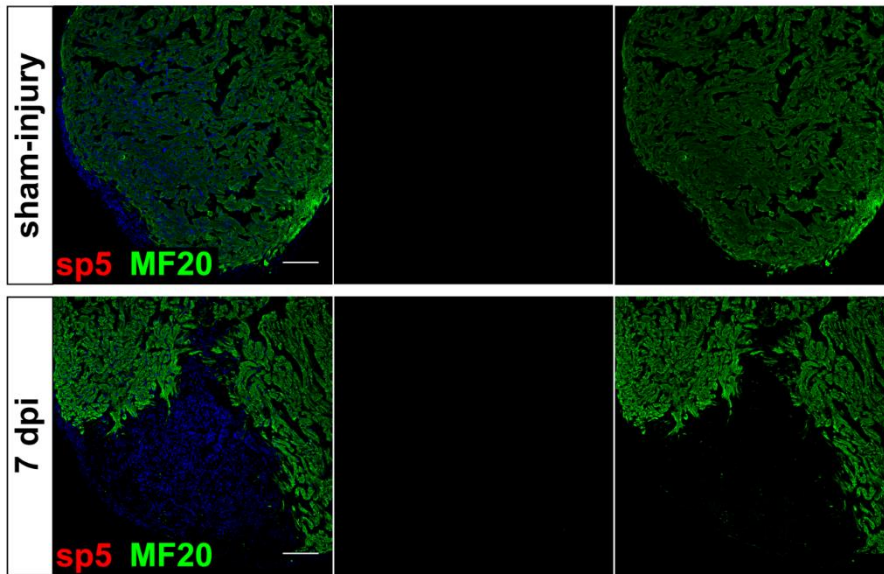
While many target genes of Wnt/ β -catenin are cell-type specific due to the numerous biological processes regulated by the pathway, a number of genes are considered common targets and thus are frequently used as readout for active signaling. Direct targets are defined as those with Tcf binding sites important for their transcriptional regulation, and include genes such as the transcription factor *lef1* and the negative feedback inhibitor *axin2* (Jho et al. 2002, Filali et al. 2002). Thus, to assess whether Wnt/ β -catenin signaling is active in injured zebrafish hearts, we performed qRT-PCR on RNA isolated from whole hearts for these two genes. Both *lef1* and *axin2* were significantly upregulated at 7 dpi compared to sham-injured hearts (Figure 8A), indicating Wnt/ β -catenin signaling activity in regenerating hearts. Next, we investigated the spatiotemporal activation of Wnt/ β -catenin by performing a time-course of *axin2* expression by in situ hybridization on cryosections of *fli1a:EGFP* transgenics hearts, which labels the endothelial cells of the endocardium and the coronary vessels, co-stained with the cardiomyocyte marker MF20. We found that *axin2* upregulation started already at 3 dpi, reached its maximum at 7 dpi and remained sustained throughout at least 30 days post injury in cardiomyocytes within the first 50 μ m from the border zone (Figure 8B,C). *axin2* was also strongly upregulated in endothelial cells in close proximity to the wound border, albeit in a more transient fashion, since its expression declined after peaking at 7 dpi (Figure 8B,C), indicating Wnt/ β -catenin activity also in the vascular plexus. Even though *axin2* is considered a commonly accepted readout for Wnt/ β -catenin signaling, we decided to test alternative targets by investigating the expression of *dkk1b*, *sp5a* and *sp5l* genes, previously reported as downstream targets of β -catenin (Niida et al. 2004, Weidinger et al. 2005), as well as the activation of transgene expression in two transgenic reporter lines for active Wnt/ β -catenin signaling, the *OTM:d2EGFP* (Optimal Tcf Motif) and *top:GFP* reporter. Both constructs contain four consensus Lef binding sites (optimal Tcf motif), driving a destabilized GFP transgene. These reporters are transcriptionally active only in the presence of both stabilized β -catenin and Lef/Tcf proteins. Unlike *axin2*, *dkk1b* was found upregulated only in cardiomyocytes close to the wound border (Figure 8D), with no detectable expression in endothelial cells inside the wound. *sp5a* and *sp5l* could not be detected in any cell type at 7 dpi (Figure 8E,F), indicating that these two genes are not Wnt/ β -catenin targets in the regenerating zebrafish hearts. Based on *in situ* for *egfp*, the *top:GFP* line displayed expression in the

entire myocardium even in sham injured hearts, with no clear upregulation upon injury (Figure 8G), indicating that the basal transcription level of this transgene is already too high in uninjured fish, thus making it not useful to detect any upregulation in regenerating hearts. We observed re-activation of the *OTM:d2EGFP* transgene in a few cardiomyocytes at the wound border (Figure 8H), resembling the expression profile of *dkk1b* at 7 dpi. Such similarity prompted us to investigate whether *dkk1b* and the *OTM:d2EGFP* transgene are expressed in the same cells. However, by double *in situ* hybridization, no overlap was observed between *dkk1b* and *egfp* (Figure 8I), suggesting that these two putative targets of Wnt/ β -catenin signaling are expressed in different subsets of border zone cardiomyocytes. Since *axin2*, *dkk1b* and the *OTM:d2EGFP* transgene showed different expression patterns, we were concerned about which readout should be trusted to faithfully recapitulate endogenous activity of the pathway. To address this issue, we measured *axin2* levels in 7 dpi hearts upon short term overexpression of either Axin1 or Dkk1b, using the *hsp70l:Mmu.Axin1-YFP* (Kagermeier-Schenk et al. 2011) or the *hsp70l:dkk1b-GFP* (Ueno et al. 2007) transgenic lines, respectively. With both lines, we observed significant reduction in *axin2* expression in border zone cardiomyocytes compared to heat shocked wild type siblings (Figure 8J). Since the *hsp70l:Mmu.Axin1-YFP* and the *hsp70l:dkk1b-GFP* transgenic lines were shown to induce the expected Wnt/ β -catenin loss of function phenotypes in zebrafish embryos (Kagermeier-Schenk et al. 2011, Ueno et al. 2007), we confirmed that *axin2* is a direct target of Wnt/ β -catenin in the adult heart. We therefore concluded that, based on *axin2* expression, Wnt/ β -catenin signaling is reactivated upon injury both in cardiomyocytes and endothelial cells proximal to the wound border. Since we did not test changes in *dkk1b* or the *OTM:d2EGFP* reporter expression after short term inhibition of Wnt/ β -catenin, we could not clearly determine whether these genes are direct targets of this signaling pathway, and therefore if they could be reliably used as Wnt/ β -catenin readouts in the regenerating zebrafish heart.

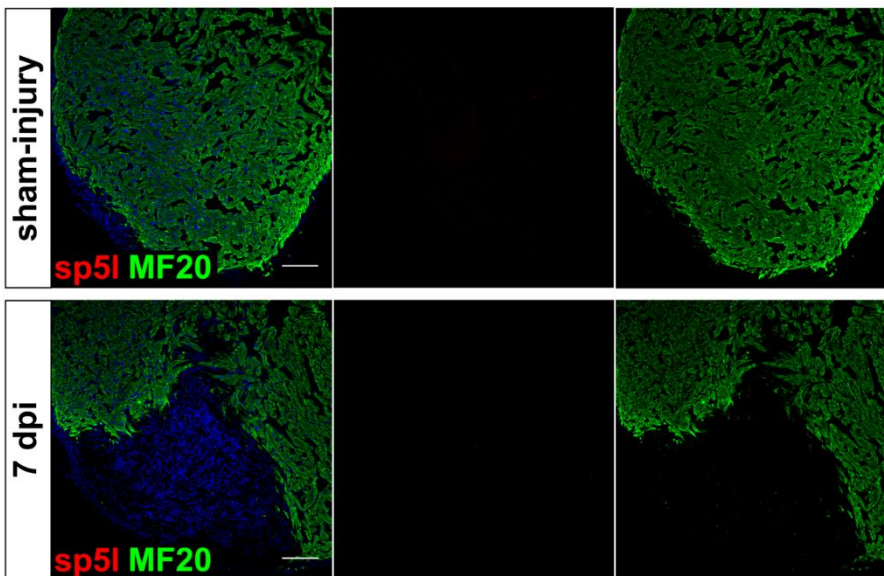




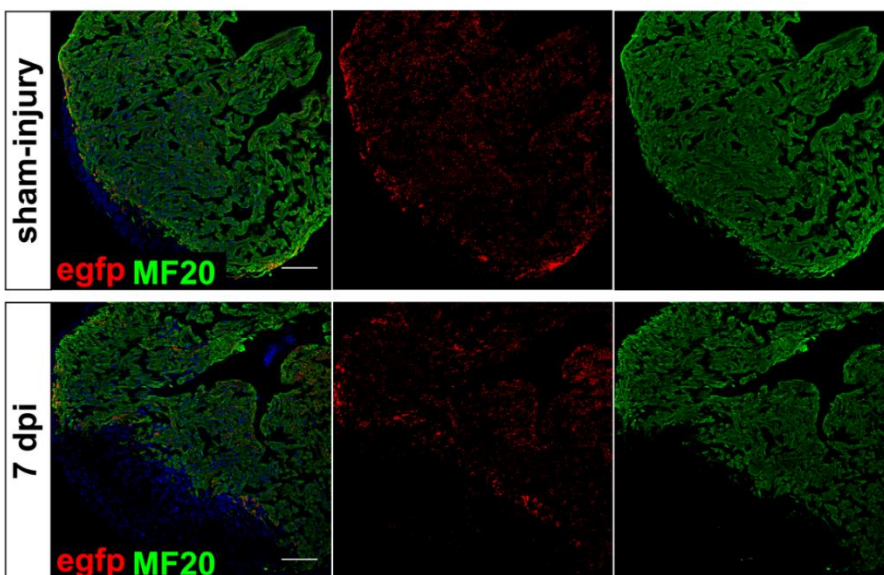
E



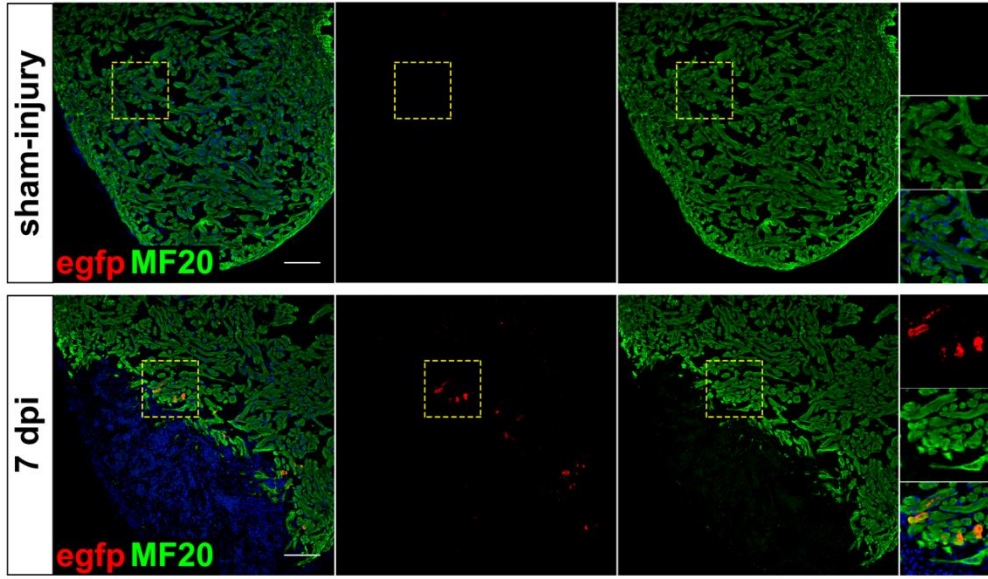
F



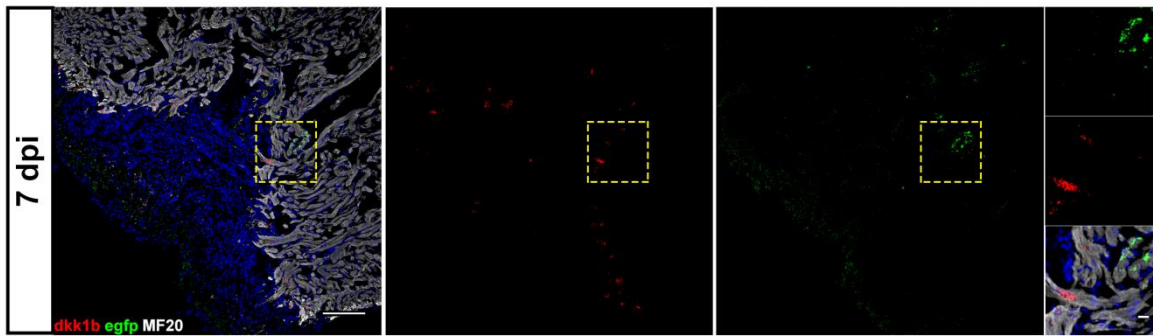
G



H



I



J

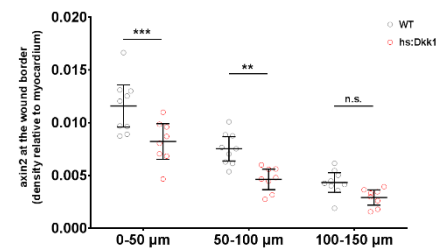
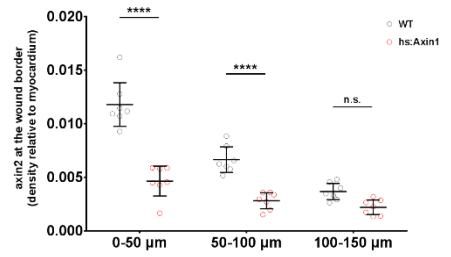
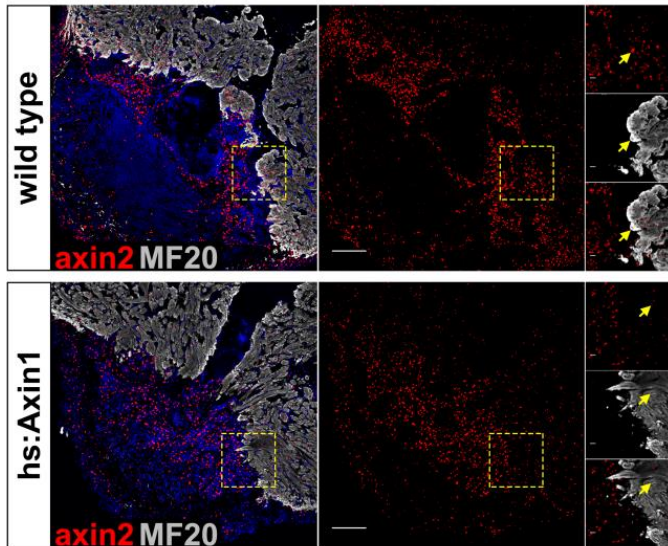
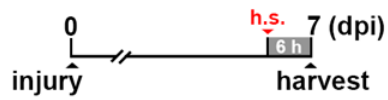


Figure 8. Wnt/ β -catenin signaling is upregulated upon cryoinjury

- (A) Wnt/ β -catenin target genes *axin2* and *lef1* are upregulated in the ventricle at 7 dpi compared to sham injured hearts, based on qRT-PCR on RNA isolated from whole hearts. Error bars, mean \pm CI 95%. n=3, 3; unpaired two-tail t-test; *: p<0.05.
- (B) *axin2* (red) is upregulated upon cryoinjury in cardiomyocytes (yellow arrow) and in endothelial cells (white arrow) at 7 dpi in *fli1a:EGFP* (endothelial marker, green) hearts co-stained with MF20 (myocyte marker, grey). Yellow rectangles mark the region magnified in the corresponding insets. Scale bar, 100 μ m. n=6, 6.
- (C) Quantification of *axin2* expression at different time points after injury shows sustained upregulation in border zone cardiomyocytes from 7 till 30 dpi, whereas *axin2* expression peaks at 7 dpi in endothelial cells close to the wound border and is progressively reduced at 14 and 30 dpi. Error bars, mean \pm CI 95%. n=5, 5, 4, 4, 3; unpaired two-tail t-test; *: p<0.05.
- (D) *dkk1b* (red) is upregulated at 3 and 7 dpi in *fli1a:EGFP* hearts only in few cardiomyocytes at the wound border (MF20, grey), but not in endothelial cells inside the wound (GFP, green). Yellow rectangles mark the region magnified in the corresponding insets. Scale bar, 100 μ m. n=6, 6.
- (E) *sp5a* (red) is not expressed either in sham injured or in cryoinjured hearts. Cardiomyocytes (MF20): green. Scale bar, 100 μ m. n=6, 6.
- (F) *sp5l* (red) is not expressed either in sham injured or in cryoinjured hearts. Cardiomyocytes (MF20): green. Scale bar, 100 μ m. n=6, 6.
- (G) *Top:GFP* transgene shows elevated expression through the whole myocardium in sham injured hearts, with no clear upregulation upon cryoinjury. *egfp*: red; cardiomyocytes (MF20): green. Scale bar, 100 μ m. n=6, 6.
- (H) *OTM:d2EGFP* transgene is upregulated at 7 dpi in few cardiomyocytes at the wound border. Yellow rectangles mark the region magnified in the corresponding insets. *egfp*: red; cardiomyocytes (MF20): green. Scale bar, 100 μ m. n=6, 6.
- (I) *dkk1b* and the *OTM:d2EGFP* reporter are not expressed within the same cardiomyocytes at the wound border. Yellow rectangles mark the region magnified in the corresponding insets. *dkk1b*: red; *egfp*: green; cardiomyocytes (MF20): grey. Scale bar, 100 μ m. n=6, 6.
- (J) In the left figure, after 6 hours post single heat shock at 7 dpi, Axin1 overexpression in hs:Axin1 fish reduces *axin2* expression in cardiomyocytes within 150 μ m from the wound border (yellow arrow), relative to heat shocked wild type siblings. Yellow rectangles mark the region magnified in the corresponding insets. *axin2*: red; cardiomyocytes (MF20): grey. Scale bar, 100 μ m. In the right graph, Axin1 or Dkk1b overexpression for 6 hours at 7 dpi is already sufficient to dampen *axin2* levels in cardiomyocytes within 100 μ m from the wound border. Error bars, mean \pm CI 95%. n=7, 7 (hs:Axin1); n=8, 8 (hs:Dkk1); one-way ANOVA plus Tukey's multiple comparisons test; n.s : p>0.05, **: p<0.01, ***: p<0.001, ****: p<0.0001.

Manipulation of Wnt/ β -catenin signaling in the adult heart using inducible transgenes

We then set out to use genetic tools to manipulate Wnt signaling upon injury. Several transgenic lines were previously established for global conditional manipulation of Wnt signaling in zebrafish embryos. The *hsp70l:Mmu.Axin1-YFP* construct overexpresses the intracellular inhibitor Axin1 fused to YFP (Kagermeier-Schenk et al. 2011), the *hsp70l:dkk1b-GFP* construct overexpresses the extracellular negative regulator Dickkopf fused to GFP (Ueno et al. 2007), *hsp70l:wnt8a-GFP* overexpresses the Wnt8a ligand fused to GFP (Weidinger et al. 2005), *HSE:Xla.Ctmb-MYC,EGFP* (Veldman et al. 2013) overexpresses a constitutively active form of β -catenin, and *hs:Xdd1-p2a-nlsTomato* (unpublished) overexpresses a Xenopus Dishevelled mutant form with a deletion of aa 301-381 (part of the PDZ domain) tagged with nuclear Tomato, originally established to achieve conditional loss of function of the Wnt/PCP pathway. All these constructs are expressed conditionally in zebrafish only after heat shock at 37 °C. Hereafter, these transgenic lines are abbreviated hs:Axin1, hs:dkk1b, hs:wnt8a, hs: β -catenin and hs:Xdd1, respectively. First, we checked whether these transgenes are expressed in the adult heart. All the tested transgenic lines were found to be expressed in the ventricle of heat shocked fish. The transgenes were expressed not only in cardiomyocytes, but also in the epicardium and the endocardium, confirming that the *hsp70l* promoter is ubiquitously activated in multiple cell types after heat shock. As a representative example, here I show immunofluorescence for YFP, the cardiomyocyte marker MF20 and *aldh1a2*, considered a *bona fide* marker for the endocardium and epicardium in injured hearts (Kikuchi et al. 2011), in heat shocked hs:Axin1 transgenic and wild type siblings at 7 dpi, which confirms overexpression of Axin1 in cardiomyocytes, endothelial and epithelial cells (Figure 9). We then verified whether these transgenic lines could effectively regulate Wnt/ β -catenin signaling in regenerating hearts, using *axin2* as standard readout for Wnt activity as previously described. Significant downregulation of *axin2* in border zone cardiomyocytes was observed with the hs:Axin1 line even after multiple daily heat shocks from 1 to 7 dpi (Figure 10A), suggesting that prolonged blockage of Wnt/ β -catenin signaling does not result in compensatory re-activation of its direct target *axin2* from other signaling pathways. Downregulation of *dkk1b* was also observed upon prolonged Axin1 overexpression (Figure 10B). Surprisingly, the hs: β -catenin line showed similar downregulation of *axin2* upon single heat shock at 7 dpi (Figure 10C), while no effect was observed after transgene overexpression from 1 to 7 dpi (Figure 10D). This suggested that transient high levels of constitutively active β -catenin can unexpectedly inhibit Wnt

activity, whereas compensatory effects might come into play to dampen the response to prolonged transgene overexpression. However, prolonged overexpression of this transgene could also downregulate *axin2* expression (Figure 10E). Therefore, this transgenic line did not prove to be specific for Wnt/PCP manipulation, since it could clearly affect Wnt/ β -catenin signaling as well. The *hs:wnt8a* line was also tested as a tool for gain of function experiments. Daily overexpression of the transgene from 1 to 7 dpi was able to boost *axin2* levels in border zone cardiomyocytes (Figure 10F), confirming that Wnt8a overexpression can upregulate Wnt/ β -catenin activity in the injured zebrafish heart. Overall, these results confirm that the *hs:Axin1*, *hs:dkk1b* and *hs:wnt8a* lines are expressed in the adult heart and exert the expected effect on *axin2* expression, thus can be reliably used to investigate the functional role of Wnt/ β -catenin signaling in zebrafish heart regeneration. Unfortunately, the *hs: β -catenin* and *hs:Xdd1* lines, despite their strong and ubiquitous expression throughout the entire myocardium, exerted opposite roles to what we expected, and thus we concluded that these two transgenic tools could not be further employed for functional studies.

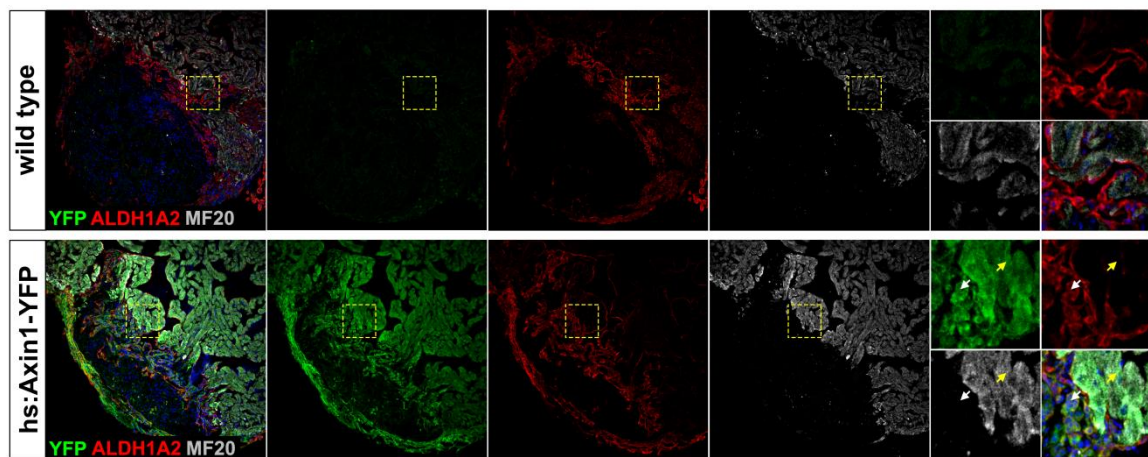


Figure 9. hs:Axin1-YFP transgene expression in the injured adult heart

Upon heat shock at 7 dpi, the *hs:Axin1-YFP* transgene, detected by immunofluorescence for YFP (green), is expressed in carrier fish in cardiomyocytes (MF20, grey) as well as in the endocardium and epicardium (*aldh1a2*, red). Only background staining for YFP is visible in heat shocked wild type siblings. Yellow rectangles mark the region magnified in the corresponding insets. Yellow arrow labels cardiomyocytes, white arrow labels endothelial cells. n=6, 6.

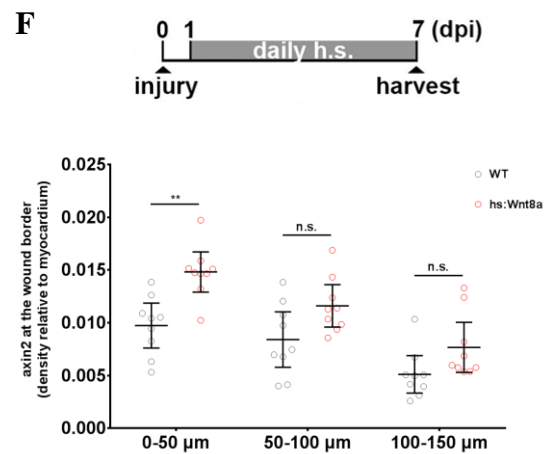
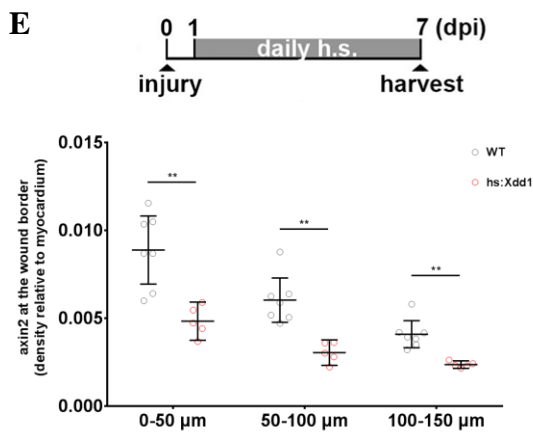
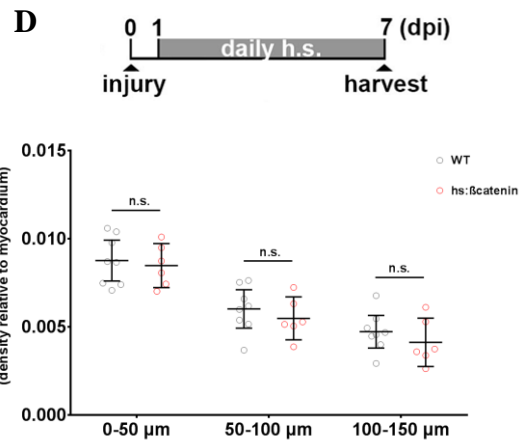
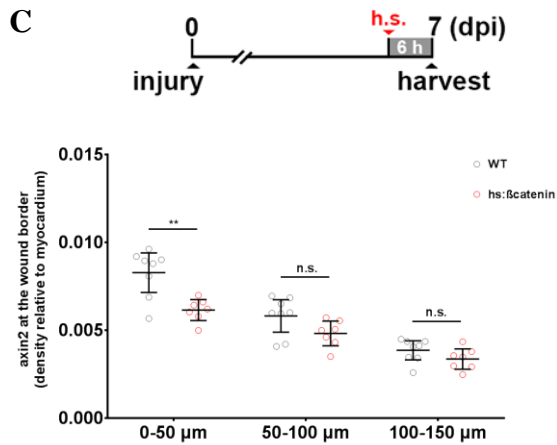
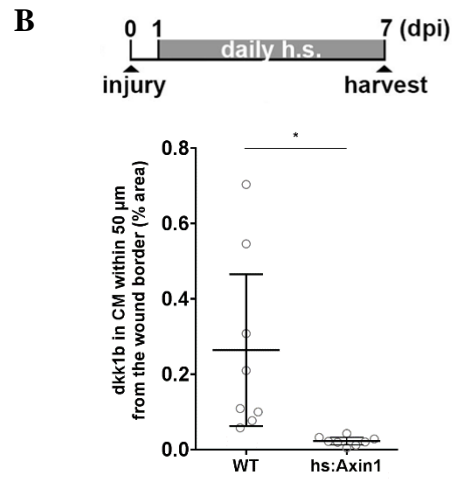
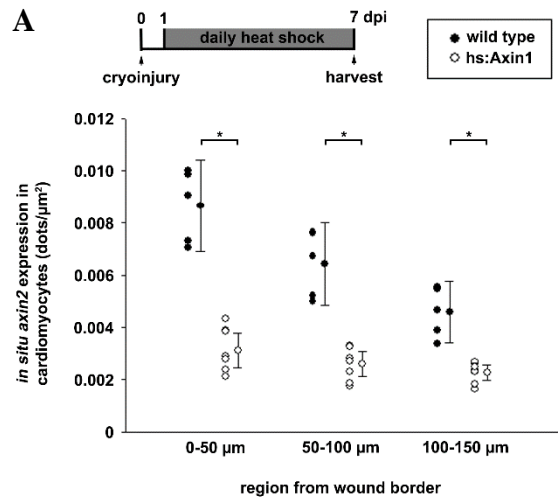


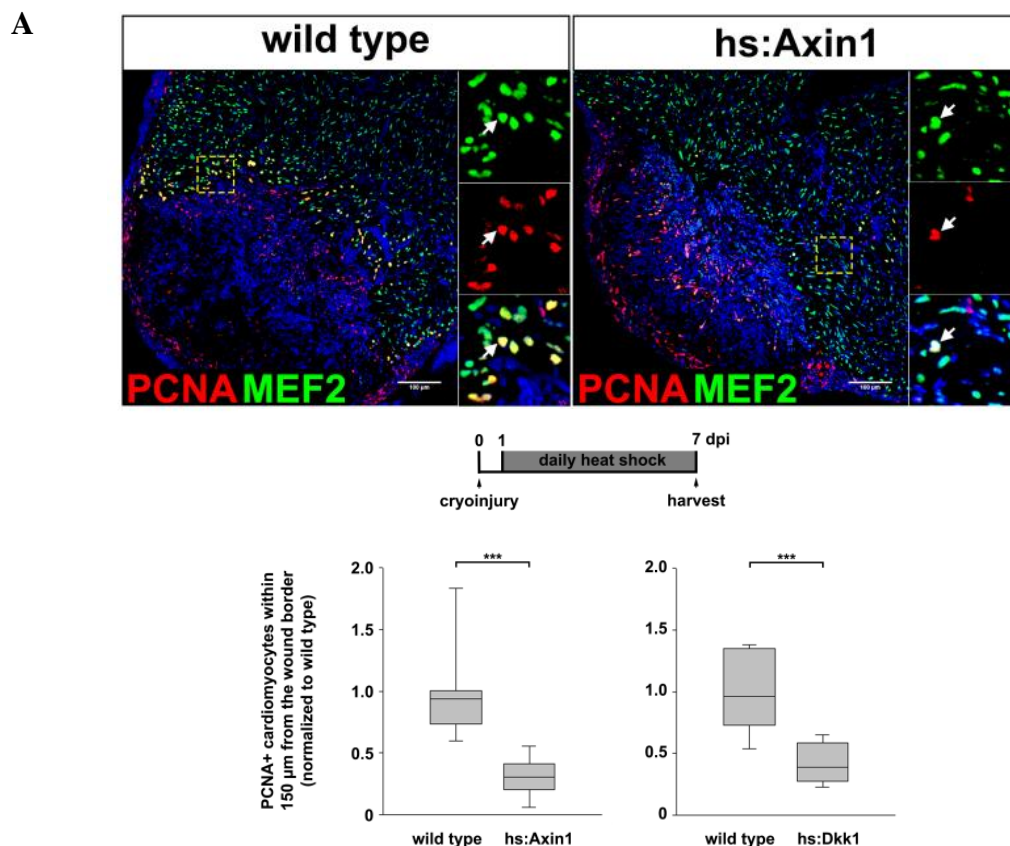
Figure 10. Effects of transgene overexpression in the injured adult heart on Wnt/ β -catenin signaling

- (A) Axin1 overexpression from 1 to 7 dpi in hs:Axin1 fish reduces *axin2* expression in cardiomyocytes within 150 μ m from the wound border relative to heat shocked wild type siblings. Error bars, mean \pm CI 95%. n=6, 6; one-way ANOVA plus Tukey's multiple comparisons test; *: p<0.05.
- (B) Axin1 overexpression from 1 to 7 dpi reduces *dkk1b* expression in cardiomyocytes within 50 μ m from the wound border, relative to heat shocked wild type siblings. Error bars, mean \pm CI 95%. n=8, 8; unpaired two-tail t-test; *: p<0.05.
- (C) After 6 hours post single heat shock at 7 dpi, β -catenin overexpression reduces *axin2* levels in border zone cardiomyocytes. Error bars, mean \pm CI 95%. n=8, 7; one-way ANOVA plus Tukey's multiple comparisons test; n.s.: p>0.05, **: p<0.01.
- (D) Prolonged overexpression of β -catenin from 1 to 7 dpi did not affect *axin2* levels in cardiomyocytes at the wound border. Error bars, mean \pm CI 95%. n=8, 6; one-way ANOVA plus Tukey's multiple comparisons test; n.s.: p>0.05.
- (E) Xdd1 overexpression from 1 to 7 dpi negatively regulates *axin2* expression in cardiomyocytes within 150 μ m from the wound border, relative to heat shocked wild type siblings. Error bars, mean \pm CI 95%. n=7, 5; one-way ANOVA plus Tukey's multiple comparisons test; **: p<0.01.
- (F) Wnt8a overexpression from 1 to 7 dpi is sufficient to boost *axin2* levels in cardiomyocytes within 50 μ m from the wound border, relative to heat shocked wild type siblings. Error bars, mean \pm CI 95%. n=9, 9; one-way ANOVA plus Tukey's multiple comparisons test; n.s.: p>0.05, **: p<0.01.

Global prolonged inhibition of Wnt/ β -catenin signaling reduces cardiomyocyte proliferation

We made use of the previously tested transgenic lines to investigate whether Wnt/ β -catenin regulates cardiomyocyte cell cycle re-entry. We assessed cardiomyocytes positive for PCNA at 7 dpi, after daily heat shocks from 1 to 7 dpi. The hs:Axin1 group showed significantly fewer PCNA+ cardiomyocytes at the wound border, compared to heat shocked wild type siblings (Figure 11A). Similar reduction of PCNA+ cardiomyocytes was observed using the hs:dkk1b line with the same heat shock regime (Figure 11A). Thus, loss of Wnt/ β -catenin signaling negatively affects cardiomyocyte cell cycle activity. To confirm that Wnt/ β -catenin is required for cardiomyocyte proliferation, we counted the number of cardiomyocytes within 150 μ m from the wound border that are positive for the mitosis marker PH3 in *myl7:H2B-GFP* fish. Since the M-phase is very short in comparison to the rest of the cell cycle, fish were treated from 5 to 7 dpi with nocodazole, which causes cell cycle arrest in the M-phase. This treatment induces accumulation of cells stuck in mitosis and thus makes analysis of the number of PH3+ cardiomyocytes possible based on

counting. The *hs:Axin1* fish had a significantly lower rate of cardiomyocytes in active mitosis compared to wild type siblings (Figure 11B), indicating that Wnt/ β -catenin signaling is important to promote cell division in cardiomyocytes. However, hearts overexpressing Axin1 or Dkk1 after a single heat shock at 7 dpi did not show a reduction in cardiomyocyte proliferation compared to wild type siblings (Figure 11C), despite lower Wnt activity as previously described using *axin2* expression (Figure 10B). This suggests that inhibition of Wnt/ β -catenin for such short time frame, while sufficient to downregulate expression of downstream target genes, might not be enough to cause a significant effect on cardiomyocyte cell cycle re-entry. In addition, overexpression of Wnt8a from 1 to 7 dpi did not show an increase in cardiomyocyte proliferation (Figure 11D), indicating that over-activation of Wnt/ β -catenin alone is not sufficient to boost the cardiomyocyte hyperplastic response beyond levels observed in wild-type siblings. We then investigated whether global Wnt/ β -catenin loss of function might also affect proliferation of endothelial cells inside the wound. After daily heat shocks from 1 till 7 dpi to *flila:nEGFP* fish, no effect was detected on endocardial proliferation in hearts overexpressing Axin1 relative to their controls (Figure 11E). We therefore concluded that Wnt/ β -catenin signaling is not required for cell cycle activity of endothelial cells in the re-vasculature.



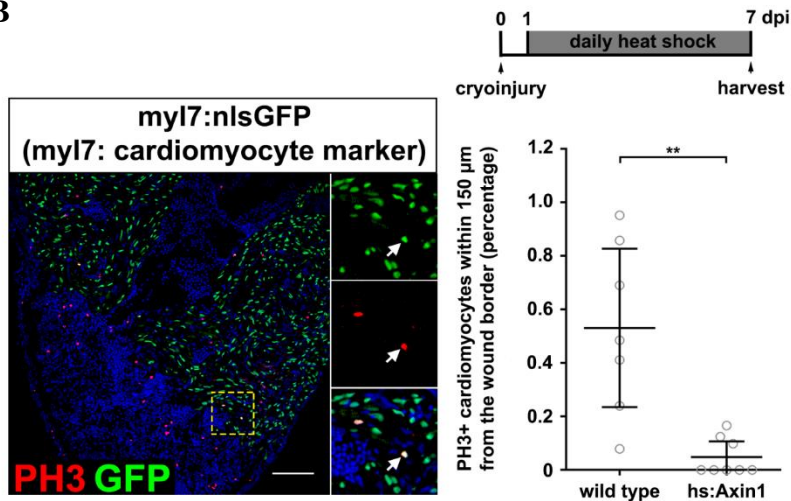
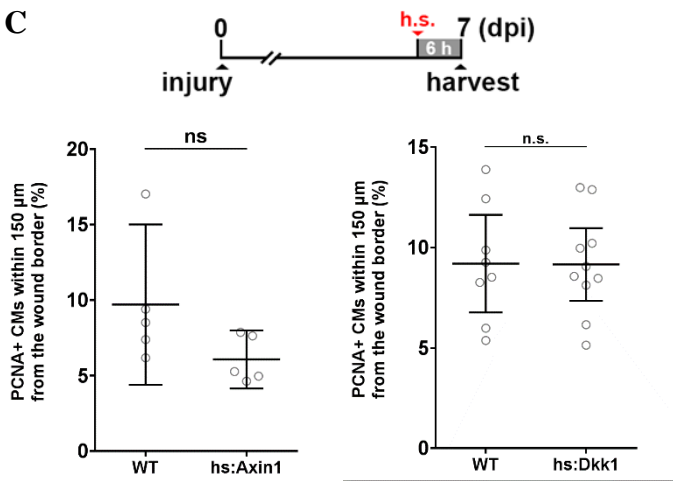
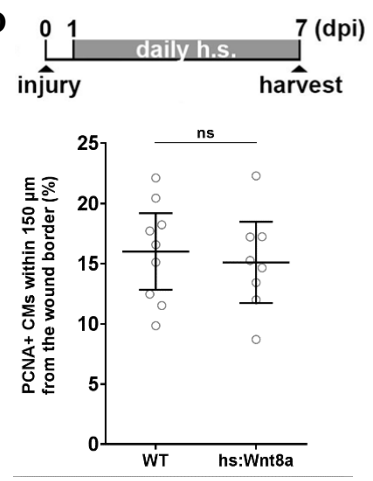
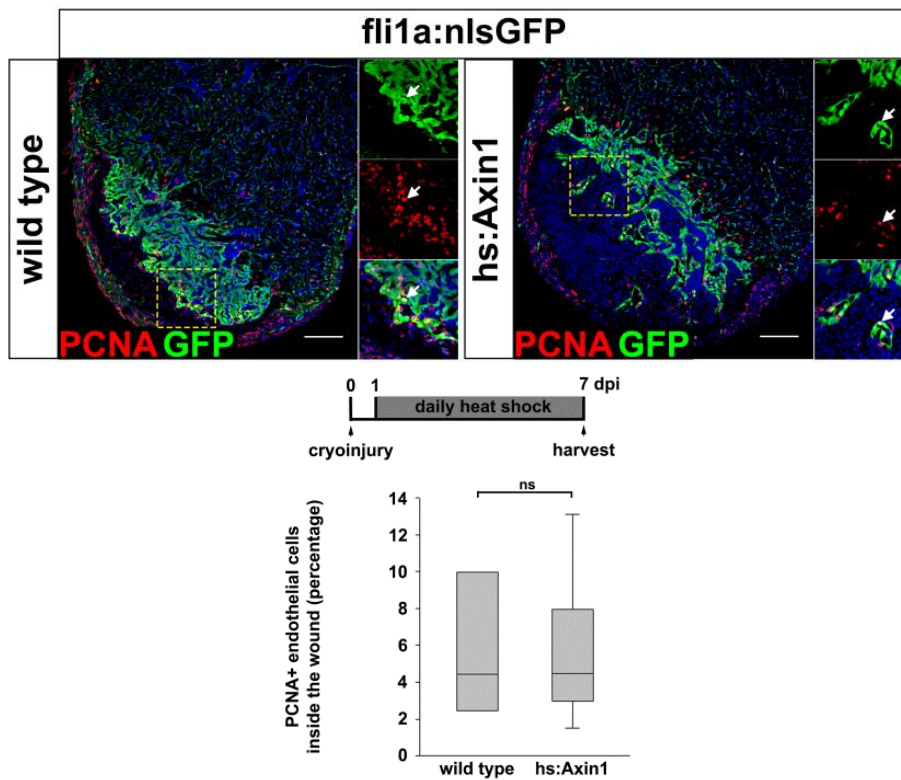
B**C****D****E**

Figure 11. Global prolonged inhibition of Wnt/ β -catenin signaling reduces cardiomyocyte proliferation

- (A) Axin1 or Dkk1 overexpression from 1 to 7 dpi impairs cell cycle re-entry of cardiomyocytes within 150 μ m from the wound border, relative to heat shocked wild type siblings. For both graphs, data from two independent experiments were merged and values normalized to wild type. PCNA: red; Mef2 (cardiomyocyte marker): green. White arrow marks PCNA+/Mef2+ cells. Yellow rectangles mark the region magnified in the corresponding insets. Scale bar, 100 μ m. Error bars, mean \pm CI 95%. n=14, 14 (hs:Axin1); n=12, 12 (hs:Dkk1); unpaired two-tail t-test; ***: p<0.001.
- (B) Axin1 overexpression from 1 to 7 dpi impairs cardiomyocyte mitosis compared to heat shocked wild type siblings. *myl7:H2B-GFP* labels cardiomyocyte nuclei. PCNA: red; GFP: green. White arrow marks PH3+/GFP+ cardiomyocytes. Yellow rectangles mark the region magnified in the corresponding insets. Scale bar, 100 μ m. Error bars, mean \pm CI 95%. n=7, 8; unpaired two-tail t-test; **: p<0.01.
- (C) Axin1 or Dkk1 overexpression for 6 hours at 7 dpi is not sufficient to reduce cardiomyocyte cell cycle re-entry, based on PCNA expression in border zone cardiomyocytes. Error bars, mean \pm CI 95%. n=5, 5 (hs:Axin1); n=8, 10 (hs:Dkk1); unpaired two-tail t-test; n.s.: p>0.05.
- (D) Wnt8a overexpression from 1 to 7 dpi does not affect cardiomyocyte cell cycle re-entry, based on PCNA expression in border zone cardiomyocytes. Error bars, mean \pm CI 95%. n=9, 8; unpaired two-tail t-test; n.s.: p>0.05.
- (E) Prolonged overexpression of Axin1 from 1 to 7 dpi in *fli1a:nEGFP* fish shows no effect on proliferation of endothelial cells inside the wound. PCNA: red; GFP: green. White arrow marks PCNA+/GFP+ endothelial cells. Yellow rectangles mark the region magnified in the corresponding insets. Scale bar, 100 μ m. Error bars, mean \pm CI 95%. n=12, 12; unpaired two-tail t-test; n.s.: p>0.05.

Global Wnt/ β -catenin inhibition impairs fetal cardiac myosin re-expression in dedifferentiating cardiomyocytes

In injured hearts, cardiomyocytes close to the wound border show signs of dedifferentiation, in addition to re-entering the cell cycle. Having previously shown that Wnt/ β -catenin affects cardiomyocyte proliferation, we then wondered if this pathway impinges on cardiomyocyte dedifferentiation as well. First, we investigated whether Wnt/ β -catenin is important for the re-activation of the regulatory regions of the developmental cardiac transcription factor *gata4*, by injuring *-14.8gata4:GFP* fish. To achieve Wnt/ β -catenin inhibition, we chose not to use the hs:Axin1 transgenic line to avoid any misinterpretation due to the concomitant immunofluorescence from both GFP and YFP. Thus, we treated injured *-14.8gata4:GFP* fish with the small molecule Wnt signaling inhibitor IWR-1 or with DMSO/PBS as control by daily intraperitoneal (IP) injection from 1 to 7 dpi, and measured GFP area in border zone cardiomyocytes at 7 dpi. We did not

detect any clear difference on GFP expression in fish injected with IWR-1 compared to the control group, indicating that Wnt/ β -catenin signaling does not affect re-activation of the -14.8*gata4*:GFP transgene upon injury (Figure 12A). We then heat shocked from 1 to 7 dpi double transgenic *myl7*:EGFP/*hs*:Axin1 fish, and measured native GFP fluorescence intensity in cardiomyocytes within 50 μ m from the wound border to assess transcriptional activity of the *myl7* promoter. No difference was observed compared to heat shocked single transgenic *myl7*:EGFP fish (Figure 12B). We therefore concluded that Wnt/ β -catenin is also not required for the downregulation of *myl7* in dedifferentiating cardiomyocytes in the border zone. Finally, we checked whether Wnt inhibition affects upregulation of *myh7*, a fetal form of cardiac myosin expressed in dedifferentiating cardiomyocytes upon injury. Axin1 overexpression from 1 to 7 dpi resulted in lower Myh7+ area in cardiomyocytes at the wound border, relative to the wild type siblings (Figure 12C). Thus, inhibition of Wnt/ β -catenin with chemical or genetic tools does not appear to affect some of the currently known readouts of cardiomyocyte dedifferentiation, but only the re-activation of such developmental myosin during heart regeneration.

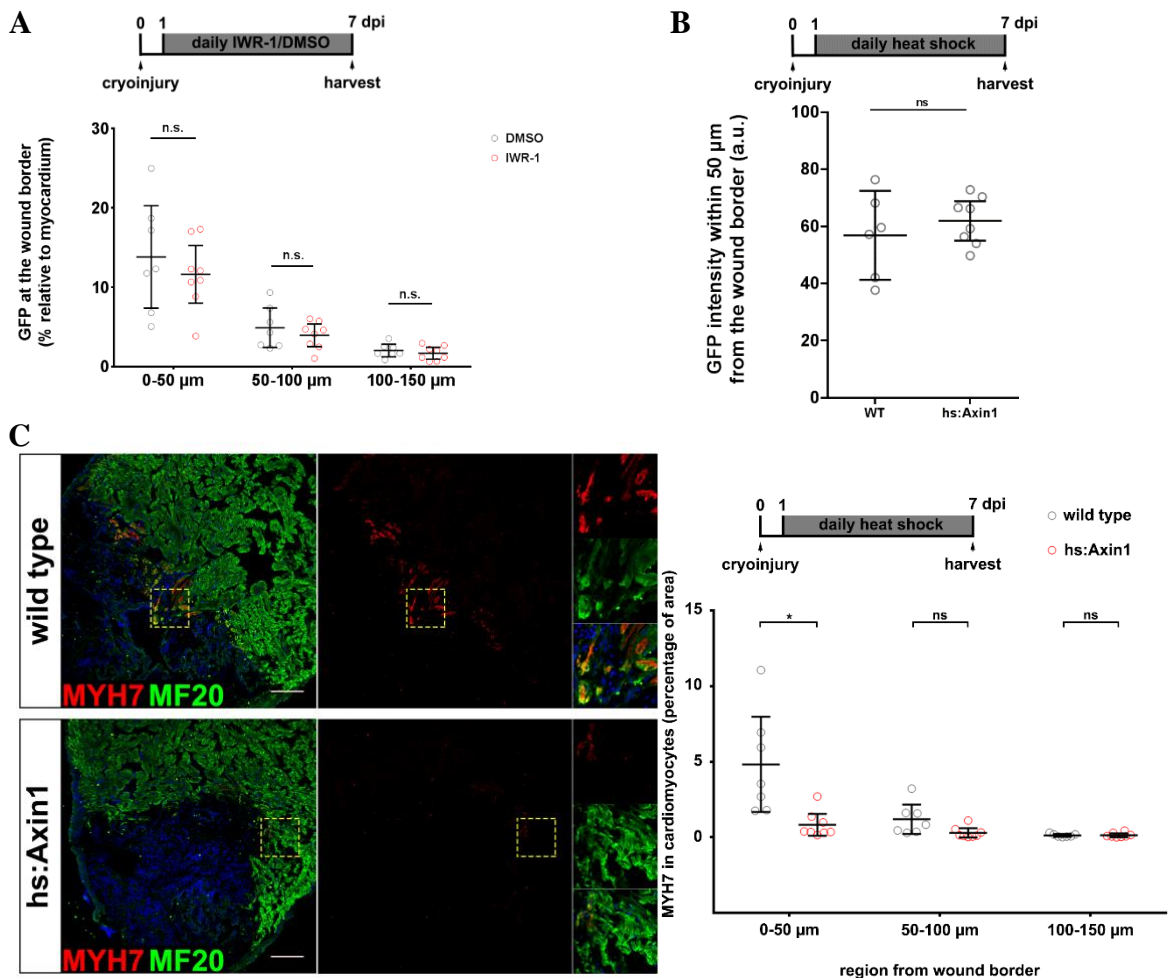


Figure 12. Global Wnt/ β -catenin inhibition impairs fetal cardiac myosin re-expression in dedifferentiating cardiomyocytes

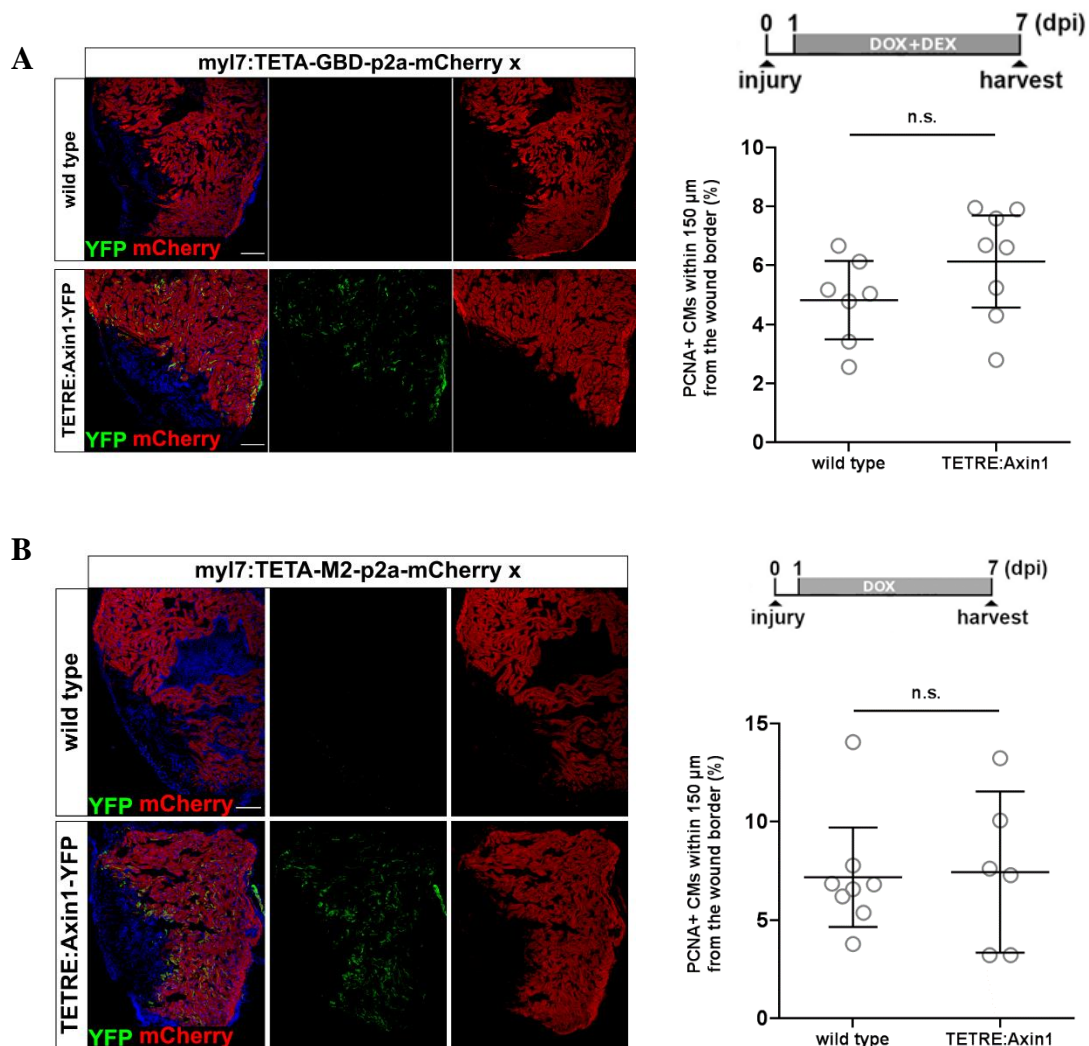
- (A) Inhibition of Wnt/ β -catenin by IWR-1 IP injections from 1 to 7 dpi does not affect regulation of the *14.8gata4:GFP* transgene in cardiomyocytes at the wound border, based on GFP+ area relative to myocardial area. Error bars, mean \pm CI 95%. n=7, 8; one-way ANOVA plus Tukey's multiple comparisons test; n.s.: p>0.05.
- (B) Axin1 overexpression from 1 to 7 dpi does not significantly affect downregulation of *myl7* in dedifferentiating cardiomyocytes within 50 μ m from the wound border, based on average native GFP fluorescence intensity in *myl7:EGFP* fish. Error bars, mean \pm CI 95%. n=6, 8; unpaired two-tail t-test; n.s.: p>0.05.
- (C) Axin1 overexpression from 1 to 7 dpi impairs *myh7* upregulation in dedifferentiating cardiomyocytes within 50 μ m from the wound border. Yellow rectangles mark the region magnified in the corresponding insets. Myh7: red; MF20: green. Scale bar, 100 μ m. In the right graph, quantification of data shown in the left picture. Error bars, mean \pm CI 95%. n=7, 8; one-way ANOVA plus Tukey's multiple comparisons test; n.s.: p>0.05, *: p<0.05.

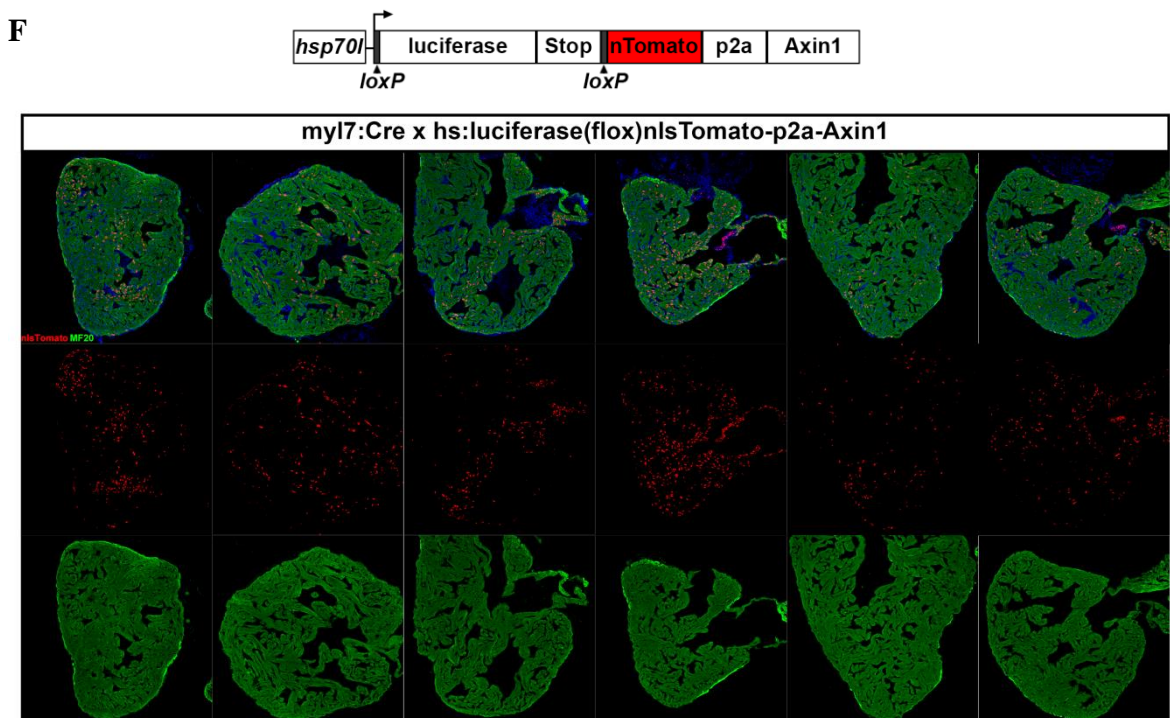
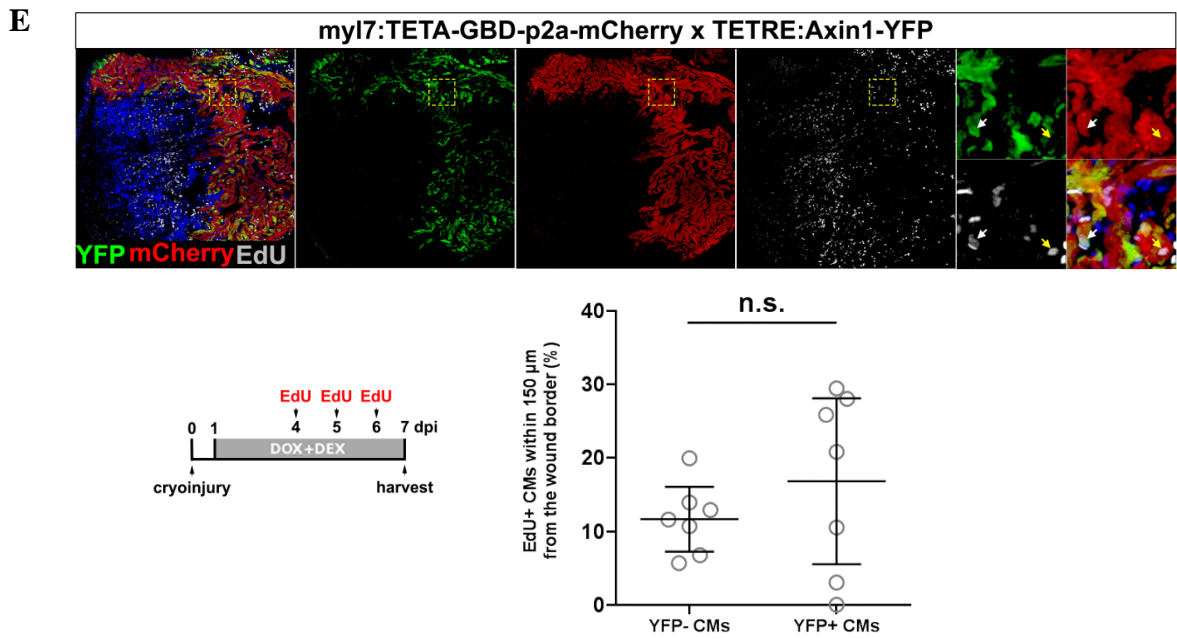
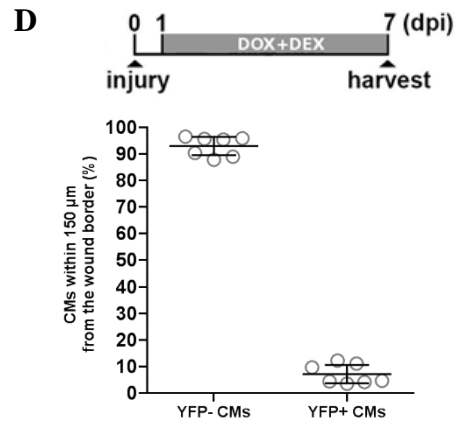
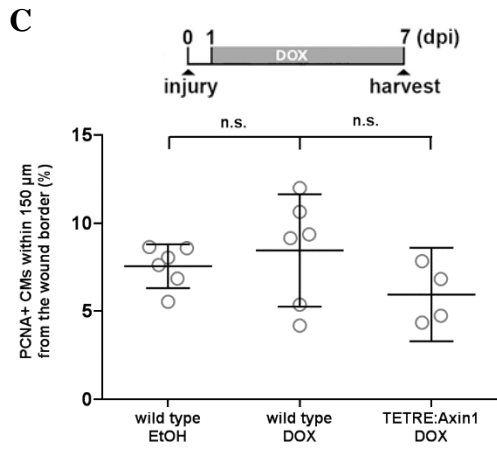
Cell-autonomous Wnt/ β -catenin inhibition impairs cardiomyocyte cell cycle re-entry

As previously shown, global Wnt/ β -catenin loss of function has a negative effect on cardiomyocyte cell cycle re-entry. However, Wnt signaling could play a role also in the response to injury of other cell types, which in turn might indirectly affect the proliferative response of cardiomyocytes. To clarify whether Wnt/ β -catenin has a direct role in cardiomyocyte proliferation, we set out to establish genetic tools to achieve cell-autonomous inhibition of Wnt/ β -catenin signaling. Initially we made use of the published TetON system established in zebrafish, which allows inducible and reversible tissue-specific transgene expression (Knopf et al. 2010). We crossed fish expressing a TET activator (inducible only in the presence of both doxycycline and dexamethasone) in cardiomyocytes, labeled by mCherry (*myl7:TETA-GBD-2A-mCherry*, hereafter abbreviated *myl7:TETA-GBD*) with fish carrying a TET responder element driving expression of Axin1 tagged with YFP (*TETRE:Mmu.Axin1-YFP*, hereafter abbreviated *TETRE:Axin1*). Upon treatment with doxycycline plus dexamethasone from 1 to 7 dpi, we did not observe any significant reduction in cardiomyocyte proliferation in double transgenics for both the *myl7:TETA-GBD* and the *TETRE:Axin1*, compared to single transgenic for the *myl7:TETA-GBD* (Figure 13A). Since we observed a low proliferation rate even in the *myl7:TETA-GBD*+ only hearts, we hypothesized that the combination of both drugs, used to induce Axin1 overexpression, might on its own dampen the

proliferative response in cardiomyocytes. It has been reported that dexamethasone is a potent stimulator of the stress response, which can impair regeneration of the zebrafish heart (Sallin and Jaźwińska 2016). Therefore, we crossed the same TETRE:Axin1 fish with an alternative TET activator line (*myl7:TETAM2-2A-mCherry*, hereafter abbreviated *myl7:TETAM2*), which requires only doxycycline for its activation. However, no difference in cardiomyocyte cell cycle re-entry was detected between *myl7:TETAM2+/TETRE:Axin1+* fish and their control *myl7:TETAM2+* only fish (Figure 13B). In another pool of fish, we did not observe any significant reduction in PCNA+ cardiomyocytes of *myl7:TETAM2* fish treated with doxycycline, when compared to ethanol treated siblings (Figure 13C). We thereby confirmed that doxycycline itself did not exert a negative effect on cardiomyocyte proliferation, suggesting that this drug can be used to activate the TetON system in cryoinjured fish without major side effects. However, based on the YFP expression pattern, we generally observed mosaic Axin1 overexpression in cardiomyocytes, in combination with both the GBD and the M2 form of the TET activator. Quantification of YFP+/mCherry+ vs YFP-/mCherry+ cells performed in *myl7:TETA-GBD+/TETRE:Axin1+* fish at 7 dpi showed that the vast majority of cardiomyocytes at the wound border (more than 90%) did not activate the TETRE:Axin1 transgene, thus making any effect on cardiomyocyte proliferation likely negligible (Figure 13D). We then decided to measure EdU incorporation in YFP+ vs YFP- cardiomyocytes of *myl7:TETA-GBD+/TETRE:Axin1+* injured hearts, but we did not observe any difference in cell cycle re-entry at 7 dpi between the YFP+ and the YFP- subsets (Figure 13E). However, since the ratio of YFP+ cardiomyocytes in the border zone was very low, we could not draw definite conclusions from this experiment. To overcome the limited expression of the TETRE:Axin1 transgene, we decided to employ a different strategy, based on the Cre-Lox system, to induce Axin1 overexpression specifically in cardiomyocytes. We constructed a heat shock inducible luciferase, flanked by LoxP sites, upstream of Axin1 tagged with nuclear Tomato (nT). In the presence of active Cre recombinase, luciferase is excised and Axin1 plus nuclear Tomato are expressed instead upon heat shock (Figure 13F). We crossed fish carrying the *hs:luciferase(flox)nlsTomato-p2a-Axin1* transgene with *myl7:Cre* fish, thus allowing inducible Axin1 overexpression only in recombined cardiomyocytes. Unfortunately, even by Cre-mediated recombination, we found that expression of Axin1 was still quite mosaic, since only a fraction of cardiomyocytes was positive for nuclear Tomato (Figure 13F). Quantification of the percentage of nT+ cardiomyocytes in the border zone showed high variability of

recombination among hearts, even though on average nT expression was less mosaic than YFP expression using the TetON system (Figure 13G, red bars). We then decided to make use of this stochasticity in transgene expression, and conducted in double transgenic hearts an analysis of nT+ vs nT- cardiomyocytes which incorporated EdU from 4 to 7 dpi. In a few sections analyzed per heart, the percentage of nT+ cells relative to EdU+ cardiomyocytes was zero, or lower than the percentage of nT+ cells relative to all border zone cardiomyocytes within the same heart (Figure 13G). This indicates that cardiomyocytes overexpressing Axin1, and thus with blocked Wnt signaling, are much less represented in the subset of cycling cardiomyocytes, when compared to expected ratio observed in the entire cardiomyocyte population at the wound border. By comparing the proliferation index between nT+ and nT- cardiomyocytes, we measured on average 2% of EdU+/nT- cardiomyocytes per heart, while almost no nT+ cardiomyocytes incorporated EdU during this time frame (Figure 13H). We concluded that Wnt/ β -catenin plays a cell-autonomous role in promoting cardiomyocyte cell cycle re-entry.





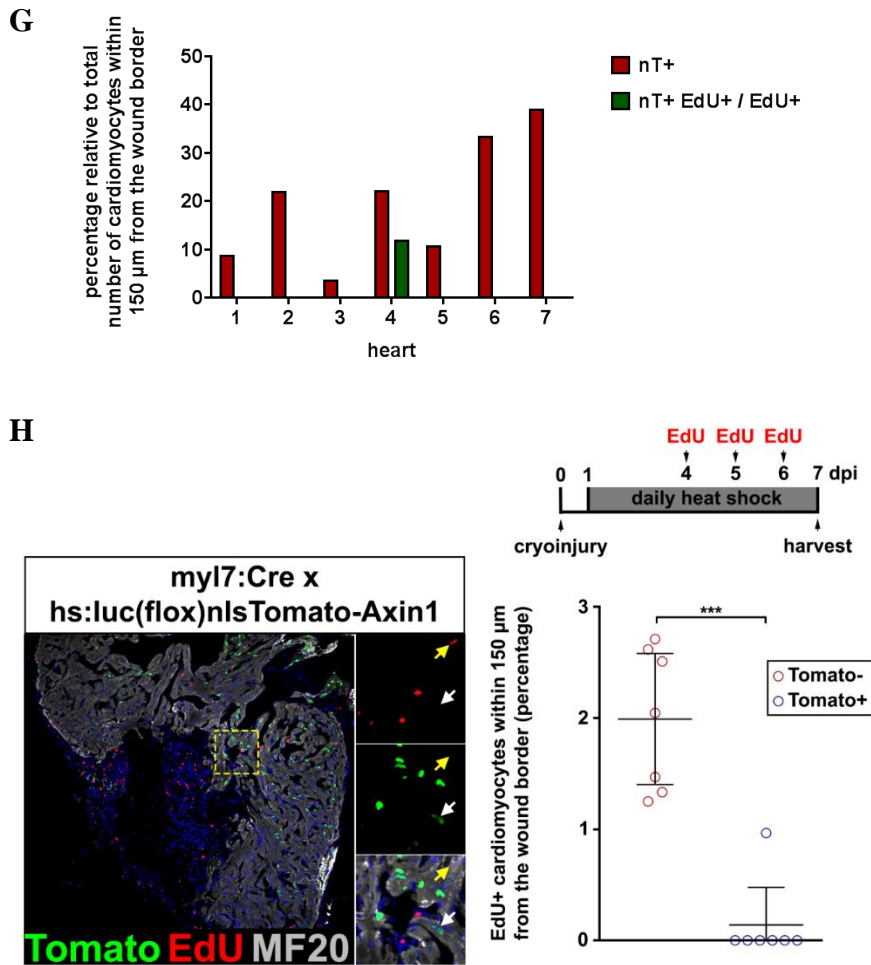


Figure 13. Cell-autonomous Wnt/ β -catenin inhibition impairs cardiomyocyte cell cycle re-entry

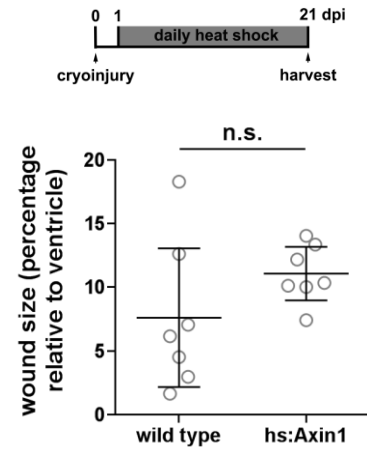
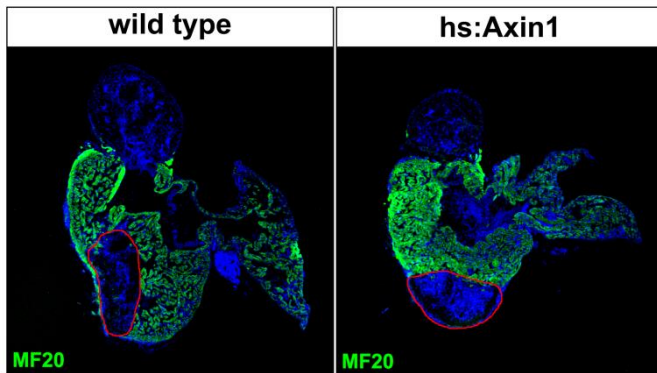
- (A) Upon treatment with doxycycline and dexamethasone from 1 to 7 dpi, no significant effect on cardiomyocyte proliferation is observed in hearts expressing both myl7:TETA-GBD and TETRE:Axin1, compared to hearts expressing only myl7:TETA-GBD (labeled as “wild type” for the TETRE:Axin1 transgene). YFP: green; mCherry: red. Scale bar, 100 μm . Error bars, mean \pm CI 95%. n=6, 8; unpaired two-tail t-test; n.s.: $p>0.05$.
- (B) In fish treated with doxycycline from 1 to 7 dpi, no significant effect on cardiomyocyte proliferation is observed in hearts expressing both myl7:TETAM2 and TETRE:Axin1, compared to hearts expressing only myl7:TETAM2 (labeled as “wild type” for the TETRE:Axin1 transgene). YFP: green; mCherry: red. Scale bar, 100 μm . Error bars, mean \pm CI 95%. n=8, 6; unpaired two-tail t-test; n.s.: $p>0.05$.
- (C) Doxycycline treatment does not clearly affect cardiomyocyte proliferation in myl7:TETAM2+ fish (labeled as “wild type” for the TETRE:Axin1 transgene) compared to clutchmates treated with ethanol. myl7:TETAM2+ / TETRE:Axin1+ fish do not have a significantly lower cardiomyocyte proliferation rate relative to the other two control groups. Error bars, mean \pm CI 95%. n=6, 6, 4; one-way ANOVA plus Tukey’s multiple comparisons test; n.s.: $p>0.05$.
- (D) Even upon continuous incubation with doxycycline plus dexamethasone from 1 to 7 dpi, the percentage of YFP+ cardiomyocytes within 150 μm from the wound border is low (7%) in fish carrying both the myl7:TETA-GBD and the TETRE:Axin1 transgene. Error bars, mean \pm CI 95%. n=7, 7.

- (E) Upper panel: representative image of a 7 dpi *myl7:TETA-GBD+/TETRE:Axin1+* ventricle from fish treated with doxycycline plus dexamethasone from 1 to 7 dpi. White arrow marks EdU+/YFP+ CM, yellow arrow marks EdU+/YFP- CM. Bottom panel: analysis of YFP- vs YFP+ cardiomyocytes showed no difference in cumulative EdU incorporation from 4 to 7 dpi in cardiomyocytes overexpressing Axin1 compared to cardiomyocytes in the YFP- control subgroup. YFP: green; mCherry: red; EdU: grey. Error bars, mean \pm CI 95%. n=7, 7; unpaired two-tail t-test; n.s.: $p > 0.05$.
- (F) Upper panel: schematic representation of the *hs:luciferase(flox)nlsTomato-p2a-Axin1* transgene. Lower panel: six uninjured fish carrying both the *myl7:Cre* and the *hs:luciferase(flox)nlsTomato-p2a-Axin1* transgene were heat shocked every 8 hours during a 24 hour time frame. Overexpression of Axin1 (denoted by immunofluorescence for nuclear Tomato) is variable among hearts and detectable only in a fraction of cardiomyocytes in the entire ventricle (marked with MF20). nlsTomato: red; MF20:green.
- (G) At 7 dpi, ratio of recombined cardiomyocytes within the border zone is variable among different hearts, in *myl7:Cre+/hs:luciferase(flox)nlsTomato-p2a-Axin1+* fish heat shocked from 1 to 7 dpi (red bars). Based on EdU incorporation from 4 to 7 dpi, the ratio of nT+ cells within the EdU+ subpopulation of cardiomyocytes (green bars) is zero or lower than the percentage of nT+ cells relative to all border zone cardiomyocytes of the same heart. n=7; Wilcoxon matched-pairs signed rank test, $p = 0.0156$.
- (H) Almost no cardiomyocytes at the wound border overexpressing Axin1 (labeled with Tomato immunofluorescence) re-entered the cell cycle, based on EdU incorporation from 4 to 7 dpi, in contrast to 2% of nT-negative cardiomyocytes in the same hearts from double transgenic fish heat shocked from 1 to 7 dpi. nlsTomato: green; EdU: red; MF20: grey. Yellow arrow marks EdU+/nT- cardiomyocytes, white arrow marks EdU-/nT+ cardiomyocytes. Yellow rectangles mark the region magnified in the corresponding insets. Error bars, mean \pm CI 95%. n=7; Mann-Whitney test, $p = 0.0006$.

Global Wnt/ β -catenin loss of function does not impact on morphological regeneration

We previously showed how Wnt/ β -catenin signaling positively regulates cardiomyocyte proliferation and dedifferentiation. We then investigated whether this pathway could also affect wound healing and morphological regeneration of the myocardium in a longer time frame. *hs:Axin1* or *hs:dkk1b* fish, together with their wild type siblings, were heat shocked daily from 1 to 21 dpi, and then wound size was assessed based on cardiac myosin immunostaining. We did not observe any significant difference in wound size at 21 dpi between the two experimental groups (Figure 14A,B). Therefore, long term inhibition of Wnt/ β -catenin is not sufficient to impair wound healing, suggesting that perhaps other mechanisms involved in scar resolution might compensate for the reduction in cardiomyocyte proliferation.

A



B

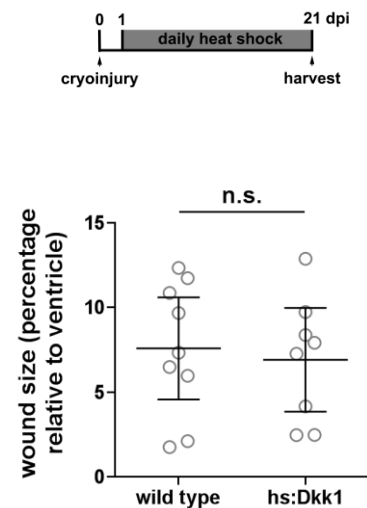
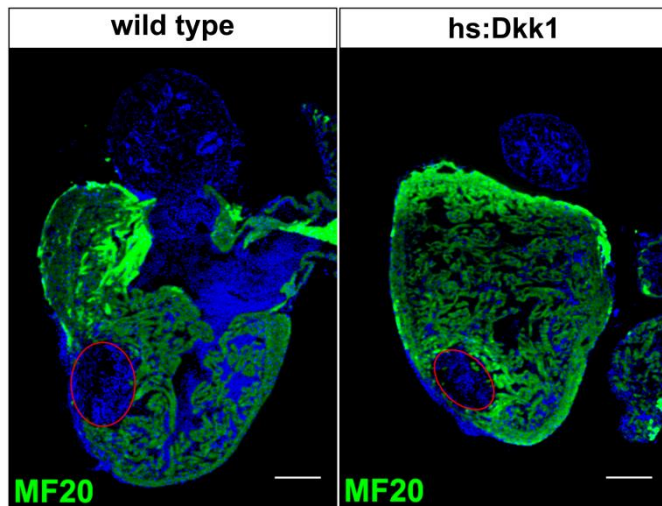
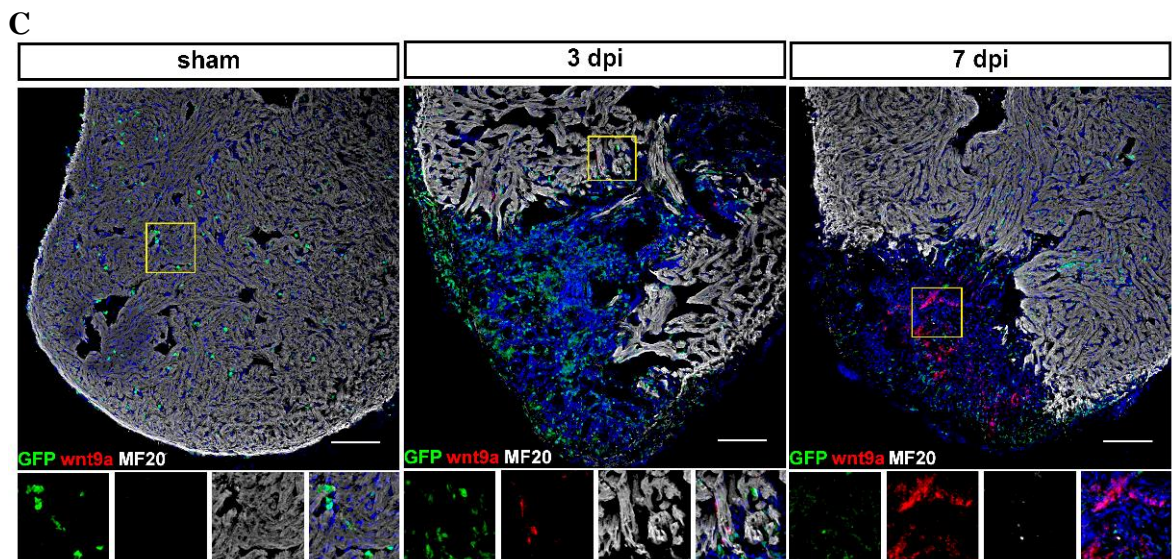
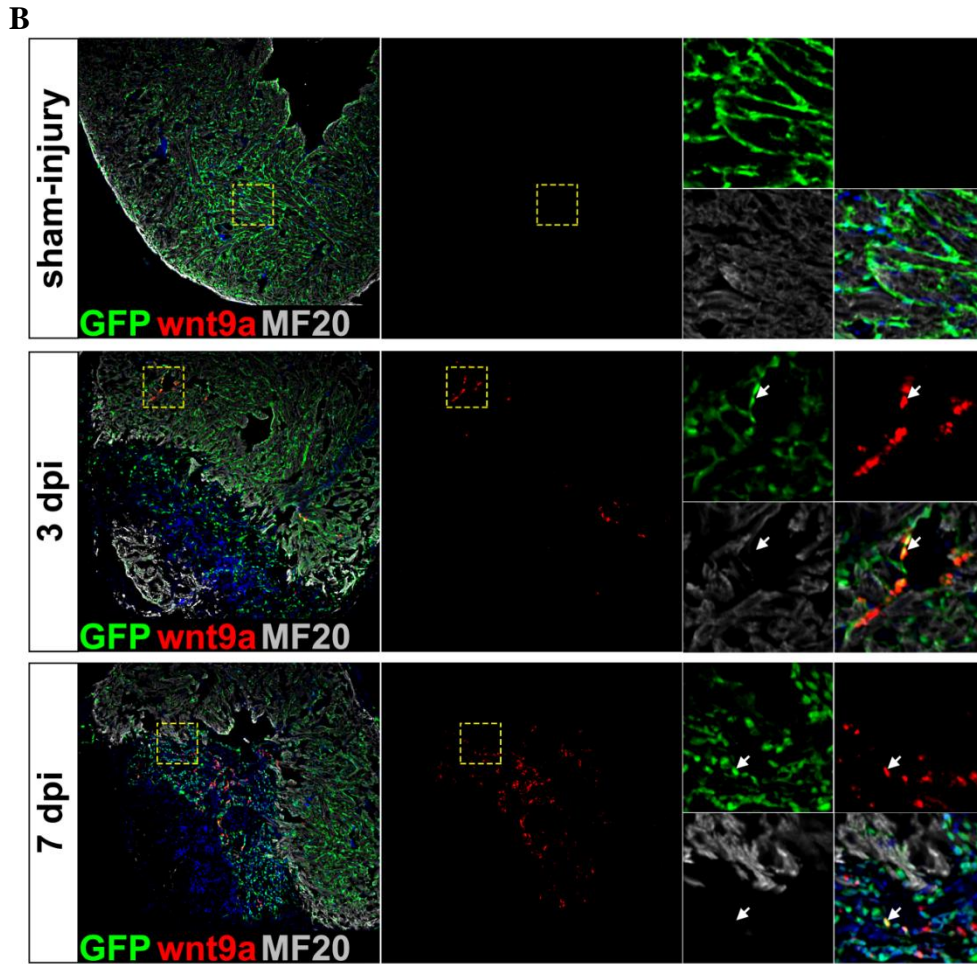
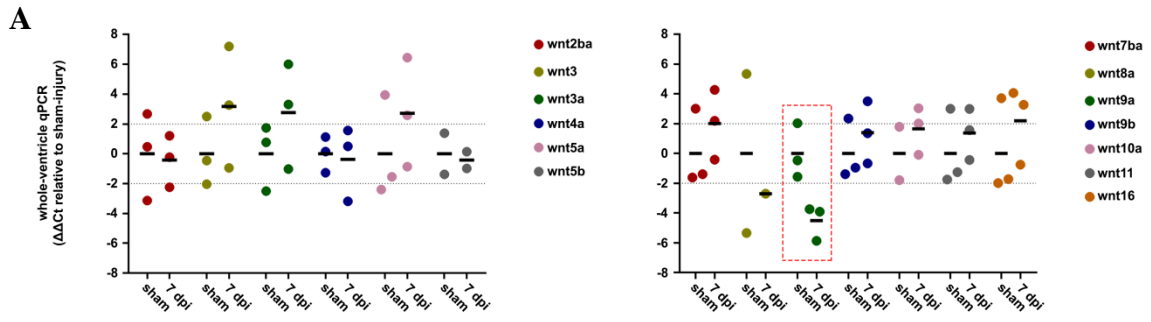


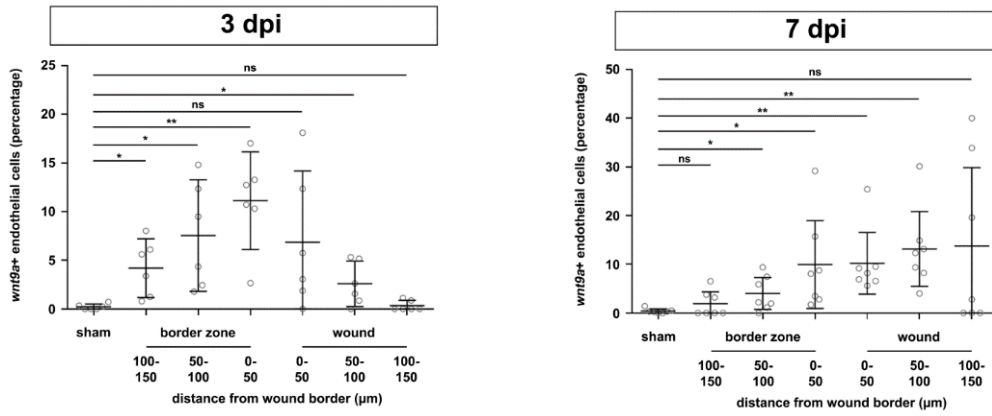
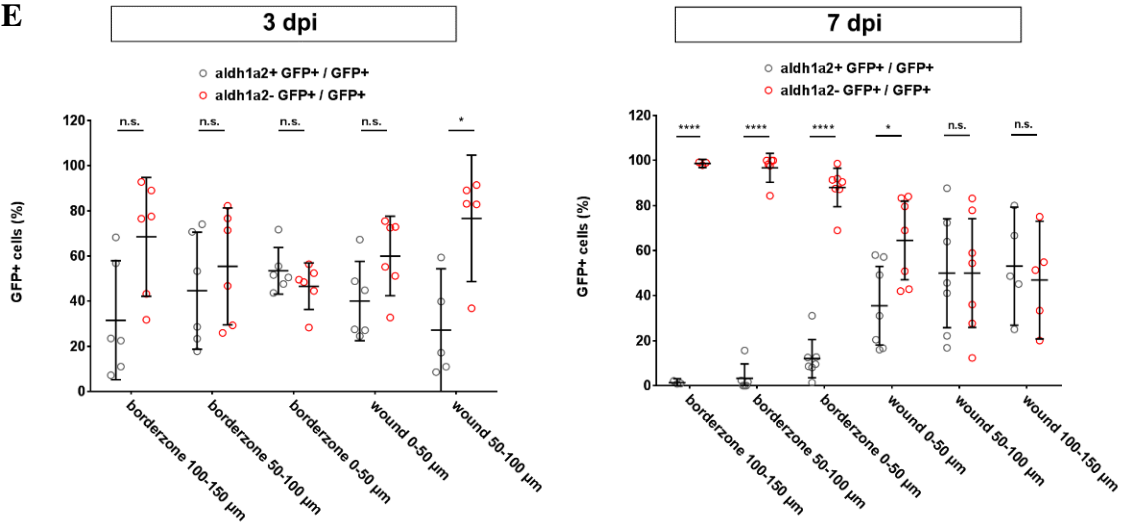
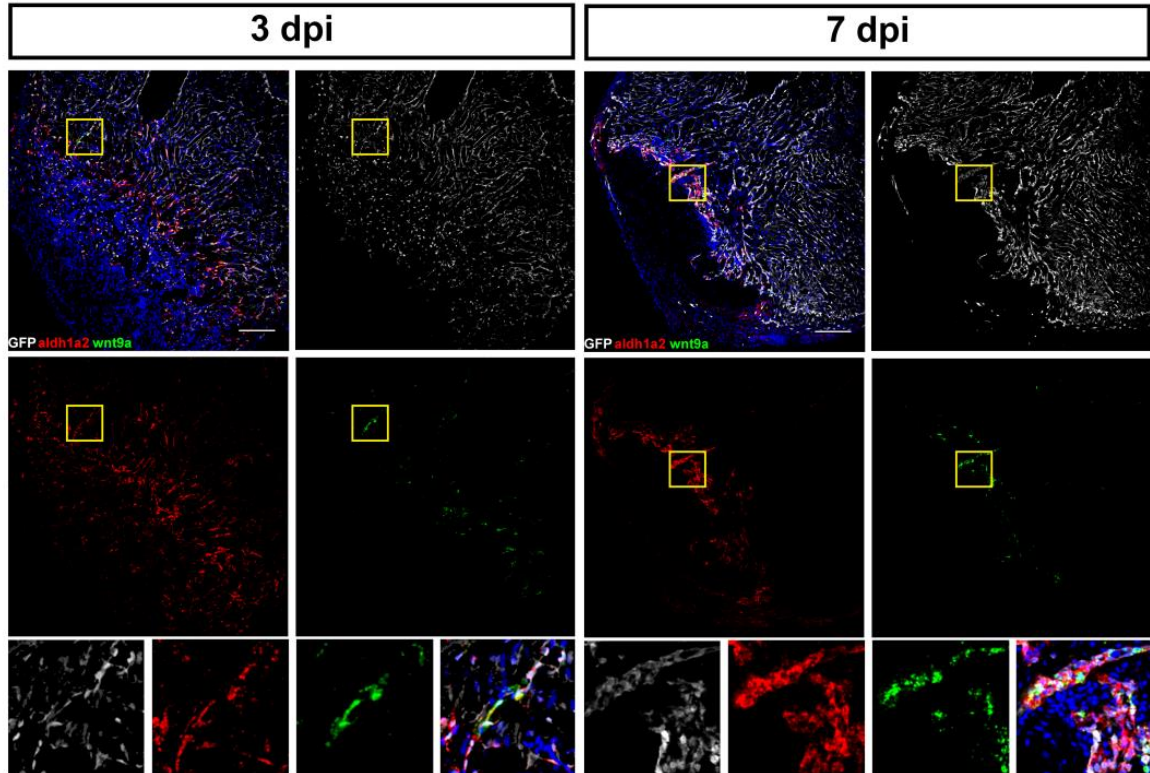
Figure 14. Global Wnt/ β -catenin loss of function does not impact on morphological regeneration

- (A) Axin1 overexpression from 1 to 21 dpi does not impair morphological regeneration compared to heat shocked wild type siblings. Wound area is outlined in red. MF20: green. Error bars, mean \pm CI 95%. n=7, 7; unpaired two-tail t-test; n.s.: $p > 0.05$.
- (B) Dkk1 overexpression from 1 to 21 dpi does not impair morphological regeneration compared to heat shocked wild type siblings. Wound area is outlined in red. MF20: green. Scale bar, 100 μ m. Error bars, mean \pm CI 95%. n=9, 8; unpaired two-tail t-test; n.s.: $p > 0.05$.

A small qPCR screen of selected Wnt ligands identifies wnt9a upregulation upon injury

According to the current model of Wnt signaling, due to the hydrophobicity of lipidated Wnt ligands, these proteins have a limited diffusion range from their secretion site. Thus, Wnt ligands must be expressed in the same cells in which the pathway is active, or in cells in their close proximity (defined as autocrine or paracrine effect, respectively) (Parchure et al. 2018). We then performed qRT-PCR for a subset of zebrafish Wnt ligands on RNA isolated from whole hearts to check which genes were upregulated in regenerating hearts (arbitrarily defined as having a $\Delta\Delta C_t$ lower than -2 relative to sham injured hearts). No tested ligand significantly changed its expression upon injury except for *wnt9a*, which showed clear upregulation at 7 dpi compared to sham injured hearts (Figure 15A). We performed *in situ* hybridization to define more clearly the expression pattern of *wnt9a*. No *wnt9a* expression was detected in sham injured hearts, while at 3 and 7 dpi it was upregulated only in endothelial cells (labeled by the *kdrl:EGFP* transgene) (Figure 15B). No expression could be detected in either cardiomyocytes or leukocytes (labeled by the *coro1a:EGFP* transgene) (Figure 15B,C). Quantification of the ratio of endothelial cells expressing *wnt9a* showed strongest upregulation in the region around the wound border at 3 dpi, whereas at 7 dpi the highest percentage of *wnt9a*⁺ cells was found in the re-vascularizing endothelium within the wound (Figure 15D). Such shift in the spatiotemporal expression of *wnt9a* resembles the pattern also observed for *aldh1a2* in endothelial cells from 3 to 7 dpi (Figure 15E). *Aldh1a2* is a limiting enzyme involved in the production of retinoic acid (RA), and is upregulated in endothelial cells in response to injury (Kikuchi et al. 2011). By double *in situ* for *wnt9a* and *aldh1a2*, we showed strong colocalization between the two transcripts (Figure 15F). Quantification of mRNA expression confirmed that *aldh1a2*⁺ endothelial cells express *wnt9a* more broadly compared to *aldh1a2*⁻ endothelial cells (Figure 15G). Thus, it seemed that retinoic acid signaling and *wnt9a* expression might be associated during regeneration. This prompted us to investigate whether retinoic acid regulates Wnt signaling, and thus we treated injured fish with drugs that induce gain of function (RA) or loss of function (DEAB and Citral) of the retinoic acid pathway. However, at 3 dpi no effect was observed in *axin2* expression in cardiomyocytes upon drug treatment from 1 to 3 dpi compared to solvent treated controls (Figure 15H,I), indicating that the retinoic acid pathway does not act upstream of Wnt/ β -catenin. Incubation with RA also did not influence overall *wnt9a* levels in the myocyte-negative border zone (Figure 15J), and therefore we concluded that over-activation of retinoic acid signaling cannot increase *wnt9a* expression.



D**E****F**

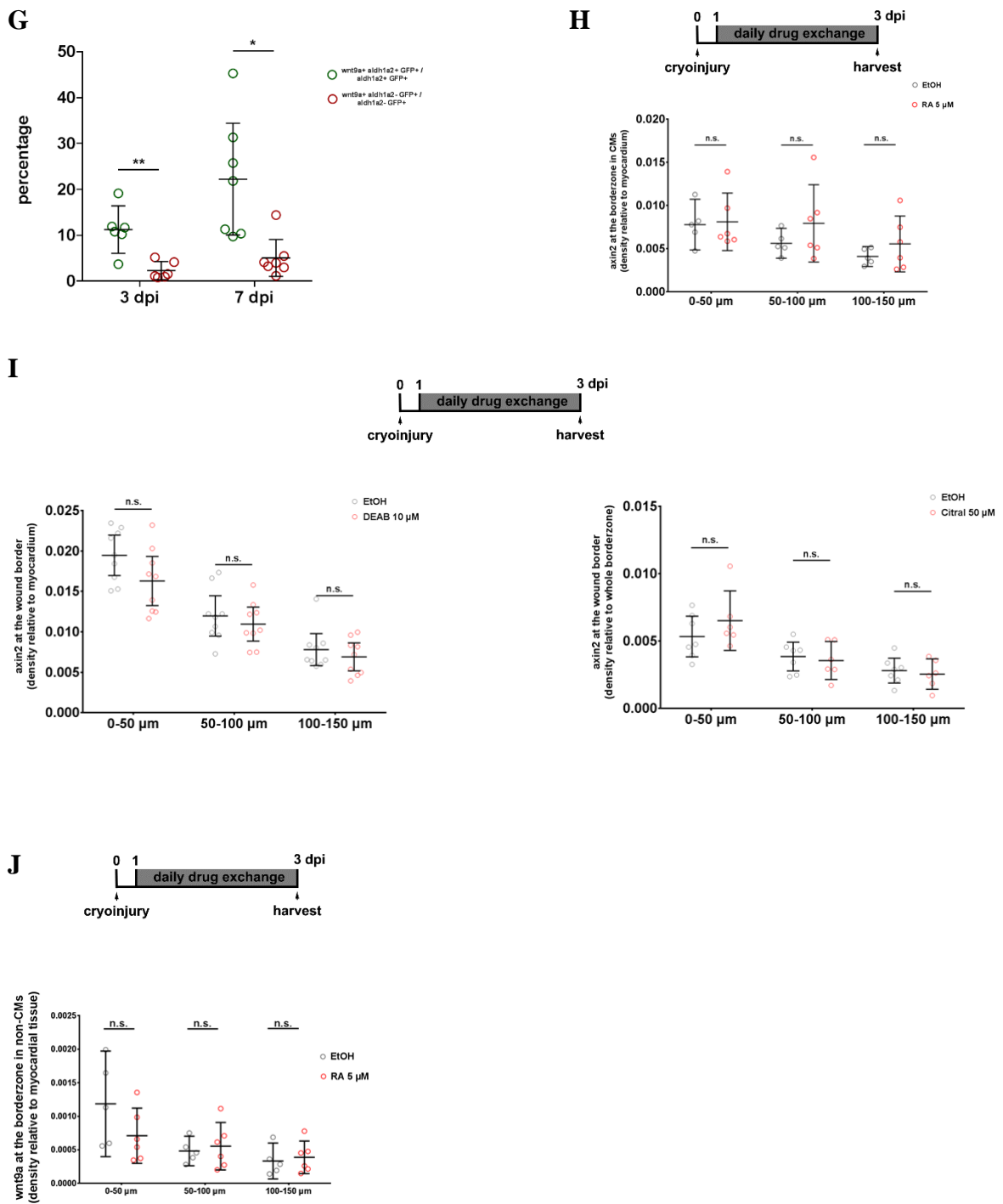


Figure 15. Wnt9a is upregulated in endothelial cells upon injury

- (A) qPCR on whole cryoinjured or sham injured ventricles shows *wnt9a* upregulation at 7 dpi compared to sham injury (outlined with dashed red line). All other tested ligands are not significantly upregulated upon cryoinjury. The two dotted grey lines mark an absolute difference in $\Delta\Delta Ct$ bigger than 2 relative to sham injured hearts.
- (B) *wnt9a* is expressed in endothelial cells (labeled by *kdrl:EGFP* transgene) at 3 and 7 dpi. No expression was detected in sham injured hearts or in cardiomyocytes (labeled by MF20) upon cryoinjury. *wnt9a*: red; GFP: green; MF20: grey. White arrow marks *wnt9a+ / GFP+* endothelial cells. Yellow rectangles mark the region magnified in the corresponding insets. n=6, 6, 6.

- (C) *wnt9a* is not expressed in leukocytes (labeled by *coro1a:EGFP* transgene) either at 3 or 7 dpi. Yellow rectangles mark the region magnified in the corresponding insets. *wnt9a*: red; GFP: green; MF20: grey. Scale bar, 100 μ m. n=6, 6, 6.
- (D) Quantification of data shown in (B). At 3 dpi, *wnt9a* is mostly expressed in endothelial cells close to the wound border and in the border zone, while at 7 dpi its expression shifts more towards the re-vascularizing endocardium inside the wound. Error bars, mean \pm CI 95%. n=6, 6 (3 dpi); n=6, 7 (7 dpi); one-way ANOVA plus Tukey's multiple comparisons test; n.s.: $p>0.05$, *: $p<0.05$, **: $p<0.01$.
- (E) At 3 dpi, *aldh1a2* expression in endothelial cells is highest in the zone around the wound border, whereas at 7 dpi almost exclusively endothelial cells inside the wound express *aldh1a2*. GFP labels endothelial cells. Error bars, mean \pm CI 95%. n=6 (3 dpi), n=7 (7 dpi); one-way ANOVA plus Tukey's multiple comparisons test; n.s.: $p>0.05$, *: $p<0.05$, **: $p<0.01$, ****: $p<0.001$.
- (F) Both at 3 and 7 dpi, most of *wnt9a* transcripts colocalize with *aldh1a2* in the same endothelial cells. Yellow rectangles mark the region magnified in the corresponding insets. *wnt9a*: green; GFP: grey; *aldh1a2*: red. Scale bar, 100 μ m. GFP labels endothelial cells. n=6, 6.
- (G) *wnt9a* is expressed more in *aldh1a2*⁺ endothelial cells (green) than in *aldh1a2*⁻ endothelial cells (red) around the wound border or inside the wound, at 3 or 7 dpi, respectively. GFP labels endothelial cells. Error bars, mean \pm CI 95%. n=6, 7; unpaired two-tail t-test; *: $p<0.05$, **: $p<0.01$.
- (H) Gain of function of retinoic acid signaling by RA treatment from 1 to 3 dpi does not affect Wnt/ β -catenin signaling at the wound border, based on *axin2* expression in cardiomyocytes. Error bars, mean \pm CI 95%. n=5, 6; one-way ANOVA plus Tukey's multiple comparisons test; n.s.: $p>0.05$.
- (I) Loss of function of retinoic acid signaling by DEAB or Citral treatment from 1 to 3 dpi does not affect Wnt/ β -catenin signaling at the wound border, based on *axin2* expression in cardiomyocytes. Error bars, mean \pm CI 95%. n=9, 9; n=7, 6; one-way ANOVA plus Tukey's multiple comparisons test; n.s.: $p>0.05$.
- (J) Over-activation of the retinoic acid pathway by RA treatment from 1 to 3 dpi does not affect overall *wnt9a* expression in the area within the first 150 μ m from the wound border negative for cardiomyocyte marker. Error bars, mean \pm CI 95%. n=5, 6; one-way ANOVA plus Tukey's multiple comparisons test; n.s.: $p>0.05$.

Discussion

The presented results focused on two different aspects in the context of cardiac repair in zebrafish, namely:

- 1) Quantitative analysis of cardiomyocyte restoration upon cryoinjury.
- 2) The role of Wnt/ β -catenin signaling in regenerating hearts.

Here I present the discussion for both topics under separate chapter headings.

A model for zebrafish heart regeneration by complete cardiomyocyte regeneration

Zebrafish heart regeneration has been described as complete based on the commonly accepted proxies of relative wound area and cardiomyocyte proliferation. However, while there is a consensus that injured zebrafish hearts can resolve most, if not all, scar tissue (Poss et al. 2002, Schnabel et al. 2011, Chablais et al. 2011, Gonzalez-Rosa et al. 2011), complete restoration of the myocardium lost to injury has actually never been proven. We settled this crucial question by providing the first quantitative report of cardiomyocyte numbers in the zebrafish heart, in which we showed that zebrafish can fully restore the pre-injury cardiomyocyte number. Based on our results, we conclude that cardiomyocyte regeneration in response to injuries that kill about 1/3 of the cardiomyocytes is already completed by four weeks post injury, and results in faithful restoration of most aspects of myocardial morphology, in particular the septation of trabecular and compact myocardial layers (Figure 16). In contrast, at this time-point, wound tissue has only been fully resorbed in 30% of injured hearts, whereas the remaining 70% still display some residual scarring (Figure 16). Interestingly, in our hands overall wound size did not change significantly between 30 dpi and 90 dpi, and the number of hearts containing wounds did not drop either. Thus, hearts with residual wounds at 30 dpi might never resolve them, or at least degrade them at an extremely slow rate (Figure 16). While the remaining scar tissue is very small (2% of ventricle area at 90 dpi), our results surprisingly indicate that - at least in response to cryoinjury - full restoration of pre-injury cardiomyocyte numbers is a more robust feature of zebrafish heart regeneration than scar-free healing. In support of this idea, ECM-producing fibroblasts have recently been shown to be incompletely eliminated in regenerating hearts (Sanchez-Iranzo et al. 2018b). Failure to fully resolve wounds or to

eliminate fibroblasts within a reasonable experimental time frame might explain why published data on restoration of heart function are somewhat conflicting. One study on cardiac performance, measured by echocardiography, reported that heart function after cardiomyocyte ablation recovered within 45 days (Wang et al. 2011), while functional recovery after cryoinjury was found to take 180 days (Hein et al. 2015). Yet other studies showed that pumping function based on relative fractional volume shortening recovered within 60 days in cryoinjured hearts, while ventricular wall motion remained altered even after 140 and 180 days (Gonzalez-Rosa et al. 2011, Hein et al. 2015). We suggest that zebrafish heart regeneration can be considered complete in the sense that all cardiomyocytes are regenerated, while in response to cryoinjury many hearts retain small, yet detectable signs of scarring. One important observation from our results is that the number of restored cardiomyocytes at any given timepoint does not fully correlate with wound size. At early stages of regeneration (up to at least 14 dpi) the relative wound area (in relation to ventricle size) appears to be lower than the ratio of restored cardiomyocytes. While this might suggest slightly different dynamics between wound shrinkage and cardiomyocyte proliferation, we cannot exclude that such differences were at least partly due to the initial discrepancy between the percentage of wound area and missing cardiomyocytes that we measured at 3 dpi. Such discrepancy might be explained by intrinsic limitations in either or both assays to capture the precise extent of both scar resolution and cardiomyocyte regeneration at the same time. However, if cardiomyocyte regeneration and wound resorption truly occur partly independently of each other, they might also be regulated independently. Indeed, miR-101a has been shown to differentially regulate cardiomyocyte proliferation and scar removal: it inhibits cardiomyocyte cell cycle entry, but promotes wound tissue resorption (Beauchemin et al. 2015). It will be interesting to see whether additional specific regulators of these processes will emerge in the future. Another conclusion that we can draw from our results is that all cardiomyocytes that show cell cycle activity based on S-phase markers indeed proliferate during regeneration. In fact, a very simple model assuming that all PCNA⁺ cardiomyocytes present at the wound border proliferate with a cell cycle length of 24 hours could predict complete cardiomyocyte regeneration within four weeks post injury. Thus cardiomyocyte cell cycle activity (PCNA or BrdU/EdU) can be used to measure cardiomyocyte proliferation, since confounding issues like endoreplication and failure to undergo cytokinesis that frequently occur in post-natal mammalian cardiomyocytes seem to be very rare in zebrafish during heart regeneration (González-Rosa et al. 2018). A previous study on zebrafish heart

regeneration has used histological methods such as AFOG staining to identify the regenerate based on locally thickened myocardium with intermingled scar, and suggested that the morphology of the myocardium is not faithfully regenerated as newly produced cardiomyocytes show a cortical-like morphology even in regions where trabecular myocardium was present before injury (Gonzalez-Rosa et al. 2018). In contrast, we found no evidence that the relative proportion of cortical and trabecular myocardium changes during regeneration based on a specific molecular marker of the cortical layer. Whereas AFOG staining, which another study has used to detect morphological alterations, can clearly label deposited scar in contrast to the healthy tissue, and to some extent distinguish gross differences in tissue morphology, its validity might be limited to reliably distinguish between cortical and trabecular myocardium. Generally, we conclude that the regenerated myocardium retains normal morphology. Only in those hearts where full resolution of wound tissue fails, some morphological alterations of a small region of the myocardium occur: since the full number of cardiomyocytes regenerates and the ventricle does not increase in size, some of the cardiomyocytes must be present in a smaller space than prior to injury. Thus, the myocardial wall that encloses the scar (which is almost always internalized) consists of cardiomyocytes that are smaller in size and cardiomyocyte density is higher in this area.

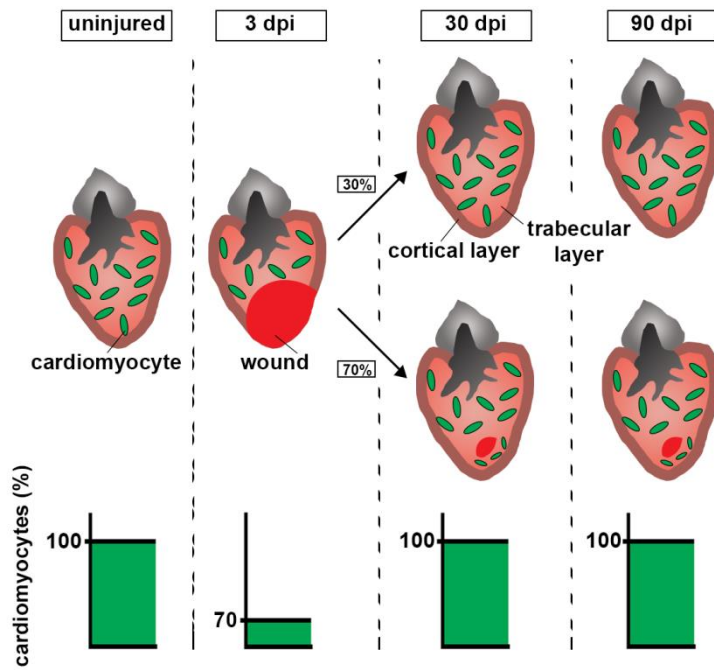


Figure 16. A model for zebrafish heart regeneration by complete cardiomyocyte regeneration

Model of the time-courses of cardiomyocyte regeneration and wound resorption. Restoration of pre-injury cardiomyocyte numbers (green) in response to cryoinjury, which kills about 30% of the cardiomyocytes, is achieved within 30 days, restoring the pre-injury morphological septation between trabecular layer (pink) and cortical layer (brown). Despite completed cardiomyocyte regeneration, the majority of hearts still contain small wounds at 30 dpi. Regenerated cardiomyocytes enclosing these wounds are smaller in size and more densely packed. After four weeks post injury, residual wounds remain mostly unresolved.

Wnt/ β -catenin signaling in zebrafish heart regeneration

Activation of Wnt/ β -catenin in the regenerating adult zebrafish hearts

In this work, we showed that Wnt/ β -catenin is upregulated in adult zebrafish hearts in response to cryoinjury. Based on *axin2* expression, Wnt signaling was found to be reactivated in border zone cardiomyocytes and in endothelial cells that form the revascularized plexus inside the wound. Upon inhibition of Wnt/ β -catenin signaling by short term overexpression of Axin1, we confirmed that *axin2* is regulated by β -catenin in cardiomyocytes in the injured adult heart, and as such it can be considered a reliable readout for the pathway. Potential alternative readouts used in this study to detect cells with active Wnt signaling gave conflicting results. *ddk1b* and the *OTM:d2EGFP* reporter showed a much more spatially restricted expression compared to *axin2*. This discrepancy indicates that *axin2* could be regarded as a broader marker for Wnt/ β -catenin in multiple cell types, while *ddk1b* and the *OTM:d2EGFP* reporter mark only a subset of cardiomyocytes close to the wound border. It is tempting to speculate that the *ddk1b*⁺ or *egfp*⁺ cardiomyocytes might represent a subpopulation of cardiomyocytes with a specific dedifferentiation or proliferation state different from the rest of cardiomyocytes in the border zone, but further experiments would be required to test this hypothesis. Other tested readouts, namely *sp5a* and *sp5l*, can be clearly considered not target genes of β -catenin in the adult regenerating hearts or, as for the *top:GFP* reporter, not responsive to changes in Wnt activity after cryoinjury. Such broadly diverse expression patterns among different (trans)genes offer a cautionary tale in the use of specific markers to detect activation of a pathway upon treatments. Multiple readouts should always be tested, in order to avoid misinterpretations due to spatiotemporal differences in expression or due to silencing in one or more cell types. Another instance of such issue was reported also in the zebrafish fin, where *lef1* was found expressed in the epidermis upon amputation. However, Wnt/ β -catenin signaling, detected with the *7xTCF-Xla.Sia:NLS-mCherry*^{ia5Tg} reporter construct, could not be reported in this tissue, suggesting that epidermal *lef1* expression is not directly regulated by the pathway (Wehner et al. 2014). Thus, even though *lef1* is a direct Wnt target gene in many other organs, it cannot be considered a proper readout for Wnt/ β -catenin signaling in the regenerating zebrafish fin.

Also in non-regenerating adult murine hearts, Wnt signaling is active in the myocardium from 7 days post-MI. Stabilized β -catenin was reported in the infarct border zone of the myocardium (Palevski et al. 2017), while a more detailed analysis found β -catenin

accumulation in the endothelium of the rat heart after ischaemic injury (Blankesteyn et al. 2000). Based on the TOPGAL reporter, Wnt/ β -catenin was found to be upregulated in endothelial cells and myofibroblasts (Aisagbonhi et al. 2011), or in the epicardium and cardiac fibroblasts (Duan et al. 2012). Using the Axin2-lacZ reporter, active Wnt/ β -catenin was detected in the whole heart after MI (Palevski et al. 2017), while another study reported activation of Wnt signaling specifically in progenitor cells, leukocytes and endothelial cells (Oerlemans et al. 2010). In the regenerating neonatal mouse heart, lineage tracing of Wnt-responsive cells based on Axin2-CreERT2 showed active Wnt signaling only in epicardial cells and fibroblasts after cryoinjury (Mizutani et al. 2016). While we observed similar upregulation of *axin2* in endothelial cells, we did not check for *axin2* expression in reporter lines for leukocytes, fibroblasts or epicardial cells, thus we cannot exclude activation of Wnt/ β -catenin also in these cell types in the zebrafish heart in response to injury. However, in none of the aforementioned studies Wnt/ β -catenin activity was clearly reported in mature cardiomyocytes in the healthy myocardium. Thus it seems that, unlike in zebrafish, murine cardiomyocytes in vivo are not Wnt-responsive after injury, at any stage after birth. This suggests that reactivation of Wnt/ β -catenin in cardiomyocytes could be one of the key features that contribute to the peculiar regenerative capacity of the adult zebrafish heart. Which stimuli might lead to activation of the endogenous Wnt pathway in zebrafish cardiomyocytes after injury is currently unknown. One intriguing possibility is hypoxia: it has been reported that in vitro embryonic stem cells respond to hypoxic environment by activating hypoxia-inducible factor HIF1 α , which in turn regulates expression of the Wnt target genes Lef1 and Tcf1 (Mazumdar et al. 2010). Since zebrafish hearts require hypoxic conditions to induce cardiomyocyte dedifferentiation and proliferation via HIF1 α (Jopling et al. 2012), this may potentially be the factor that triggers activation of the Wnt pathway upon injury.

The role of Wnt/ β -catenin in zebrafish cardiac repair

Wnt/ β -catenin signaling can play opposite effects on the proliferative response after injury in different organs or species. In zebrafish, for instance, it is known that Wnt/ β -catenin is required and sufficient to promote proliferation of mesenchymal and epithelial cells during fin regeneration (Stoick-Cooper et al. 2007). In adult mammals, active Wnt/ β -catenin signaling in physiological conditions is maintained only in specific organs with high cell turnover, such as the hematopoietic niche, the intestinal epithelium and the epidermis, and it is considered a promoting factor for stem cell renewal. However, in other organs or

tissues, the Wnt pathway is usually silent and is reactivated only after injury, as reported for instance in lung, kidney, skin, skeletal muscle and liver (reviewed in Bastakoty and Young 2016), as well as in osteoprogenitor cells during bone regeneration in mice (Kim et al. 2007). In such organs with moderate to high regenerative capacity, active Wnt/ β -catenin contributes to proliferation and differentiation of progenitor cells during the repair process. However, in the injured adult rodent heart, Wnt/ β -catenin exerts an anti-proliferative and anti-differentiation effect on cardiac progenitors (Oikonomopoulos et al. 2011, Zelarayán et al. 2008). In addition, the Wnt pathway was reported to be detrimental to cardiomyocyte survival by stimulating apoptosis in the infarct zone (Zhang et al. 2009, Mirotsoou et al. 2007, Oikonomopoulos et al. 2011), even though a different study demonstrated an opposite pro-survival effect of Wnt/ β -catenin in cardiomyocytes (Hahn et al. 2006). Hence, there is a consensus that Wnt/ β -catenin usually plays a positive role on proliferation in most organs capable to regenerate at least to some extent, whereas it has a detrimental effect on the proliferative response in a non-regenerative organ such as the adult mammalian heart. Thus, the finding that Wnt/ β -catenin positively regulates zebrafish cardiomyocyte proliferation in the injured heart fits this notion. A short inhibition of the pathway (6 hours) was not sufficient to reduce the proliferation index of cardiomyocytes, which might potentially indicate an indirect effect on cardiomyocyte cell cycle re-entry. However, in most of the studies on zebrafish heart regeneration published so far, the proliferation index was measured at least 24 hours post treatment (Karra et al. 2015, Zhao et al. 2014, Huang et al. 2013, Chablais and Jazwińska, 2012, Kikuchi et al. 2011), except for Wu et al. 2016, in which a difference in cardiomyocyte proliferation was detectable already after 6 hours post treatment. Thus, up to date, evidence for such a fast-acting effect on cardiomyocyte cell cycle re-entry is reported solely for BMP signaling. Wnt/ β -catenin, as well as possibly other signaling pathways, might require a longer time frame to exert its pro-proliferative role.

In this study, we tried to achieve cell autonomous inhibition of Wnt/ β -catenin by employing two different genetic tools, the TetON- and the Cre/Lox-based system. However, based on the analysis of mosaic expression in border zone cardiomyocytes, we could observe an effect on cycling activity only with the Cre/Lox recombination. This might reflect unknown limitations of the TetON system related to this kind of analysis. One possibility could be that expression level of the transgene by drug treatment is lower than what obtained by heat shock treatment, even though, by immunofluorescence for YFP

and nlsTomato, no clear difference in average intensity was visible in the subset of cardiomyocytes expressing the transgenes.

Despite these technical obstacles, our data on impaired cardiomyocyte cell cycle re-entry upon cell autonomous inhibition of Wnt/ β -catenin suggest that Wnt signaling acts directly in cardiomyocytes to promote their proliferative response. Since cardiac progenitors do not contribute significantly to the regenerated myocardium in zebrafish (Jopling et al. 2010; Kikuchi et al. 2010), such direct effect on mature cardiomyocytes appears in contrast to what happens in mammals; in fact, in the infarcted murine heart, Wnt/ β -catenin does not affect proliferation of pre-existing cardiomyocytes, but rather represses differentiation of cardiac progenitor cells (Zelarayán et al. 2008), consistently with the negative role of this pathway in the later phases of heart development. However, since over-activation of the pathway was not sufficient to increase proliferation rate in zebrafish cardiomyocytes beyond physiological levels, we must conclude that Wnt/ β -catenin acts in concert with other mechanisms to induce cardiomyocyte cell cycle re-entry.

In this work we showed that Wnt/ β -catenin signaling promotes partly also cardiomyocyte dedifferentiation. In studies employing gain or loss of function approaches, many pathways known to affect cardiomyocyte proliferation have been shown to induce changes in diverse cardiomyocyte differentiation markers. For instance, BMP signaling is required for downregulation of *myl7* and re-expression of *myh7* (Wu et al. 2016), Notch induces *hand2* and *nkx2.5* expression while dampening *mylk3*, *vmhc* and *tcap* levels (Münch et al. 2017), NF- κ B is important for the re-activation of the *-14.8gata4:GFP* transgene and downregulation of Troponin T (Karra et al. 2015) and Nrg1 is sufficient to induce *-14.8gata4:GFP* reporter activity as well as disorganization of sarcomeres (Gemberling et al. 2015). While this variability might simply reflect a limitation in which differentiation markers were reported in such studies, it is entirely possible that different pathways regulate different features of the dedifferentiation process in cardiomyocytes. Hence, our results suggest that Wnt/ β -catenin is required, among the differentiation markers tested so far, only for the upregulation of *myh7*. This gene, also referred to as embryonic cardiac myosin heavy chain (embCMHC), encodes the beta (or slow) heavy chain subunit of cardiac myosin and is normally expressed in the ventricle during embryogenesis and in regenerating adult zebrafish hearts (Sallin et al. 2015). Of note, Wnt/ β -catenin signaling induces formation of slow myosin heavy chains, both in cultured fetal myoblasts and in embryonic skeletal muscles (Kuroda et al 2013), and β -catenin positively modulates the

number of slow myofibers during fetal myogenesis (Hutcheson et al. 2009). However, the functional significance of developmental myosins during regeneration is still unclear. This myosin isoform may permit the modification of the sarcomere structure providing a higher cellular plasticity that is needed for proliferation, migration and morphogenesis (Maggs et al. 2000). It is thus possible that Wnt-dependent re-expression of this embryonic form of myosin heavy chain is important to allow cytokinesis in zebrafish cardiomyocytes.

In the adult murine heart, Wnt/ β -catenin promotes a pro-fibrotic response important for preserving cardiac function in the days immediately after MI, which is however detrimental to heart repair and eventually leads to pathological remodeling in the long term (Duan et al. 2012, Palevski et al. 2017, Moon et al. 2017, Bastakoty et al. 2016). In the injured zebrafish heart, even though Wnt/ β -catenin inhibition impaired cardiomyocyte proliferation, it did not affect the dynamics of scar resorption. It is possible that blockage of Wnt signaling for 21 days post injury is not sufficient to detect an effect on morphological regeneration. In many studies on zebrafish heart repair, the time point to assess the extent of regeneration upon treatment was usually set at 30 days post amputation or cryoinjury (Karra et al. 2015, Zhao et al. 2014, Huang et al. 2013, Chablais and Jaźwińska, 2012), with the exception of the study on BMP signaling, in which wound size was measured at 21 dpi (Wu et al. 2016). An alternative explanation would imply that Wnt/ β -catenin is not required for scar removal. Such exclusive effect on cardiomyocyte proliferation would not be unprecedented, since retinoic acid production, important for the proliferative response in cardiomyocytes, was not proven necessary for morphological regeneration of the myocardium (Kikuchi et al. 2011).

Expression of Wnt ligands in the zebrafish heart in response to injury

Within the first two weeks post MI in adult mice, several Wnt ligands show increased expression in the whole heart, including Wnt1, Wnt2, Wnt4, Wnt7a, Wnt10b, and Wnt11 (reviewed in Deb 2014). A more recent study reported upregulation of Wnt9a, Wnt4 and Wnt3a and downregulation of Wnt8a, Wnt5a, Wnt11 and Wnt7b in the infarcted murine heart (Palevski et al. 2017). A comprehensive analysis of Wnts *in situ* expression in the neonatal mouse heart upon cryoinjury (Mizutani et al. 2016) showed upregulation of Wnt2b and Wnt5a in the epicardium, Wnt9a in both epicardium and myocardium, while Wnt3a, Wnt4, Wnt5b, Wnt6, Wnt8a, Wnt9b and Wnt10b only in the myocardium.

Since we observed upregulation of Wnt9a also in the regenerating zebrafish heart, this suggests that expression of this ligand is a response to cardiac injury conserved both in zebrafish and mice, although its role in this context is currently unknown. In chick, Wnt9a is essential for morphogenesis and proliferation of the hepatic epithelium (Matsumoto et al. 2008) and mediates atrioventricular cardiac cushion development (Person et al. 2005). In zebrafish, Wnt9a regulates palate morphogenesis (Rochard et al. 2016) and hematopoietic stem cell development (Grainger et al. 2016). Interestingly, Wnt9a has been reported to signal in both a β -catenin-dependent (Matsumoto et al. 2008, Grainger et al. 2016) and -independent (Landeira et al. 2015, Ali et al. 2016) manner; Wnt9a has also been described to signal in a paracrine fashion in different organs (Matsumoto et al. 2008, Grainger et al. 2016, Rochard et al. 2016). Thus, expression of Wnt9a in the endocardium of injured zebrafish hearts could potentially activate Wnt/ β -catenin both in neighbouring endothelial cells and in cardiomyocytes at the wound border, although we cannot exclude that it might not act through β -catenin. In cultured endothelial cells, activation of Wnt/ β -catenin was sufficient to induce EndMT and myofibroblast formation (Aisagbonhi et al. 2011). This suggests that, if Wnt9a acts through β -catenin, it might be involved in a similar function also in the injured zebrafish heart.

In murine ESCs, administration of RA increases the expression of Wnt ligands and receptors, as well as β -catenin-mediated downstream signaling (Osei-Sarfo and Gudas 2014). In our study, significant enrichment of *wnt9a* transcripts in endothelial cells expressing *aldh1a2* suggested a similar role for retinoic acid signaling in regulating Wnt ligands or their downstream effectors. However, manipulation of retinoic acid signaling did not result in changes in Wnt activity, indicating that after injury this pathway does not act upstream of β -catenin. While retinoic acid signaling gain of function by RA treatment did not induce increased *wnt9a* expression, a loss of function approach would be required to clearly verify if retinoic acid is required for the expression of this ligand. Interestingly, in zebrafish fin regeneration, *aldh1a2* is actually a downstream target of Wnt/ β -catenin that regulates blastemal cell proliferation (Wehner et al. 2014). In future work, it might be interesting to investigate whether this direct Wnt/ β -catenin – retinoic acid signaling axis is also conserved in the regenerating heart.

Finally, changes in expression, or lack thereof, of Wnt ligands upon injury based on analysis of whole hearts might hide subtle or even opposite changes in specific cell types. For instance, *wnt5a* expression was found to be generally lower in the entire myocardium

after MI, while the same study reported strong upregulation of this ligand in macrophages (Palevski et al. 2017). Hence, ligands other than Wnt9a might also be expressed during zebrafish heart regeneration in specific cell populations or in different regions of the injured ventricle.

Conclusion

Overall, our data suggest that regeneration of cardiomyocytes is complete and happens surprisingly fast within four weeks post cryoinjury, with faithful restoration of overall myocardial morphology. Only in those hearts that have not fully resolved residual scar by the time cardiomyocyte regeneration is complete, the subset of cardiomyocytes that encloses the wound border is smaller than usual and more densely packed.

Wnt/ β -catenin signaling gets reactivated during regeneration both in cardiomyocytes and endothelial cells, and expression of Wnt9a ligand is prominent in endothelial cells after injury. Wnt/ β -catenin is required, likely in a cell autonomous manner, to promote cardiomyocyte dedifferentiation and proliferation, while it is dispensable for morphological regeneration of the myocardium.

Summary

Background

Unlike mammals, zebrafish can achieve scar-free healing of heart injuries, which is associated with dedifferentiation and cell cycle re-entry of cardiomyocytes. However, it is unknown to which extent cardiomyocytes lost to injury are restored, since only indirect evidences of myocardial regeneration exist thus far. In addition, while Wnt signaling has been shown to induce fibrosis and prevent production of new cardiomyocytes in the infarcted murine heart, involvement of this pathway in zebrafish cardiac regeneration has not been yet investigated. Hence, we set out to provide the first absolute quantification of cardiomyocyte numbers before and after injury in zebrafish, as well as to address whether Wnt signaling impinges on cardiomyocyte proliferation and wound healing.

Methods

Firstly, we used stereological methods to quantify the number of cardiomyocytes on heart sections at 3, 14, 30 and 90 days post cryoinjury. Based on histological markers, we investigated the morphology of the regenerated myocardium. Secondly, we performed quantitative PCR and in situ hybridization to check whether Wnt signaling is active, and which Wnt ligands are expressed in the injured heart. Finally, we employed genetic tools for Wnt/ β -catenin manipulation and measured proliferation and dedifferentiation in cardiomyocytes, as well as wound resorption, upon inhibition of the pathway.

Results

We found that injured zebrafish hearts did regenerate to the pre-injury number of cardiomyocytes already within four weeks. Mathematical modeling indicated that all cardiomyocytes that enter the cell cycle at the wound border actually proliferate. The regenerated myocardium does not display signs of altered morphology compared to uninjured hearts. Thus, we establish that zebrafish can indeed completely and faithfully regenerate the ventricular myocardium. Surprisingly, full cardiomyocyte regeneration also occurred in hearts that retained scars, indicating that cardiomyocyte regeneration is more efficient than scar-free healing. In addition, we found that Wnt/ β -catenin signaling is active in regenerating hearts both in cardiomyocytes and in endothelial cells. Blockade of the pathway impairs cardiomyocyte dedifferentiation and proliferation, likely in a cell autonomous manner. However, Wnt signaling has no significant effect on scar removal.

Finally, we found significant upregulation of the Wnt9a ligand in endothelial cells after injury.

Conclusions

Our results show that zebrafish cardiomyocyte regeneration is efficient and complete, and it does not require complete scar removal. Wnt/ β -catenin is an important player in this process, since it is required to promote cell cycle re-entry and dedifferentiation of pre-existing cardiomyocytes.

List of references

- Aisagbonhi, O., Rai, M., Ryzhov, S., Atria, N., Feoktistov, I., Hatzopoulos, A.K. (2011). Experimental myocardial infarction triggers canonical Wnt signaling and endothelial-to-mesenchymal transition. *Dis Model Mech.* 4:469-83.
- Ali, I., Medegan, B., Braun, D.P. (2016). Wnt9A Induction Linked to Suppression of Human Colorectal Cancer Cell Proliferation. *Int J Mol Sci.* 17:495.
- Angers, S., Moon, R.T. (2009). Proximal events in Wnt signal transduction. *Nat Rev Mol Cell Biol.* 10:468-77.
- Bastakoty, D., Young, P.P. (2016). Wnt/ β -catenin pathway in tissue injury: roles in pathology and therapeutic opportunities for regeneration. *FASEB J.* 30:3271-3284.
- Bastakoty, D., Saraswati, S., Joshi, P., Atkinson, J., Feoktistov, I., Liu, J., Harris, J.L., Young, P.P. (2016). Temporary, Systemic Inhibition of the WNT/ β -Catenin Pathway promotes Regenerative Cardiac Repair following Myocardial Infarct. *Cell Stem Cells Regen Med.* 2.
- Beauchemin, M., Smith, A., Yin, V.P. (2015). Dynamic microRNA-101a and Fosab expression controls zebrafish heart regeneration. *Development.* 142:4026-37.
- Beers, M.F., Morrisey, E.E. (2011). The three R's of lung health and disease: repair, remodeling, and regeneration. *J Clin Invest.* 121:2065-73.
- Behrens, J., von Kries, J.P., Kühl, M., Bruhn, L., Wedlich, D., Grosschedl, R., Birchmeier, W. (1996). Functional interaction of beta-catenin with the transcription factor LEF-1. *Nature.* 382:638-42.
- Blankesteyn, W.M., van Gijn, M.E., Essers-Janssen, Y.P., Daemen, M.J., Smits, J.F. (2000). Beta-catenin, an inducer of uncontrolled cell proliferation and migration in malignancies, is localized in the cytoplasm of vascular endothelium during neovascularization after myocardial infarction. *Am J Pathol.* 157:877-83.
- Cadigan, K.M., Waterman, M.L. (2012). TCF/LEFs and Wnt signaling in the nucleus. *Cold Spring Harb Perspect Biol.* 4.
- Chablais, F., Veit, J., Rainer, G., and Jaźwińska, A. (2011). The zebrafish heart regenerates after cryoinjury-induced myocardial infarction. *BMC Dev. Biol.* 11, 21.

Chablais, F., and Jazwinska, A. (2012). The regenerative capacity of the zebrafish heart is dependent on TGF β signaling. *Development* 139, 1921–1930.

Chen, L., Wu, Q., Guo, F., Xia, B., Zuo, J. (2004). Expression of Dishevelled-1 in wound healing after acute myocardial infarction: possible involvement in myofibroblast proliferation and migration. *J Cell Mol Med.* 8:257-64.

Chen, Y., Whetstone, H.C., Lin, A.C., Nadesan, P., Wei, Q., Poon, R., Alman, B.A. (2007). Beta-catenin signaling plays a disparate role in different phases of fracture repair: implications for therapy to improve bone healing. *PLoS Med.* 4:e249.

Choi, W.-Y., Gemberling, M., Wang, J., Holdway, J.E., Shen, M.-C., Karlstrom, R.O., and Poss, K.D. (2013). In vivo monitoring of cardiomyocyte proliferation to identify chemical modifiers of heart regeneration. *Development* 140, 660–666.

Clevers, H., Nusse, R. (2012). Wnt/ β -catenin signaling and disease. *Cell.* 149:1192-205.

Deb, A. (2014). Cell-cell interaction in the heart via Wnt/ β -catenin pathway after cardiac injury. *Cardiovasc Res.* 102:214-23.

Dorsky, R.I., Sheldahl, L.C., Moon, R.T. (2002). A transgenic Lef1/ β -catenin-dependent reporter is expressed in spatially restricted domains throughout zebrafish development. *Developmental Biology.* 241:229-237.

Duan, J., Gherghe, C., Liu, D., Hamlett, E., Srikantha, L., Rodgers, L., Regan, J.N., Rojas, M., Willis, M., Leask, A., Majesky, M., Deb, A. (2012). Wnt1/ β catenin injury response activates the epicardium and cardiac fibroblasts to promote cardiac repair. *EMBO J.* 31:429-42.

Figeac, F., Uzan, B., Faro, M., Chelali, N., Portha, B., Movassat, J. (2010). Neonatal growth and regeneration of beta-cells are regulated by the Wnt/ β -catenin signaling in normal and diabetic rats. *Am J Physiol Endocrinol Metab.* 298:E245-56.

Filali, M., Cheng, N., Abbott, D., Leontiev, V., Engelhardt, J.F. (2002). Wnt-3A/ β -catenin signaling induces transcription from the LEF-1 promoter. *J Biol Chem.* 277:33398-410.

Galliot, B., Chera, S. (2010). The Hydra model: disclosing an apoptosis-driven generator of Wnt-based regeneration. *Trends Cell Biol.* 20:514-23.

Gemberling, M., Bailey, T.J., Hyde, D.R., and Poss, K.D. (2013). The zebrafish as a model for complex tissue regeneration. *Trends Genet.* 29, 611–620.

Gemberling, M., Karra, R., Dickson, A.L., and Poss, K.D. (2015). *Nrg1* is an injury-induced cardiomyocyte mitogen for the endogenous heart regeneration program in zebrafish. *Elife* 4.

Gessert, S., Köhl, M. (2010). The multiple phases and faces of wnt signaling during cardiac differentiation and development. *Circ Res.* 107:186-99.

González-Rosa, J.M., Martín, V., Peralta, M., Torres, M., and Mercader, N. (2011). Extensive scar formation and regression during heart regeneration after cryoinjury in zebrafish. *Development* 138, 1663–1674.

González-Rosa, J.M., Sharpe, M., Field, D., Soonpaa, M.H., Field, L.J., Burns, C.E., Burns, C.G. (2018). Myocardial Polyploidization Creates a Barrier to Heart Regeneration in Zebrafish. *Dev Cell.* 44:433-446.

Grainger, S., Richter, J., Palazón, R.E., Pouget, C., Lonquich, B., Wirth, S., Grassme, K.S., Herzog, W., Swift, M.R., Weinstein, B.M., Traver, D., Willert, K. (2016). *Wnt9a* Is Required for the Aortic Amplification of Nascent Hematopoietic Stem Cells. *Cell Rep.* 17:1595-1606.

Gupta, V., Gemberling, M., Karra, R., Rosenfeld, G.E., Evans, T., Poss, K.D. (2013). An injury-responsive *gata4* program shapes the zebrafish cardiac ventricle. *Curr Biol.* 23:1221-7.

Gurung, A., Uddin, F., Hill, R.P., Ferguson, P.C., Alman, B.A. (2009). Beta-catenin is a mediator of the response of fibroblasts to irradiation. *Am J Pathol.* 174:248-55.

Hahn, J.Y., Cho, H.J., Bae, J.W., Yuk, H.S., Kim, K.I., Park, K.W., Koo, B.K., Chae, I.H., Shin, C.S., Oh, B.H., Choi, Y.S., Park, Y.B., Kim, H.S. (2006). Beta-catenin overexpression reduces myocardial infarct size through differential effects on cardiomyocytes and cardiac fibroblasts. *J Biol Chem.* 281:30979-89.

Hayashi, T., Mizuno, N., Kondoh, H. (2008). Determinative roles of FGF and Wnt signals in iris-derived lens regeneration in newt eye. *Dev Growth Differ.* 50:279-87.

- Heallen, T., Zhang, M., Wang, J., Bonilla-Claudio, M., Klysiak, E., Johnson, R.L., Martin, J.F. (2011). Hippo pathway inhibits Wnt signaling to restrain cardiomyocyte proliferation and heart size. *Science*. 332:458-61.
- Heicklen-Klein, A., Evans, T. (2004). T-box binding sites are required for activity of a cardiac GATA-4 enhancer. *Developmental Biology*. 267:490-504.
- Hein, S.J., Lehmann, L.H., Kossack, M., Juergensen, L., Fuchs, D., Katus, H.A., Hassel, D. (2015). Advanced echocardiography in adult zebrafish reveals delayed recovery of heart function after myocardial cryoinjury. *PLoS One*. 10:e0122665.
- Huang, C.-J., Tu, C.-T., Hsiao, C.-D., Hsieh, F.-J., Tsai, H.-J. (2003). Germ-line transmission of a myocardium-specific GFP transgene reveals critical regulatory elements in the cardiac myosin light chain 2 promoter of zebrafish. *Developmental dynamics* 228:30-40
- Huang, Y., Harrison, M.R., Osorio, A., Kim, J., Baugh, A., Duan, C., Sucov, H.M., and Lien, C.-L. (2013). Igf Signaling is Required for Cardiomyocyte Proliferation during Zebrafish Heart Development and Regeneration. *PLoS One* 8, e67266.
- Huelsken, J., Birchmeier, W. (2001). New aspects of Wnt signaling pathways in higher vertebrates. *Curr Opin Genet Dev*. 11:547-53.
- Hutcheson, D.A., Zhao, J., Merrell, A., Haldar, M., Kardon, G. (2009). Embryonic and fetal limb myogenic cells are derived from developmentally distinct progenitors and have different requirements for beta-catenin. *Genes Dev*. 23:997-1013.
- Ito, M., Yang, Z., Andl, T., Cui, C., Kim, N., Millar, S.E., Cotsarelis, G. (2007). Wnt-dependent de novo hair follicle regeneration in adult mouse skin after wounding. *Nature*. 447:316-20.
- Itou, J., Akiyama, R., Pehoski, S., Yu, X., Kawakami, H., and Kawakami, Y. (2014). Regenerative responses after mild heart injuries for cardiomyocyte proliferation in zebrafish. *Dev. Dyn*. 243, 1477–1486.
- Jho, E.H., Zhang, T., Domon, C., Joo, C.K., Freund, J.N., Costantini, F. (2002). Wnt/beta-catenin/Tcf signaling induces the transcription of Axin2, a negative regulator of the signaling pathway. *Mol Cell Biol*. 22:1172-83.

- Jin, S.W., Beis, D., Mitchell, T., Chen, J.N., Stainier, D.Y. (2005). Cellular and molecular analyses of vascular tube and lumen formation in zebrafish. *Development* 132:5199-5209.
- Jopling, C., Sleep, E., Raya, M., Martí, M., Raya, A., and Belmonte, J.C.I. (2010). Zebrafish heart regeneration occurs by cardiomyocyte dedifferentiation and proliferation. *Nature* 464, 606–609.
- Jopling, C., Suñé, G., Faucherre, A., Fabregat, C., Izpisua Belmonte, J.C. (2012). Hypoxia induces myocardial regeneration in zebrafish. *Circulation*. 126:3017-27.
- Kagermeier-Schenk, B., Wehner, D., Ozhan-Kizil, G., Yamamoto, H., Li, J., Kirchner, K., Hoffmann, C., Stern, P., Kikuchi, A., Schambony, A., Weidinger, G. (2011). Waif1/5T4 inhibits Wnt/ β -catenin signaling and activates noncanonical Wnt pathways by modifying LRP6 subcellular localization. *Dev Cell*. 21:1129-43.
- Karra, R., Knecht, A.K., Kikuchi, K., and Poss, K.D. (2015). Myocardial NF- κ B activation is essential for zebrafish heart regeneration. *Proc. Natl. Acad. Sci. U. S. A.* 112, 13255–13260.
- Kikuchi, K., Holdway, J.E., Werdich, A.A., Anderson, R.M., Fang, Y., Egnaczyk, G.F., Evans, T., MacRae, C.A., Stainier, D.Y.R., and Poss, K.D. (2010). Primary contribution to zebrafish heart regeneration by *gata4*⁺ cardiomyocytes. *Nature* 464, 601–605.
- Kikuchi, K., Gupta, V., Wang, J., Holdway, J.E., Wills, A.A., Fang, Y., Poss, K.D. (2011). *tcf21*⁺ epicardial cells adopt non-myocardial fates during zebrafish heart development and regeneration. *Development*. 138:2895-902.
- Kikuchi, K., Holdway, J.E., Major, R.J., Blum, N., Dahn, R.D., Begemann, G., and Poss, K.D. (2011). Retinoic acid production by endocardium and epicardium is an injury response essential for zebrafish heart regeneration. *Dev. Cell* 20, 397–404.
- Kikuchi, K., Poss, K.D. (2012). Cardiac regenerative capacity and mechanisms. *Annu Rev Cell Dev Biol*. 28:719-41.
- Kim, J.B., Leucht, P., Lam, K., Luppen, C., Ten Berge, D., Nusse, R., Helms, J.A. (2007). Bone regeneration is regulated by wnt signaling. *J Bone Miner Res*. 22:1913-23.
- Kimelman, D., Xu, W. (2006). beta-catenin destruction complex: insights and questions from a structural perspective. *Oncogene*. 25:7482-91.

- Klaus, A., Saga, Y., Taketo, M.M., Tzahor, E., Birchmeier, W. (2007). Distinct roles of Wnt/beta-catenin and Bmp signaling during early cardiogenesis. *Proc Natl Acad Sci U S A*. 104:18531-6.
- Knopf, F., Schnabel, K., Haase, C., Pfeifer, K., Anastassiadis, K., Weidinger, G. (2010). Dually inducible TetON systems for tissue-specific conditional gene expression in zebrafish. *Proc Natl Acad Sci U S A*. 107:19933-8.
- Kubo, F., Nakagawa, S. (2008). Wnt signaling in retinal stem cells and regeneration. *Dev Growth Differ*. 50:245-51.
- Kuroda, K., Kuang, S., Taketo, M.M., Rudnicki, M.A. (2013). Canonical Wnt signaling induces BMP-4 to specify slow myofibrogenesis of fetal myoblasts. *Skelet Muscle*. 3:5.
- Laflamme, M.A., and Murry, C.E. (2011). Heart regeneration. *Nature* 473, 326-335.
- Lai, S.-L., Marín-Juez, R., Moura, P.L., Kuenne, C., Lai, J.K.H., Tsedeke, A.T., Guenther, S., Looso, M., and Stainier, D.Y. (2017). Reciprocal analyses in zebrafish and medaka reveal that harnessing the immune response promotes cardiac regeneration. *Elife* 6.
- Landeira, D., Bagci, H., Malinowski, A.R., Brown, K.E., Soza-Ried, J., Feytout, A., Webster, Z., Ndjetehe, E., Cantone, I., Asenjo, H.G., Brockdorff, N., Carroll, T., Merckenschlager, M., Fisher, A.G. (2015). Jarid2 Coordinates Nanog Expression and PCP/Wnt Signaling Required for Efficient ESC Differentiation and Early Embryo Development. *Cell Rep*. 12:573-86.
- Lawson, N.D., Weinstein, B.M. (2002). In vivo imaging of embryonic vascular development using transgenic zebrafish. *Developmental Biology*. 248:307-318.
- Lepilina, A., Coon, A.N., Kikuchi, K., Holdway, J.E., Roberts, R.W., Burns, C.G., and Poss, K.D. (2006). A Dynamic Epicardial Injury Response Supports Progenitor Cell Activity during Zebrafish Heart Regeneration. *Cell* 127, 607–619.
- Leucht, P., Kim, J.B., Helms, J.A. (2008). Beta-catenin-dependent Wnt signaling in mandibular bone regeneration. *J Bone Joint Surg Am*. 90 Suppl 1:3-8.
- Li, L., Yan, B., Shi, Y.Q., Zhang, W.Q., Wen, Z.L. (2012). Live imaging reveals differing roles of macrophages and neutrophils during Zebrafish tail fin regeneration. *The Journal of biological chemistry*. 287:25353-25360.

- Lickert, H., Kutsch, S., Kanzler, B., Tamai, Y., Taketo, M.M., Kemler, R. (2002). Formation of multiple hearts in mice following deletion of beta-catenin in the embryonic endoderm. *Dev Cell*. 3:171-81.
- Livak, K.J., Schmittgen, T.D. (2001). Analysis of relative gene expression data using real-time quantitative PCR and the 2(-Delta Delta C(T)) Method. *Methods*. 25:402-8.
- Logan, C.Y., Nusse, R. (2004). The Wnt signaling pathway in development and disease. *Annu Rev Cell Dev Biol*. 20:781-810.
- MacDonald, B.T., Tamai, K., He, X. (2009). Wnt/beta-catenin signaling: components, mechanisms, and diseases. *Dev Cell*. 17:9-26.
- MacDonald, B.T., He, X. (2012). Frizzled and LRP5/6 receptors for Wnt/ β -catenin signaling. *Cold Spring Harb Perspect Biol*. 4.
- Maggs, A.M., Taylor-Harris, P., Peckham, M., Hughes, S.M. (2000). Evidence for differential post-translational modifications of slow myosin heavy chain during murine skeletal muscle development. *J. Muscle Res. Cell Motil*. 21, 101–113.
- Marín-Juez, R., Marass, M., Gauthier, S., Rossi, A., Lai, S.-L., Materna, S.C., Black, B.L., and Stainier, D.Y.R. (2016). Fast revascularization of the injured area is essential to support zebrafish heart regeneration. *Proc. Natl. Acad. Sci. U. S. A.* 113, 11237–11242.
- Masters, M., Riley, P.R. (2014). The epicardium signals the way towards heart regeneration. *Stem Cell Res*. 13: 683–692.
- Matsumoto, K., Miki, R., Nakayama, M., Tatsumi, N., Yokouchi, Y. (2008). Wnt9a secreted from the walls of hepatic sinusoids is essential for morphogenesis, proliferation, and glycogen accumulation of chick hepatic epithelium. *Dev Biol*. 319:234-47.
- Mazumdar, J., O'Brien, W.T., Johnson, R.S., LaManna, J.C., Chavez, J.C., Klein, P.S., Simon, M.C. (2010). O₂ regulates stem cells through Wnt/ β -catenin signalling. *Nat Cell Biol*. 12:1007-13.
- Mickoleit, M., Schmid, B., Weber, M., Fahrbach, F.O., Hombach, S., Reischauer, S., Huisken, J. (2014). High-resolution reconstruction of the beating zebrafish heart. *Nature Methods*. 11:919-22.

Mirotsov, M., Zhang, Z., Deb, A., Zhang, L., Gneccchi, M., Noiseux, N., Mu, H., Pachori, A., Dzau, V. (2007). Secreted frizzled related protein 2 (Sfrp2) is the key Akt-mesenchymal stem cell-released paracrine factor mediating myocardial survival and repair. *Proc Natl Acad Sci U S A.* 104:1643-8.

Mizutani, M., Wu, J.C., Nusse, R. (2016). Fibrosis of the Neonatal Mouse Heart After Cryoinjury Is Accompanied by Wnt Signaling Activation and Epicardial-to-Mesenchymal Transition. *J Am Heart Assoc.* 5:e002457.

Moon, R.T., Kohn, A.D., De Ferrari, G.V., Kaykas, A. (2004). WNT and beta-catenin signalling: diseases and therapies. *Nat Rev Genet.* 5:691-701.

Moon, J., Zhou, H., Zhang, L.S., Tan, W., Liu, Y., Zhang, S., Morlock, L.K., Bao, X., Palecek, S.P., Feng, J.Q., Williams, N.S., Amatruda, J.F., Olson, E.N., Bassel-Duby, R., Lum, L. (2017). Blockade to pathological remodeling of infarcted heart tissue using a porcupine antagonist. *Proc Natl Acad Sci U S A.* 114:1649-1654.

Münch, J., Grivas, D., González-Rajal, Á., Torregrosa-Carrión, R., de la Pompa, J.L. (2017). Notch signalling restricts inflammation and *serpine1* expression in the dynamic endocardium of the regenerating zebrafish heart. *Development.* 144:1425-1440.

Naito, A.T., Shiojima, I., Akazawa, H., Hidaka, K., Morisaki, T., Kikuchi, A., Komuro, I. (2006). Developmental stage-specific biphasic roles of Wnt/beta-catenin signaling in cardiomyogenesis and hematopoiesis. *Proc Natl Acad Sci U S A.* 103:19812-7.

Niida, A., Hiroko, T., Kasai, M., Furukawa, Y., Nakamura, Y., Suzuki, Y., Sugano, S., Akiyama, T. (2004). DKK1, a negative regulator of Wnt signaling, is a target of the beta-catenin/TCF pathway. *Oncogene.* 23:8520-6.

Oerlemans, M.I., Goumans, M.J., van Middelaar, B., Clevers, H., Doevendans, P.A., Sluijter, J.P. (2010). Active Wnt signaling in response to cardiac injury. *Basic Res Cardiol.* 105:631-41.

Oikonomopoulos, A., Sereti, K.I., Conyers, F., Bauer, M., Liao, A., Guan, J., Crapps, D., Han, J.K., Dong, H., Bayomy, A.F., Fine, G.C., Westerman, K., Biechele, T.L., Moon, R.T., Force, T., Liao, R. (2011). Wnt signaling exerts an antiproliferative effect on adult cardiac progenitor cells through IGFBP3. *Circ Res.* 109:1363-74.

- Osei-Sarfo, K., Gudas, L.J. (2014). Retinoic acid suppresses the canonical Wnt signaling pathway in embryonic stem cells and activates the noncanonical Wnt signaling pathway. *Stem Cells*. 32:2061-71.
- Ozhan, G., Weidinger, G. (2015). Wnt/ β -catenin signaling in heart regeneration. *Cell Regen (Lond)*. 4:3.
- Paige, S.L., Osugi, T., Afanasiev, O.K., Pabon, L., Reinecke, H., Murry, C.E. (2010). Endogenous Wnt/beta-catenin signaling is required for cardiac differentiation in human embryonic stem cells. *PLoS One*. 5.
- Palevski, D., Levin-Kotler, L.P., Kain, D., Naftali-Shani, N., Landa, N., Ben-Mordechai, T., Konfino, T., Holbova, R., Molotski, N., Rosin-Arbesfeld, R., Lang, R.A., Leor, J. (2017). Loss of Macrophage Wnt Secretion Improves Remodeling and Function After Myocardial Infarction in Mice. *J Am Heart Assoc*. 6. pii: e004387.
- Parchure, A., Vyas, N., Mayor, S. (2018). Wnt and Hedgehog: Secretion of Lipid-Modified Morphogens. *Trends Cell Biol*. 28:157-170.
- Parente, V., Balasso, S., Pompilio, G., Verduci, L., Colombo, G.I., Milano, G., Guerrini, U., Squadroni, L., Cotelli, F., Pozzoli, O. (2013). Hypoxia/Reoxygenation Cardiac Injury and Regeneration in Zebrafish Adult Heart. *PLoS One* 8, e53748.
- Person, A.D., Garriock, R.J., Krieg, P.A., Runyan, R.B., Klewer, S.E. (2005). Frzb modulates Wnt-9a-mediated beta-catenin signaling during avian atrioventricular cardiac cushion development. *Dev Biol*. 278:35-48.
- Petersen, C.P., Reddien, P.W. (2009). A wound-induced Wnt expression program controls planarian regeneration polarity. *Proc Natl Acad Sci U S A*. 106:17061-6.
- Porrello, E.R., Mahmoud, A.I., Simpson, E., Hill, J.A., Richardson, J.A., Olson, E.N., and Sadek, H.A. (2011). Transient regenerative potential of the neonatal mouse heart. *Science* 331, 1078–1080.
- Poss, K.D., Shen, J., Keating, M.T. (2000). Induction of *lef1* during zebrafish fin regeneration. *Dev Dyn*. 219:282-6.
- Poss, K.D., Wilson, L.G., and Keating, M.T. (2002). Heart regeneration in zebrafish. *Science* 298, 2188–2190.

Reuter, H., März, M., Vogg, M.C., Eccles, D., Grífol-Boldú, L., Wehner, D., Owlarn, S., Adell, T., Weidinger, G., Bartscherer, K. (2015). B-catenin-dependent control of positional information along the AP body axis in planarians involves a teashirt family member. *Cell Rep.* 10:253-65.

Richardson, W.J., Clarke, S.A., Quinn, T.A., Holmes, J.W. (2015). Physiological Implications of Myocardial Scar Structure. *Compr Physiol.* 5: 1877–1909.

Rochard, L., Monica, S.D., Ling, I.T., Kong, Y., Roberson, S., Harland, R., Halpern, M., Liao, E.C. (2016). Roles of Wnt pathway genes *wls*, *wnt9a*, *wnt5b*, *frzb* and *gpc4* in regulating convergent-extension during zebrafish palate morphogenesis. *Development.* 143:2541-7.

Roman, B.L., Pham, V., Lawson, N.D., Kulik, M., Childs, S., Lekven, A.C., Garrity, D.M., Moon, R.T., Fishman, M.C., Lechleider, R.J., Weinstein, B.M. (2002). Disruption of *acvr11* increases endothelial cell number in zebrafish cranial vessels. *Development* 129:3009-3019.

Sallin, P., de Preux Charles, A.-S., Duruz, V., Pfefferli, C., and Jazwińska, A. (2015). A dual epimorphic and compensatory mode of heart regeneration in zebrafish. *Dev. Biol.* 399, 27–40.

Sallin, P., Jazwińska, A. (2016). Acute stress is detrimental to heart regeneration in zebrafish. *Open Biol.* 6. pii: 160012.

Sánchez-Iranzo, H., Galardi-Castilla, M., Minguillón, C., Sanz-Morejón, A., González-Rosa, J.M., Felker, A., Ernst, A., Guzmán-Martínez, G., Mosimann, C., Mercader, N. (2018). *Tbx5a* lineage tracing shows cardiomyocyte plasticity during zebrafish heart regeneration. *Nat Commun.* 9:428.

Sánchez-Iranzo, H., Galardi-Castilla, M., Sanz-Morejón, A., González-Rosa, J.M., Costa, R., Ernst, A., Sainz de Aja, J., Langa, X., Mercader, N. (2018). Transient fibrosis resolves via fibroblast inactivation in the regenerating zebrafish heart. *Proc Natl Acad Sci U S A.* 115:4188-4193.

Schnabel, K., Wu, C.C., Kurth, T., and Weidinger, G. (2011). Regeneration of cryoinjury induced necrotic heart lesions in zebrafish is associated with epicardial activation and cardiomyocyte proliferation. *PLoS One* 6, e18503.

- Sehring, I.M., Jahn, C., and Weidinger, G. (2016). Zebrafish fin and heart: what's special about regeneration? *Curr. Opin. Genet. Dev.* 40, 48–56.
- Shimizu, N., Kawakami, K., Ishitani, T. (2012). Visualization and exploration of Tcf/Lef function using a highly responsive Wnt/beta-catenin signaling-reporter transgenic zebrafish. *Developmental Biology.* 370:71-85
- Stamos, J.L., Weis, W.I. (2013). The β -catenin destruction complex. *Cold Spring Harb Perspect Biol.* 5.
- Stoick-Cooper, C.L., Weidinger, G., Riehle, K.J., Hubbert, C., Major, M.B., Fausto, N., Moon, R.T. (2007). Distinct Wnt signaling pathways have opposing roles in appendage regeneration. *Development.* 134:479-89.
- Sugimoto, K., Hui, S.P., Sheng, D.Z., and Kikuchi, K. (2017). Dissection of zebrafish shha function using site-specific targeting with a Cre-dependent genetic switch. *Elife* 6.
- Tseng, A.S., Engel, F.B., Keating, M.T. (2006). The GSK-3 inhibitor BIO promotes proliferation in mammalian cardiomyocytes. *Chem Biol.* 13:957-63.
- Ueno, S., Weidinger, G., Osugi, T., Kohn, A.D., Golob, J.L., Pabon, L., Reinecke, H., Moon, R.T., Murry, C.E. (2007). Biphasic role for Wnt/beta-catenin signaling in cardiac specification in zebrafish and embryonic stem cells. *Proc Natl Acad Sci U S A.* 104:9685-90.
- Veldman, M.B., Zhao, C., Gomez, G.A., Lindgren, A.G., Huang, H., Yang, H., Yao, S., Martin, B.L., Kimelman, D., Lin, S. (2013). Transdifferentiation of fast skeletal muscle into functional endothelium in vivo by transcription factor Etv2. *PLoS Biol.* 11:e1001590.
- Villar, J., Cabrera, N.E., Casula, M., Valladares, F., Flores, C., López-Aguilar, J., Blanch, L., Zhang, H., Kacmarek, R.M., Slutsky, A.S. (2011). WNT/ β -catenin signaling is modulated by mechanical ventilation in an experimental model of acute lung injury. *Intensive Care Med.* 37:1201-9.
- Wang, J., Panáková, D., Kikuchi, K., Holdway, J.E., Gemberling, M., Burriss, J.S., Singh, S.P., Dickson, A.L., Lin, Y.-F., Sabeh, M.K., et al. (2011). The regenerative capacity of zebrafish reverses cardiac failure caused by genetic cardiomyocyte depletion. *Development* 138, 3421–3430.

- Wang, W.E., Li, L., Xia, X., Fu, W., Liao, Q., Lan, C., Yang, D., Chen, H., Yue, R., Zeng, C., et al. (2017). Dedifferentiation, Proliferation, and Redifferentiation of Adult Mammalian Cardiomyocytes After Ischemic Injury. *Circulation* 136, 834–848.
- Wehner, D., Cizelsky, W., Vasudevarao, M.D., Ozhan, G., Haase, C., Kagermeier-Schenk, B., Röder, A., Dorsky, R.I., Moro, E., Argenton, F., et al. (2014). Wnt/ β -catenin signaling defines organizing centers that orchestrate growth and differentiation of the regenerating zebrafish caudal fin. *Cell Rep.* 6, 467–481.
- Wehner, D., Jahn, C., Weidinger, G. (2015). Use of the TetON System to Study Molecular Mechanisms of Zebrafish Regeneration. *Journal of visualized experiments JoVE*:e52756.
- Weidinger, G., Thorpe, C.J., Wuennenberg-Stapleton, K., Ngai, J., Moon, R.T. (2005). The Sp1-related transcription factors sp5 and sp5-like act downstream of Wnt/ β -catenin signaling in mesoderm and neuroectoderm patterning. *Curr Biol.* 15:489-500.
- Willert, K., Nusse, R. (2012). Wnt proteins. *Cold Spring Harb Perspect Biol.* 4.
- Wills, A.A., Holdway, J.E., Major, R.J., Poss, K.D. (2008). Regulated addition of new myocardial and epicardial cells fosters homeostatic cardiac growth and maintenance in adult zebrafish. *Development.* 135:183-92.
- Wu, C.-C., Kruse, F., Vasudevarao, M.D., Junker, J.P., Zebrowski, D.C., Fischer, K., Noël, E.S., Grün, D., Berezikov, E., Engel, F.B., et al. (2016). Spatially Resolved Genome-wide Transcriptional Profiling Identifies BMP Signaling as Essential Regulator of Zebrafish Cardiomyocyte Regeneration. *Dev. Cell* 36, 36–49.
- Yokoyama, H., Ogino, H., Stoick-Cooper, C.L., Grainger, R.M., Moon, R.T. (2007). Wnt/ β -catenin signaling has an essential role in the initiation of limb regeneration. *Dev Biol.* 306:170-8.
- Zebrowski, D.C., Engel, F.B. (2013). The cardiomyocyte cell cycle in hypertrophy, tissue homeostasis, and regeneration. *Rev Physiol Biochem Pharmacol.* 165:67-96.
- Zelarayán, L.C., Noack, C., Sekkali, B., Kmecova, J., Gehrke, C., Renger, A., Zafiriou, M.P., van der Nagel, R., Dietz, R., de Windt, L.J., Balligand, J.L., Bergmann, M.W. (2008). β -Catenin downregulation attenuates ischemic cardiac remodeling through enhanced resident precursor cell differentiation. *Proc Natl Acad Sci U S A.* 105:19762-7.

Zhang, Y., Goss, A.M., Cohen, E.D., Kadzik, R., Lepore, J.J., Muthukumaraswamy, K., Yang, J., DeMayo, F.J., Whitsett, J.A., Parmacek, M.S., Morrisey, E.E. (2008). A Gata6-Wnt pathway required for epithelial stem cell development and airway regeneration. *Nat Genet.* 40:862-70.

Zhang, Z., Deb, A., Zhang, Z., Pachori, A., He, W., Guo, J., Pratt, R., Dzau, V.J. (2009). Secreted frizzled related protein 2 protects cells from apoptosis by blocking the effect of canonical Wnt3a. *J Mol Cell Cardiol.* 46:370-7.

Zhao, L., Borikova, A.L., Ben-Yair, R., Guner-Ataman, B., MacRae, C.A., Lee, R.T., Burns, C.G., Burns, C.E. (2014). Notch signaling regulates cardiomyocyte proliferation during zebrafish heart regeneration. *Proc Natl Acad Sci U S A.* 111:1403-8.

Statutory Declaration:

I hereby declare that I wrote the present dissertation with the topic:

Investigation of the extent of cardiomyocyte regeneration in the injured zebrafish heart and the role of Wnt signaling during cardiac repair

independently and used no other aids than those cited. In each individual case, I have clearly identified the source of the passages that are taken word for word or paraphrased from other works.

I also hereby declare that I have carried out my scientific work according to the principles of good scientific practice in accordance with the current „Satzung der Universität Ulm zur Sicherung guter wissenschaftlicher Praxis“ [Rules of the University of Ulm for Assuring Good Scientific Practice].

Ulm, 05.11.2018

(Alberto Bertozzi)